

INFORMATION TO USERS

This material was produced from a microfilm copy of the original document. While the most advanced technological means to photograph and reproduce this document have been used, the quality is heavily dependent upon the quality of the original submitted.

The following explanation of techniques is provided to help you understand markings or patterns which may appear on this reproduction.

1. The sign or "target" for pages apparently lacking from the document photographed is "Missing Page(s)". If it was possible to obtain the missing page(s) or section, they are spliced into the film along with adjacent pages. This may have necessitated cutting thru an image and duplicating adjacent pages to insure you complete continuity.
2. When an image on the film is obliterated with a large round black mark, it is an indication that the photographer suspected that the copy may have moved during exposure and thus cause a blurred image. You will find a good image of the page in the adjacent frame.
3. When a map, drawing or chart, etc., was part of the material being photographed the photographer followed a definite method in "sectioning" the material. It is customary to begin photoing at the upper left hand corner of a large sheet and to continue photoing from left to right in equal sections with a small overlap. If necessary, sectioning is continued again — beginning below the first row and continuing on until complete.
4. The majority of users indicate that the textual content is of greatest value, however, a somewhat higher quality reproduction could be made from "photographs" if essential to the understanding of the dissertation. Silver prints of "photographs" may be ordered at additional charge by writing the Order Department, giving the catalog number, title, author and specific pages you wish reproduced.
5. PLEASE NOTE: Some pages may have indistinct print. Filmed as received.

Xerox University Microfilms

300 North Zeeb Road
Ann Arbor, Michigan 48106

77-1487

TUNCER, Erdil Riza, 1946-
ENGINEERING BEHAVIOR AND CLASSIFICATION
OF LATERITIC SOILS IN RELATION TO SOIL
GENESIS.

Iowa State University, Ph.D., 1976
Engineering, civil

Xerox University Microfilms, Ann Arbor, Michigan 48106

Engineering behavior and classification of
lateritic soils in relation to soil genesis

by

Erdil Riza Tuncer

A Dissertation Submitted to the
Graduate Faculty in Partial Fulfillment of
The Requirements for the Degree of
DOCTOR OF PHILOSOPHY

Department: Civil Engineering
Major: Soil Engineering

Approved:

Signature was redacted for privacy.

In Charge of Major Work

Signature was redacted for privacy.

For the Major Department

Signature was redacted for privacy.

For the Graduate College

Iowa State University
Ames, Iowa

1976

TABLE OF CONTENTS

	Page
INTRODUCTION	1
LITERATURE REVIEW ON LATERITES AND LATERITIC SOILS	3
METHODS OF INVESTIGATION AND RESULTS	15
ANALYSIS AND DISCUSSION OF TEST RESULTS	61
CONCLUSIONS	113
LITERATURE CITED	116
ACKNOWLEDGMENTS	122
APPENDIX A: QUANTITATIVE X-RAY DIFFRACTION AND FLUORESCENCE ANALYSES RESULTS	123
APPENDIX B: PORE SIZE DISTRIBUTION CURVES OBTAINED FROM MERCURY POROSIMETRY	125

INTRODUCTION

To the soil engineer, the word "soil" means a material which is used in any kind of civil engineering job, either as foundation material to support the load exerted by structures, or as construction material itself, as in the cases of earthfill dam and highway constructions.

From this point of view, the soil engineer is mainly interested in the engineering behavior of soils as foundation and construction material, and he needs a kind of classification system that would establish boundaries between differently behaving soils on the basis of soil properties which can be easily measured. American Association of State Highway Officials and Unified systems are classifications which have been used satisfactorily for years in the case of temperate soils, and they are based upon the plasticity and gradation characteristics of soils. However, it has been observed for a long time that these classification systems fail to accurately predict the engineering behavior of laterites and lateritic soils. The reason for this failure is the variation in plasticity and gradation characteristics of these soils resulting from sample preparation and handling which disrupt the natural structure of the soils. Therefore, engineering index properties of laterites and lateritic soils are not reproducible (25,35,44,38,24). In order to avoid such difficulties many authors have advocated a classification of laterites and lateritic soils for engineering purposes, based on parent material and degree of weathering (46,35,19,11,26). The weathering becomes an

important factor in the case of tropical soils, simply because the environment in tropics leads to intense weathering.

It is the purpose of this thesis to investigate the engineering behavior of selected Hawaiian lateritic soils derived from basalt, in relation to degree of weathering and search for any possible engineering classification.

The following sections of the thesis contain a brief literature review on laterites and lateritic soils, methods of investigation and results, discussion of test results and conclusions.

LITERATURE REVIEW ON LATERITES AND LATERITIC SOILS

In this section, a brief literature review on laterities and lateritic soils will be presented. The information which will be compiled here was selected to be directly related to the scope of this particular study. More detailed information obtained from the literature on these soils can be found in Paulson's (49) and Fish's (23) theses.

Definition and Genesis of Laterites and Lateritic Soils

The recognition of laterite as an earth material, with unique properties, dates back to 1807 when Buchanan first encountered a material in India which he called laterite and defined as "soft enough to be readily cut into blocks by an iron instrument, but which upon exposure to air quickly becomes as hard as brick, and is reasonably resistant to the action of air and water" (74).

Since Buchanan's time, the word laterite has been used to describe a wide variety of tropical soils without reaching an agreement on the exact origin, composition and properties of laterites. If one attempts to find the definition of laterite by searching the literature, he will encounter several different definitions. Among them, the one of Alexander and Cady (3) is widely accepted: "Laterite is a highly weathered material rich in secondary oxides of iron, aluminum, or both. It is nearly void of bases and primary silicates, but it may contain large amounts of quartz and kaolinite. It is either hard or capable of hardening on exposure to wetting and drying." Among those characteristics listed in the above definition; hardness is the only one which makes laterite unique. Later

on, Lohnes and Demirel (37) used the same definition in their studies on tropical soils, with the slight modification that "hardness means there is sufficient induration of the soil that it cannot be readily excavated by a shovel or spade."

There are certain tropical soils which have not weathered as severely as laterites, but still have high sesquioxide and kaolinite contents, and low base and primary silicate contents, however, they are neither hard nor capable of hardening. According to Lohnes and Demirel (37), such soils can be referred to as lateritic soils.

In this thesis, the terms laterite and lateritic soils will be used in accordance with the definitions made by Lohnes and Demirel.

A complete accumulation of information on laterites prior to 1966 can be found in Maignien's (42) UNESCO report, "Review of Research on Laterites," in which he condensed the information contained in more than 2000 bibliographical references.

There are numerous hypotheses on the genesis of laterites, differing from each other one way or another. The following points, however, remain common in most of them. The weathering process involves leaching of silica, formation of colloidal sesquioxides, and precipitation of the oxides with increasing crystallinity and dehydration as the rock becomes more weathered. The parent rock which contains primary feldspars, quartz, and ferromagnesian minerals is transformed to a porous clayey system containing kaolinite, sesquioxides, and some residual quartz. The primary feldspars are converted to kaolinite and then, kaolinite is transformed to gibbsite. Primary ferromagnesian minerals, on the other hand, are

eventually converted to diffuse goethite, followed by well-crystallized goethite, and finally hematite. The crystallization leads to the formation of iron and/or aluminum oxide concretions, coalescence of concretions and their cementation by iron and/or aluminum colloids, until the entire system is a continuous iron and/or aluminum oxide cemented crust (55,3, 60,27,37).

The weathering process of soils is very much dependent on the environmental conditions in which soils are occurring. There are five major factors influencing the formation of soils and they are: parent material, climate, topography, vegetation, and time. From this point of view, the tropical regions with high temperature and humid conditions provide a favorable environment for intense weathering.

It is quite difficult to differentiate which factors have more influence on weathering than the others. One may intuitively say that the properties of a soil, which is the product of weathering, should be directly dependent on the properties and features of the parent material from which the soil is derived (45,42).

The influence of climate on weathering, on the other hand, is a commonly accepted fact. In discussing the factors influencing soil weathering, Mohr and Van Baren (45) put considerable emphasis on the rainfall distribution. In his study on Hawaiian soils, Sherman (54) observed the influence of rainfall intensity on the mineral composition of soils. Although many investigators (65,18,36) reported certain relationships between rainfall and mineral composition, there are some discrepancies. Dean (18) and Tanada (65), for example, observed that in Hawaiian

soils, high kaolinite content occurs in regions receiving small amount of rainfall (65-90 cm annually), and that the kaolinite content decreases with increasing rainfall. Some other publications on Hawaiian soils, on the other hand, present cases in which kaolinite does not exist at all under a rainfall of 90 cm per year; instead, high amounts of sesquioxides of secondary origin occur. This difference in occurrence is attributed to the age of the soils (54,58).

The influence of topography on weathering, also, cannot be overlooked. Since topography has influence on ground and surface water movement, it has a direct influence on the development of soil profile. Mohr and Van Baren (45) point out that the same type of rock may yield a weathering product of completely different composition if different topography and accordingly different drainage processes are involved.

Vegetation is another important factor in the formation of laterites. As Sherman et al. (59) point out dehydration of the colloidal hydrated oxides of the soil has a very important role in the development of laterite; and vegetation is one of the factors which determine the rate of dehydration. Vegetation also has a protective effect on runoff and erosion which are important environmental factors influencing the genesis of soils (42).

Finally, the role of time in the formation of laterites and lateritic soils, is a well-recognized point introduced by many investigators (54,51, 45,42,14). Sherman (54) states that "since the geological ages of the parent materials vary greatly, the time of exposure of the parent material

to soil forming processes will also have had a major effect on soil development."

As a result of the preceding discussions, it is concluded that because of the combined effects of those several soil forming factors, laterites and lateritic soils exhibit a very complex pattern of soil development.

Engineering Properties of Laterites and Lateritic Soils

Many studies have shown that plasticity and grain size distribution data for lateritic soils are extremely varied and erratic (79,44,74,38). The reasons for this are discussed in detail by several investigators (44,69,26). When soils are manipulated their characteristics vary a lot. Pre-testing drying causes variations in some properties of lateritic soils and this behavior is commonly attributed to the dehydration of the colloidal hydrated oxides occurring in these soils. In most of the cases the variation, resulting from drying, is irreversible and results in a soil with more granular characteristics. To disperse such a system for plasticity and grain size determinations is almost impossible (74). Because of such difficulties it is extremely difficult to derive an acceptable generalization for lateritic soils with regard to plasticity and gradation.

Lohnes and Demirel (37) are the first investigators who have put emphasis on using specific gravity as an indicator for engineering behavior of lateritic soils. By definition specific gravity is the weighted average of the specific gravities of the minerals which comprise the soil.

In the weathering process of lateritic soils, it is always stated that the contents of high specific gravity minerals increase with age of formation. This fact, of course, should be reflected in the value of specific gravity, that is, specific gravity of lateritic soils should increase with increasing degree of weathering. Lohnes and Demirel made an attempt to verify this thought by plotting extractable iron content versus specific gravity for several selected Puerto Rican soils and ended up with a good correlation between increasing specific gravity and increasing iron content. They also used the data presented by Trow and Morton (70) on Dominican Republic soils to show increasing specific gravity with increasing amount of goethite.

Thus it appears that specific gravity of lateritic soils can be regarded as a parameter which can be used for a better understanding of the engineering behavior of tropical soils in relation to degree of weathering.

Other engineering properties of lateritic soils, such as wet and dry densities, moisture content, and void ratio (or porosity), have not been taken into account in the majority of studies. There are very limited data on such properties of lateritic soils in the literature. This is an unfortunate situation, because these properties have an advantage over plasticity and gradation, in that, the majority of them are determined by bulk measurements and as such are not influenced by degree of manipulation. Specific gravity, which is used in determining the void ratio, is also a parameter not affected much by the manipulation of soils prior to testing. In addition, the bulk properties, reflect the behavior of

undisturbed soils; so, from the engineering point of view, they provide better information on laterites and lateritic soils.

In their study on Puerto Rican soils, Lohnes and Demirel (37) observed a relationship between void ratio and specific gravity, indicating a decrease in void ratio as specific gravity increases. Besides that, they observed increasing cohesion with decreasing void ratio. By making use of these relationships, they suggested the possibility of an engineering classification system for lateritic soils which relates void ratio, strength and degree of weathering to each other.

Structure of Laterites and Lateritic Soils

The size, shape, and arrangement of mineral grains which form the soil mass is known as soil structure. The importance of soil structure in explaining the engineering behavior of soils is emphasized by many investigators (29,43,62,6). In this section of the literature review the soil properties which have been inferred as having direct relationships with the soil structure will be introduced.

Soil mineralogy

Soil minerals occurring in the soil mass apparently have direct influence on the size, shape and arrangement of the soil aggregates. According to many investigators the predominant minerals occurring in lateritic soils are kaolinite, gibbsite, and iron compounds (65,18,16,57, 21,36,38). It has also been inferred that the occurrence of kaolinite in large amounts comes first in the course of weathering. With continued weathering the kaolinite content decreases, while the sesquioxides of iron and aluminum become larger in amount (3,27). Peterson (50) made an

attempt to measure the capacity of kaolinite to form water stable aggregates under the influence of cyclic wetting and drying, and found out that kaolinite is very inert as a binding agent which has very little effect on aggregation. Oxides of iron and aluminum, on the other hand, are reported as being very active as binding agents by many investigators (40,66,69,5,8). Arca and Weed (5) point out that the relationship between aggregate occurrence and free iron oxide content remains highly significant and fairly constant at all sizes studied (0.1-2.0 mm diameter). These observations suggest that the soils with high kaolinite content would show low aggregation, and soils with large amount of sesquioxides would exhibit good soil aggregation. In his study on some residual soils from the highlands of Papua, New Guinea, Wallace (75) made an attempt to idealize the structure of lateritic soils. According to him, soil aggregates are cemented together at their contacts to form a continuous three-dimensional structural framework and the precipitation of iron and aluminum hydroxides is responsible for the cementation. This is verified somewhat by the scanning electron microscope photos of Lohnes and Demirel (37).

As it is stated by many investigators (54,45,42), the ultimate end product of laterization in tropical soils could be either iron oxide rich laterite or aluminum oxide rich laterite. According to Sherman (54) the end product of weathering is closely related to the distribution of rainfall. He states that an alternating wet and dry season climate results in the stabilization of the iron oxide. Under continuously wet conditions, however, the alumina becomes the stabilized free oxide, while iron oxide

becomes unstable and leaches away. This explains the difference in formation of so called ferruginous and aluminous, or bauxite, laterites.

Titanium oxide, in the form of anatase, is occasionally encountered in tropical soils (16,56). Sherman (56) studied the titanium content of Hawaiian soils and discussed its significance in the weathering process of soils. The data presented by him suggest that the occurrence of titanium element usually takes place in the surface of soils, more specifically in A-horizon, under a climate which has definite wet and dry seasons.

Soil pore structure

Besides studying the size, shape and arrangement of solid phase in a soil mass, it should be worthwhile to study the pore phase of soils as well.

Mercury injection technique is a method recently developed, and can be used for analyzing several aspects of porous materials. Diamond (20) introduced the method first for studying the pore size distribution of soils. After him, several pore size studies have been performed on temperate soils (64,6,2), but not on tropical soils. It is the belief of the author that such a useful tool should be utilized in studying the pore structure of lateritic soils in order to be able to understand the behavior of these soils better, with regard to soil weathering and soil strength.

The most common methods utilized in studying the structure of lateritic soils have been light microscopy and recently, scanning electron microscopy (30,71,37). It is extremely difficult to define the soil structure quantitatively from the micrographs obtained from microscopic

studies. The mercury porosimetry, however, gives the opportunity to generate several parameters from the pore size distribution curves and to quantify, at least, the pore structure of soils (39).

Strength of Laterites and Lateritic Soils

A literature review on the strength characteristics of undisturbed samples of laterites and lateritic soils reveals that the investigation of these soils from an engineering point of view has been greatly overlooked, although such soils have been used as a primary engineering construction material in tropical and equatorial countries for many years. Some studies performed recently on the strength behavior of laterites and lateritic soils have added little because either they are incomplete or they deal with localized problems and in restricted areas.

The available reported test results can be summarized in the following manner. Lateritic soils usually have relatively high to very high cohesion and internal friction angle (23). This behavior is generally attributed to the cementation which is taking place among the individual soil grains by the binding action of sesquioxides (23,37,49). The strength behavior of lateritic soils was observed to be very much dependent on the moisture content of the sample tested (7,49). Decreasing moisture content usually causes an increase both in cohesion and internal friction angle (7,49). This behavior is attributed to the variation in soil structure with varying moisture content, such that, as the soil dries out part of the hydrated colloidal iron and aluminum oxides dehydrates

and forms strong bonds among certain soil grains which, in turn, causes an increase in strength.

In their study on Puerto Rican soils, Lohnes and Demirel (37) made an attempt to relate cohesion to degree of weathering and they observed that cohesion increases with increasing weathering.

Classification of Laterites and Lateritic Soils

There have been several attempts to classify laterites and lateritic soils for many years, but none of the proposed classification systems has been accepted universally. According to Maignien (42), these classification systems can be grouped as (a) analytical classifications which are based mainly on morphological characteristics with a bias toward soil genetic considerations, and (b) synthetic classifications which are based on genetic factors or soil-genetic processes or on properties of pedo-genetic factors or processes.

As Mohr and Van Baren (45) point out every classification system should have some predetermined purposes. None of the classification systems mentioned above has an aim to classify the soils according to their engineering behavior. Although there are some popular engineering classification systems, such as the Unified system or the American Association of State Highway Officials system, which have been used satisfactorily in the temperate environments of the world for years, they have not been so successful in the case of tropical soils. These classification systems are based on plasticity and gradation data of the soils; but as discussed previously, such characteristics of tropical soils are not

reproducible by standard laboratory tests. The reasons for this, once again, are the influences of sample preparation and handling which disrupt the natural structure of the soil.

In order to avoid such problems, several authors (46,35,26) have advocated a classification of laterites and lateritic soils for engineering purposes, based on parent material and degree of weathering.

Fish (23) and Gidigas (26) made attempts to use pedological classifications for engineering purposes. Ruddock (53) has suggested an engineering classification based on topographic position, sample depth and depth to water table which are, in fact, factors influencing the degree of weathering. Lohnes and Demirel (37) have suggested to use specific gravity, void ratio and degree of weathering for engineering classification of tropical soils. None of these proposed engineering classification systems, however, has found a broad acceptance yet.

From the above discussion, it becomes evident that an appropriate classification of laterites and lateritic soils for engineering purposes is still nonexistent.

METHODS OF INVESTIGATION AND RESULTS

Geographic Location and Sample Sites

The soils investigated in this study were collected from the islands of Oahu and Kauai, Hawaii. The islands of Hawaii are located in the central part of the Pacific Ocean, between 19° and 23° latitude and 154° and 161° longitude, and they line up in the direction of northwest to southeast.

In selecting the specific sampling locations, the main consideration was to obtain soils which were derived from the same parent material, but formed under the influence of various environmental conditions. The soil series collected from the island of Oahu are Molokai, Lahaina, Wahiawa, Manana and Paaloa. All of these soils were derived from the Koolau basalt series on the leeward side of the Koolau mountain range. According to Wentworth and Winchell (78), this basalt series is very uniform chemically and petrologically, so it may be assumed that the soils were derived from essentially the same parent rock. The sample locations are along a three mile traverse on the divide between Kipapa stream and Panakauki Gulch about three and one-half miles northwest of Pearl City. Generalized geologic map of Oahu and location of soil sampling sites are shown in Figure 1.

The soil series collected from the island of Kauai are Lihue, Puhi, Kapaa and Halii. All were derived from Koloa basalt series on the windward side of the island. Beinroth et al. (10) state that these soil

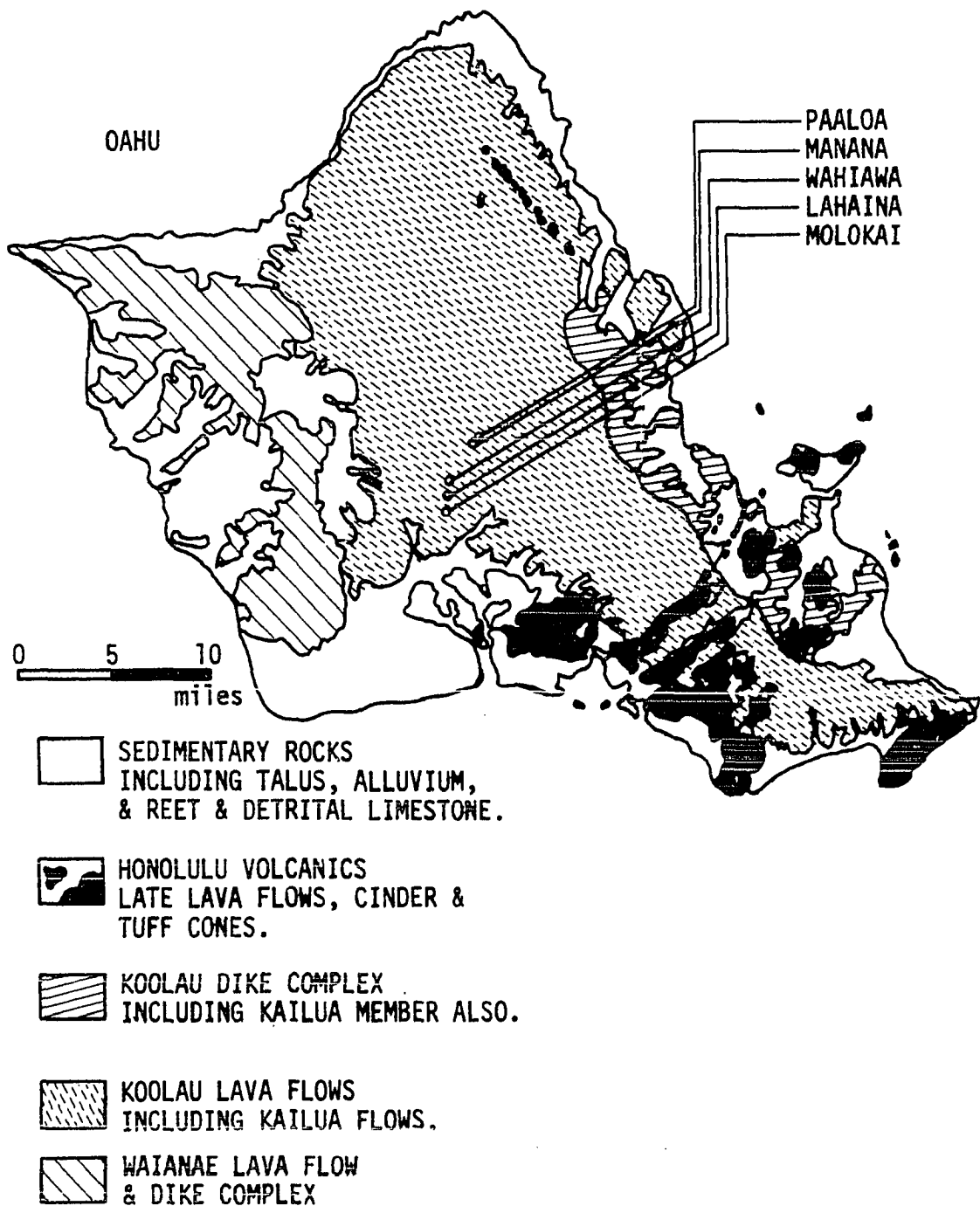


Figure 1. Generalized geologic map of Oahu, Hawaii, showing location of soil sampling sites

series can be considered as derived from the same parent material. Generalized geologic map of Kauai and location of soil sampling sites are shown in Figure 2.

According to the most recent pedological classification of the U.S. Department of Agriculture (72), the soils which are the subject of this study are oxisols and ultisols. Table 1 outlines the USDA classification and environmental factors of the soils. Complete profile descriptions can be found in the soil survey of the islands (73).

Method of Sampling, Shipping, and Storage

Thin walled Shelby tubes were hydraulically pushed into the soil by a Soiltest Model DR-2000 Hydraulic Porta-Sampler to collect undisturbed samples. Description and efficiency of this method of sampling is explained in detail in Paulson's (49) and Fish's (23) theses.

Two or three borings were made at each location. All the samples were collected from B-horizon of the profile, since it is influenced by the weathering process more than the other horizons, and it can form a good basis for the comparison of different soils from the genesis point of view. Therefore, highly organic A-horizon and relatively unweathered C-horizon were eliminated from the investigation.

Permission was obtained from the U.S. Department of Agriculture to ship the soils into the continental United States without sterilization, so that the relatively undisturbed nature of the soils could be preserved. The method of handling and shipping the samples was the same as explained in Paulson's and Fish's theses.

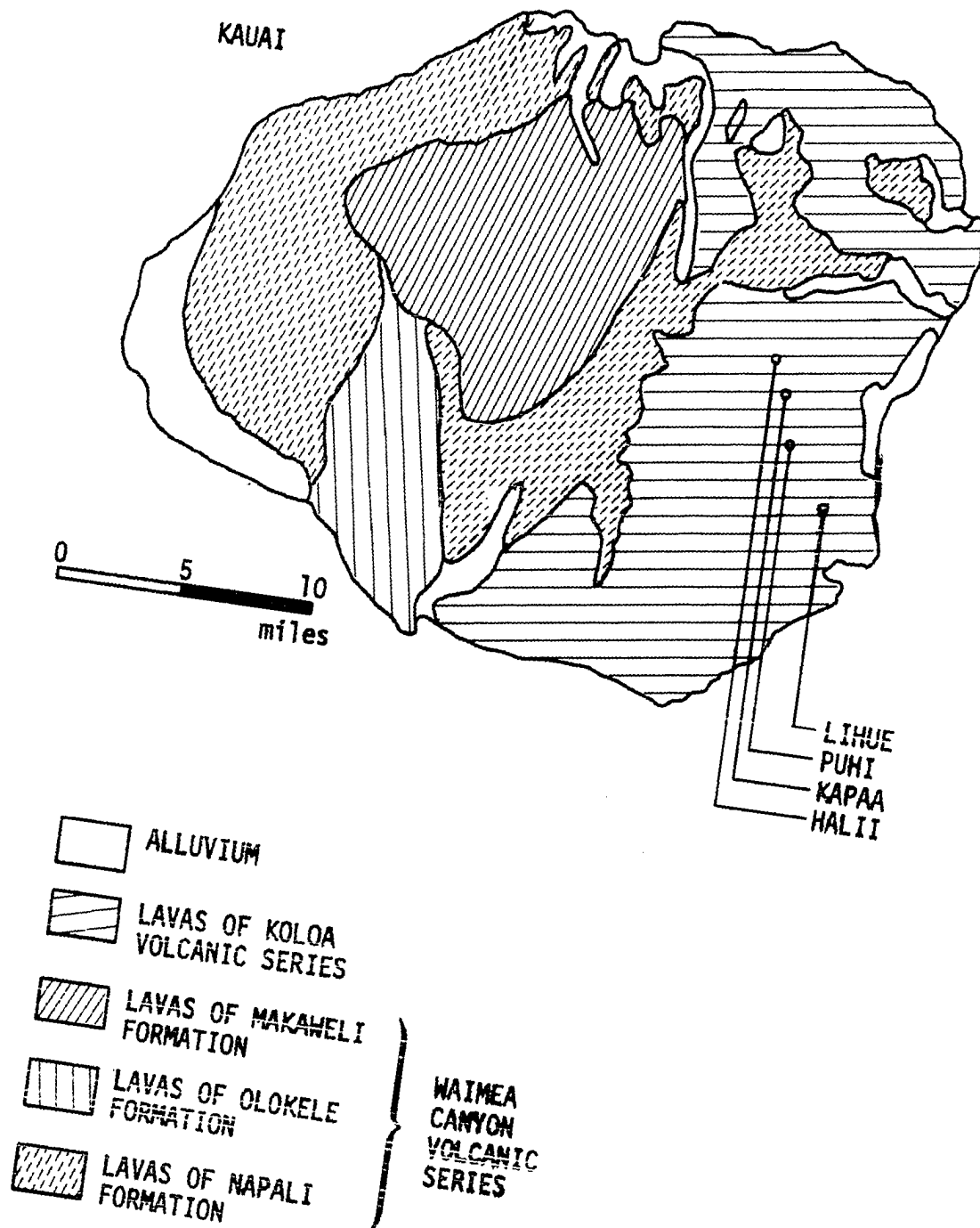


Figure 2. Generalized geologic map of Kauai, Hawaii, showing location of soil sampling sites

Table 1. Environmental factors and USDA classification of selected Hawaiian soils

Soil series	Location	Rainfall cm/yr	Slope %	Pedologic classification	Order	Great soil group (1938 classification)
Molokai	Oahu	57	2-6	Typic torrox	Oxisol	Low-humic latosol
Lahaina	Oahu	70	2-6	Typic torrox	Oxisol	Low-humic latosol
Wahiawa	Oahu	127	0-3	Tropeptic eustrtox	Oxisol	Low-humic latosol
Manana	Oahu	127	6-12	Orthoxic tropohumults	Ultisol	Humic ferruginous latosol
Paaloa	Oahu	203	3-8	Humoxic tropohumults	Ultisol	Humic latosol
Lihue	Kauai	127	0-8	Tropeptic eustrtox	Oxisol	Low-humic latosol
Puhi	Kauai	178	3-8	Typic umbriorthox	Oxisol	Humic ferruginous latosol
Kapaa	Kauai	254	3-8	Typic gibbsihumox	Oxisol	Humic ferruginous latosol
Halii	Kauai	381	3-8	Typic gibbsihumox	Oxisol	Humic ferruginous latosol

When the samples arrived at the laboratory, the sealed Shelby tubes were removed from wooden crates and stored in a 100 percent relative humidity, in order to prevent any moisture loss during storage.

Laboratory Testing and Results

Bulk measurements and determination of index properties

Although it was stated earlier that standard engineering index tests are not adequate to accurately predict the field behavior of lateritic soils, they were performed for the completeness, and for any possible correlation that may show up in the analysis.

Wet densities were determined by bulk measurements, that is, by obtaining weight and bulk dimensions of the undisturbed, cylindrical soil samples. Moisture contents were calculated on oven dry weight basis and used together with wet densities to compute dry densities.

In the determination of specific gravities, Atterberg limits, and grain size distributions, the samples were prepared by mixing the trimmings from thin-walled tube samples obtained from various depths within the B-horizon, and then, the mixture was quartered with a sample splitter and used for testing. That way, it was attempted to analyze material that is representative of the B-horizon. In this thesis, the samples so prepared will be referred to as composite samples. All of these common soil tests were conducted in accordance with the standard AASHTO procedures (4).

Porosity and void ratio values were calculated by using dry densities and specific gravities.

Figures 3 and 4 show the grain size distribution curves of the soils from Oahu and Kauai, respectively. Table 2 and 3 summarize the results of the standard laboratory tests.

In pore size analysis which will be discussed in one of the coming sections, it was observed that Puhi and Halii soil series are not consistent within themselves. Puhi gives different characteristic pore size distribution curves for samples from shallow and deep depths, and Halii has different curves for soil matrix and concretions it contains. So, each of these two soil series was treated as being two different soils and whenever it was possible the other soil properties of each were determined separately. Table 2 is an example of this.

Mineralogical analysis

Qualitative mineralogical analysis In the first step of mineralogical analysis, minerals which are present in the composite samples of each soil series were identified qualitatively. X-ray diffraction and differential thermal analysis were utilized for this purpose.

A GE-XRD-5 spectrogoniometer was used in all X-ray work. Composite samples for X-ray diffraction were prepared by first oven drying the soils and then sieving them through a No. 200 sieve. Either copper-K α or molybdenum-K α radiation was used. Besides oven drying, each soil was subjected to glycol and heat treatments and the effects of these treatments on the X-ray patterns were observed (15).

Analysis of the X-ray patterns exhibited that kaolinite and gibbsite are the main clay minerals present. Hematite is the most abundant iron

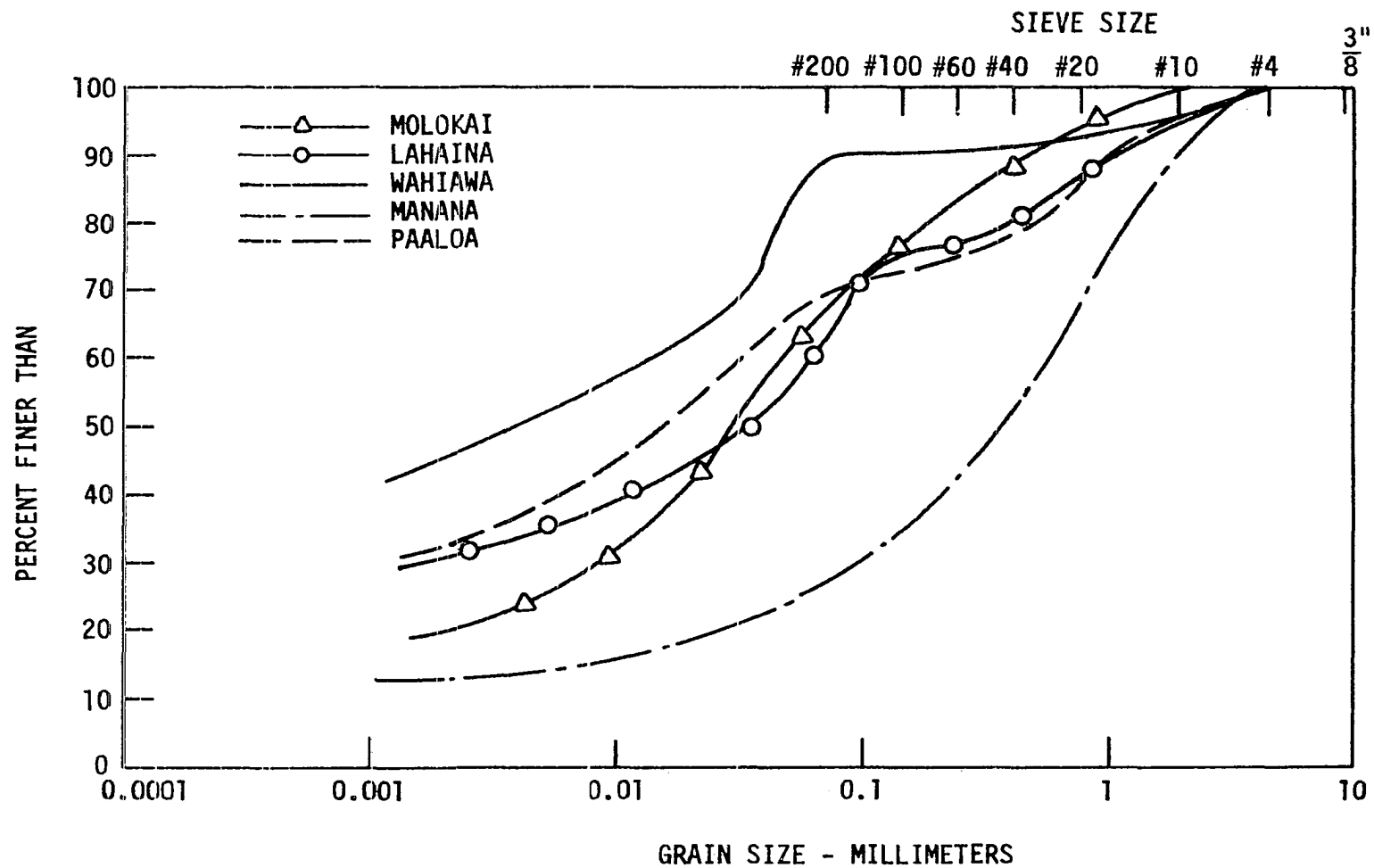


Figure 3. Grain size distribution curves for soils from the island of Oahu, Hawaii

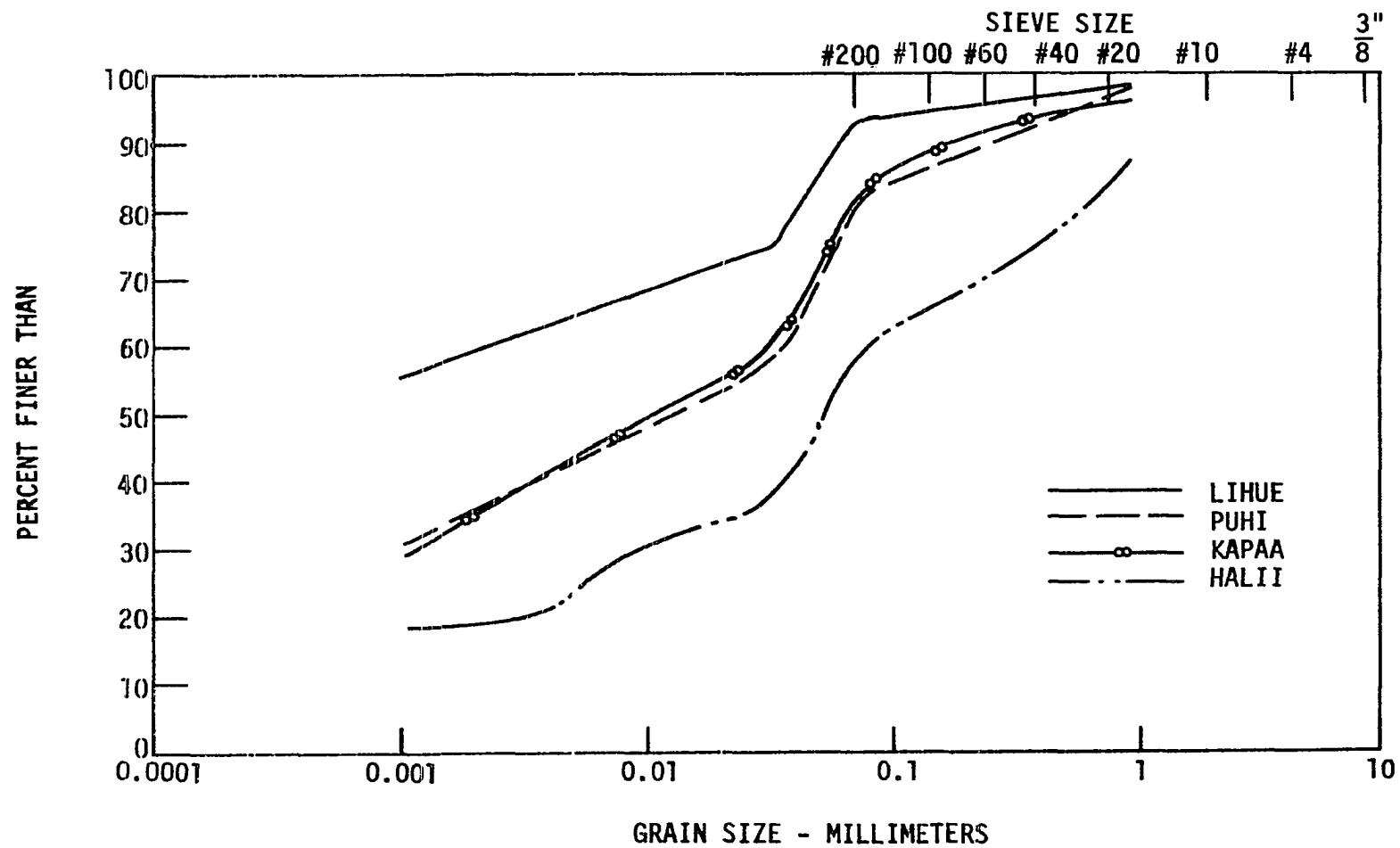


Figure 4. Grain size distribution curves for soils from the island of Kauai, Hawaii

Table 2. Some engineering properties of selected Hawaiian soils

Soil series	Depth cm	Moisture content %	Hygroscopic moisture content ^a %	Dry density gm/cc	Specific gravity	Void ratio
Molokai	43-137	23.03	3.77	1.41	2.946	1.088
Lahaina	48-122	22.82	3.10	1.35	2.937	1.174
Wahiawa	30-104	27.28	3.50	1.48	2.989	1.020
Manana	25-124	33.85	4.20	1.40	2.991	1.137
Paaloa	38-135	39.56	3.46	1.32	3.098	1.347
Lihue	25-147	35.54	2.20	1.33	3.112	1.342
Puhi	61-177	41.33	7.57	1.29	3.326	1.577
(shallow)	61-114	43.09	9.62	1.26	3.297	1.660
(deep)	114-177	39.14	5.51	1.34	3.351	1.463
Kapaa	38-159	45.79	1.99	1.17	3.395	1.899
Halii	27-155	43.74	4.19	1.23	3.391	1.755
(soil matrix)	27-155	52.53	4.94	1.17 ^b	3.493	1.905 ^b
(concretion)	27-155	24.77	3.43	1.66 ^b	2.985	0.802 ^b

^aDetermined for powder samples which are sieved through No. 200 sieve.

^bDetermined from mercury porosimetry data.

Table 3. Physical properties of selected Hawaiian soils

Soil series	Sand (2.0-0.06 mm) %	Silt (0.06-0.002 mm) %	Clay (<0.002 mm) %	Liquid limit	Plastic limit	Shrinkage limit	Plasticity index	Activity
Molokai	28.7	51.0	20.3	45.5	38.7	24.6	6.8	0.33
Lahaina	31.0	38.7	30.3	49.1	38.5	32.6	10.6	0.35
Wahiawa	10.7	45.5	43.8	51.3	36.0	26.0	15.3	0.35
Manana	69.3	16.7	14.0	67.1	50.4	39.1	16.7	1.19
Paaloa	27.8	39.2	33.0	57.1	39.3	23.8	17.8	0.54
Lihue	12.4	28.8	58.8	72.6	54.9	34.2	17.7	0.30
Puhi	24.5	39.9	35.6	44.0	40.3	36.2	3.7	0.10
Kapaa	24.0	41.7	34.3	52.0	42.0	31.0	10.0	0.29
Halii	45.1	34.4	20.5	40.0	35.4	29.8	4.6	0.22

compound detected. Goethite and magnetite are the other iron compounds occurring in these soils in smaller amounts.

Differential thermal analysis (DTA) was conducted by making use of a Rigaku Thermal Analyzer. Composite samples of each soil series, oven dried and sieved through a No. 200 sieve, were tested over a temperature range of 20-1000°C. The DTA curves were compared with the standard curves given in the literature (41,63), to identify unknown minerals which are present in the samples. Kaolinite and gibbsite minerals were identified readily by this technique. Hematite, on the other hand, does not have any particular reaction within the temperature range covered, so it was not included in DTA study.

Quantitative mineralogical analysis In this part of the study, the main concern was to determine the contents of predominant minerals which occur in these soils, i.e., kaolinite, gibbsite, and iron oxides.

The determination of kaolinite and gibbsite contents of the soils was achieved by making use of thermal gravimetric analysis (TGA) together with differential thermal analysis. The method used is as follows: First, a sample, which contains only the pure mineral in question, is prepared with a known weight, approximately 40 milligrams, and the weight loss corresponding to the most characteristic reaction of the mineral determined. Then, the weight loss corresponding to the same reaction is obtained for the natural sample having the same weight as the pure mineral sample. Direct proportioning of these weight loss values gives the fraction of the mineral to be determined in the unknown sample (77).

The kaolinite and gibbsite contents determined by this technique are listed in Table 4 which summarizes all the mineralogical and chemical analyses results.

Hematite, which commonly occurs in all the soils, was determined quantitatively by X-ray diffraction. For this purpose, a quantitative X-ray diffraction method, which is applicable for the determination of any soil mineral, was developed. The theory and the application of the method are given below.

The basis of the proposed method is the comparison of X-ray diffraction peak intensities of the mineral in the sample with the intensities of the same peak in specimens which are a mixture of the original soil sample and known additional amounts of the mineral in question, that is, the component to be determined is used as an internal standard.

Norrish and Taylor (48) expanded upon the ideas of Klug and Alexander (34) to demonstrate that the measured intensity of an X-ray diffraction peak of a crystalline component in a sample is related to the weight fraction of that component in the sample by the equation:

$$I_0 = \frac{Kx}{\rho A_s} \quad (\text{Eq. 1})$$

where I_0 is the measured intensity of the diffraction peak of a crystalline component in a soil sample, ρ is the true density of the component used to make the diffraction pattern, x is the weight fraction of the component being estimated, K is a constant for any particular peak of a particular component, and A_s is the mass absorption coefficient of the sample. Norrish and Taylor state that the use of this equation without

Table 4. Mineralogical and chemical analyses results

Soil series	Kaolinite content ^a %	Gibbsite content ^a %	Hematite content ^b %	Total iron content		Total Fe ₂ O ₃ content ^c %	Organic matter mg/gm
				by X-ray fluor. %	by atomic absorption spec. %		
Molokai	52	9	12.6	11.4	13.5	16.3	4.28
Lahaina	60	9	10.3	11.9	12.7	17.0	4.14
Wahiawa	54	5	13.3	12.4	14.3	17.7	3.81
Manana	43	16	6.4	16.3	17.1	23.3	8.43
Paaloa	30	33	20.1	17.3	18.9	24.7	8.67
Lihue	51	10	3.8	14.3	14.3	20.4	8.91
Puhi	11	47	15.0	17.7	25.1	25.3	11.30
(shallow)	10	42	12.1	14.2	26.0	20.3	12.10
(deep)	13	52	8.6	19.3	24.1	27.6	10.50
Kapaa	10	48	6.6	24.8	26.5	35.4	12.12
Halii	11	53	12.1	28.1	30.4	40.1	15.40
(soil matrix)	11	52	16.2	18.6	28.5	26.6	13.21
(concretion)	0	76	13.6	19.2	32.2	27.4	17.58

^aBy thermal gravimetric analysis.

^bBy X-ray diffraction.

^cFrom X-ray fluorescence.

internal standards is difficult because the mass absorption coefficients of the standard mixtures vary as the amount of known mineral content changes in the specimen. The derivation here takes this variable into account but assumes that the ratio of K/ρ will remain constant so long as the crystalline structure of the standard component which is added to the soil sample is essentially the same as that of the component which occurs in the soil sample.

Equation 1 can be written as

$$I_o = \frac{Kx}{\rho(xA_m + x_2A_2 + x_3A_3 + \dots)}$$

where A_m is the mass absorption coefficient of the component being measured, A_2 , A_3 , etc. are the mass absorption coefficients of the other minerals in the soil, and x_2 , x_3 , etc. are the weight fractions of those other minerals. The true mass absorption coefficient of the sample consisting of components exclusive of the one being measured is A_i . These minerals exclusive of the one being estimated will be referred to as the "matrix minerals." The true mass absorption coefficient of the matrix minerals is given by the equation:

$$A_i = \frac{x_2}{1-x} A_2 + \frac{x_3}{1-x} A_3 + \dots$$

therefore

$$A_i = \frac{1}{1-x} (x_2A_2 + x_3A_3 + \dots)$$

the term $x_2A_2 + x_3A_3 + \dots$ can be called the apparent mass absorption coefficient of the matrix minerals, \bar{A}_i . Therefore,

$$I_o = \frac{Kx}{\rho(xA_m + \bar{A}_i)} \quad (\text{Eq. 2})$$

If a known quantity of the component being estimated is added to the sample, this mixture can be referred to as a specimen. Let c be the known added weight fraction of the component in the specimen, and X is the composite or total weight fraction of the component in the specimen. The weight fraction of the sample in the specimen is $1 - c$ and the unknown weight fraction of the component in the specimen is $(1-c)x$. Therefore, the total weight fraction of the component in the specimen is: $X = (1-c)x + c$. And the peak intensity produced by the total amount of the component in the specimen is:

$$I_c = \frac{KX}{\rho A_c} = \frac{K[(1-c)x + c]}{\rho A_c} \quad (\text{Eq. 3})$$

where I_c is the peak intensity and A_c is the complete mass absorption coefficient of the specimen. The mass absorption in terms of the total and added weight fractions in the specimen is:

$$A_c = XA_m + (1-c)x_2A_2 + (1-c)x_3A_3 + \dots$$

which can also be written in terms of the unknown weight fraction of the component in the sample:

$$A_c = [(1-c)x + c]A_m + (1-c)[x_2A_2 + x_3A_3 + \dots]$$

The value of the apparent mass absorption coefficient of the matrix minerals can be substituted into the above equation to give:

$$A_c = [(1-c)x + c]A_m + (1-c) \bar{A}_i \quad (\text{Eq. 4})$$

Substitution of Equation 4 into Equation 3 gives:

$$I_c = \frac{K[(1-c)x + c]}{\rho \{[(1-c)x + c]A_m + (1-c) \bar{A}_i\}}$$

The ratio of the peak intensities produced by the sample and the specimen is:

$$\frac{I_c}{I_o} = \frac{[(1-c)x + c][xA_m + \bar{A}_i]}{\{[(1-c)x + c]A_m + (1-c)\bar{A}_i\}x}$$

which can be written as:

$$\frac{I_c}{I_o} = \frac{\frac{A_m}{\bar{A}_i} + \frac{1}{x}}{\frac{A_m}{\bar{A}_i} + \frac{1-c}{(1-c)x + c}} \quad (\text{Eq. 5})$$

If

$$\frac{A_m}{\bar{A}_i} = A$$

and this term is substituted into Equation 5 then by adding and subtracting 1 the equation becomes:

$$\frac{I_c}{I_o} = \frac{c/x}{Ax - Acx + Ac + 1 - c} + 1 \quad (\text{Eq. 6})$$

Let $\frac{I_c}{I_o} - 1 = 1$ and substitute it into Equation 6 to give:

$$\frac{c}{I} = Ax^2 - Acx^2 + Acx + x - cx$$

grouping terms:

$$\frac{c}{I} = c[Ax - x(Ax+1)] + x(Ax+1) \quad (\text{Eq. 7})$$

Let $m = [Ax - x(Ax+1)]$ and $n = x(Ax+1)$. Equation 7 becomes a linear equation:

$$\frac{c}{I} = mc + n \quad (\text{Eq. 8})$$

such that if the concentration of the component added to the sample divided by the intensity ratio minus one is plotted versus the concentration of the component added to the sample for various concentrations, then a straight line should result with a slope of m and an intercept of n . From these experimentally determined values it is possible to compute x , the unknown amount of the component in the soil sample. The values of m and n give two equations with two unknowns, x and A . By eliminating A , x can be related to m and n in the following manner:

$$x = \frac{n}{m + n + 1} \quad (\text{Eq. 9})$$

It is also possible to compute experimentally the ratio of the mass absorption coefficient of the mineral A_m to the mass absorption coefficient of the matrix minerals.

In order to evaluate the reliability of this method an "artificial soil" was prepared containing 5% hematite ground from a naturally occurring hematite and 95% kaolinite. This "soil" sample was then mixed with additional known amounts (5, 8, 12, 15, and 20%) of a chemically pure hematite. For consistency of volume and weight percentages, specimens were compressed into rings at a constant porosity. The intensities of the 100 peaks for the sample and each specimen were measured. The intensity ratio for each specimen was computed and a plot of c/I versus c was prepared. The radiation used was molybdenum- $K\alpha$ and the 100 reflection gives a peak at the 2θ angle of 15.15 degrees. As can be seen in Figure 5, there is an overlap of the 15.15 degree peak and the next peak corresponding to both hematite and kaolinite at around 16.4 degrees. Therefore it is necessary to sketch the lower portion of both peaks to the baseline

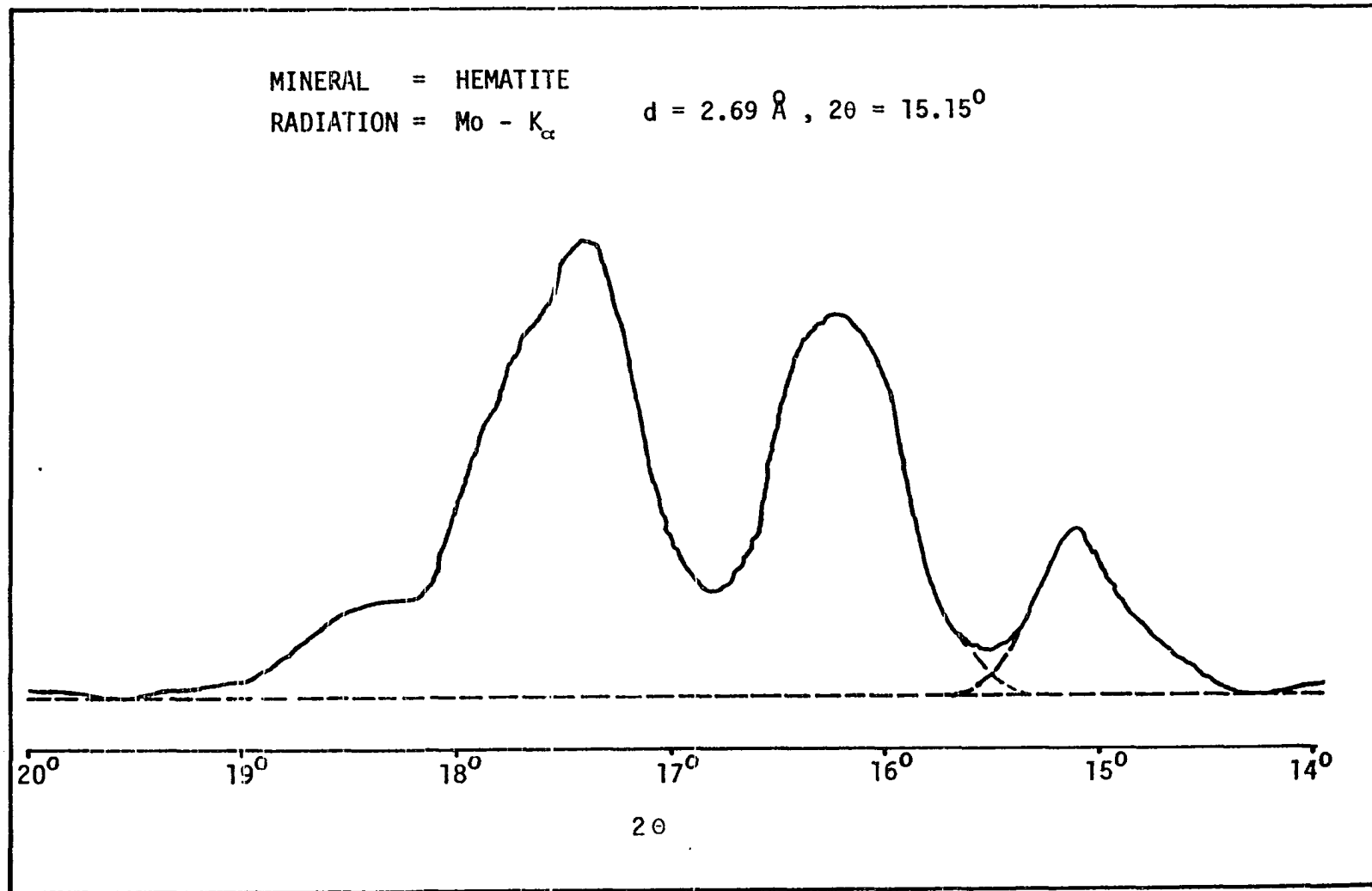


Figure 5. Example of definition of X-ray peak for intensity measurements

so that the higher intensity caused by the overlap is equal to the sum of the areas of the two tails. The baseline is determined by extending a straight line from one background level at a lower 2θ angle where there are no peaks to another low background at a higher 2θ angle. The area of the peak so defined was then measured with a planimeter.

Four separate intensity measurements were made on each specimen and the "soil" sample, then the intensity ratios were calculated using the average intensities. The values of c/I then were calculated and plotted versus c . The graph is shown in Figure 6 with the regression line and 95% confidence limits. The hematite content which was determined from m and n is 5.15% which compares favorably with the 5.00% which is in the artificial soil sample. The calculus method of error analysis (67) revealed that at the 5% significance level the range in calculated hematite contents is from 4.6% to 5.7%. Theoretical mass absorption characteristics for hematite and kaolinite were determined as 27.26 and 3.4, respectively. The theoretical value of the mixture of 5% hematite and 95% kaolinite is therefore 8.4. The mass absorption coefficient that was determined from Figure 6, and the parameters m and n , is 6.11.

Based upon the good agreement between the amount of hematite in the artificial "soil" sample and the amount of hematite estimated by the method described here, it is concluded that this method offers promise of being a reliable method for the determination of various mineral components in natural soils. The fair agreement between theoretical and experimentally determined mass absorption coefficient is taken as further evidence of the reliability of this method.

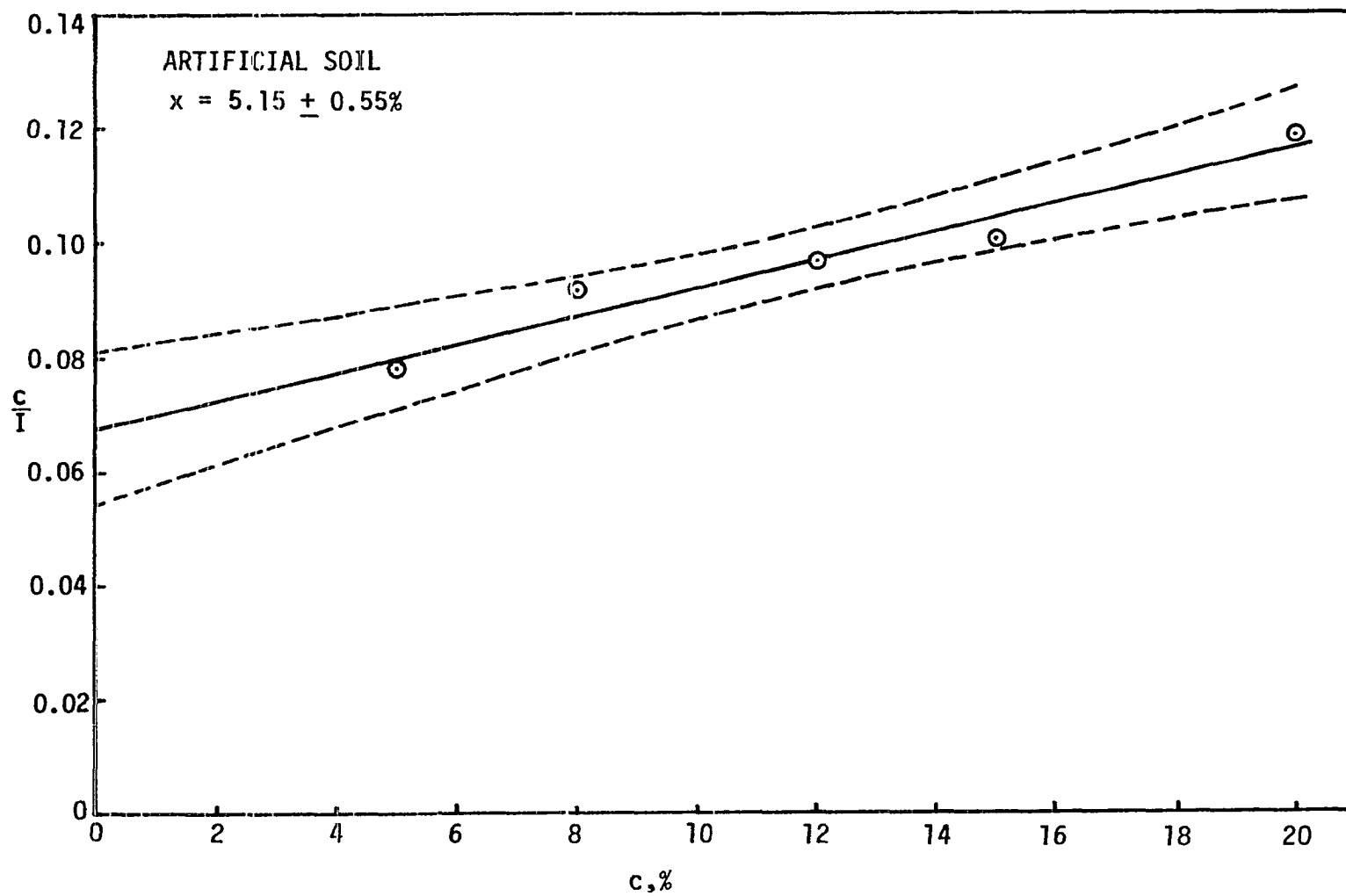


Figure 6. Average values of peak intensity resulted in this relationship of concentration to intensity ratio versus concentration of added hematite

One source of the variability in the four individual values is interpreted as arising from the judgment that goes into the definition of each peak due to the overlap of sequential peaks.

Another source of scatter in the values may be the result of variability in the time rate of X-ray photon densities due to voltage alternation. Thus on any given determination, a different population of grains in the powder will be irradiated; this will result in varying intensities for each individual determination. Rotating the sample should minimize this effect. By taking this into account, the composite samples of Hawaiian soils, subjected to this analysis, were rotated in the plane of the sample holder so as to give a better statistical sample of the crystallites being irradiated.

Application of this method for Hawaiian soils to determine the hematite contents gave the results listed in Table A1 in Appendix A. The hematite content values were then corrected for hygroscopic moisture, in order to have the contents on dry weight basis. The corrected values are listed in Table 4.

The importance of iron oxides in lateritic soils was discussed earlier. In order to get the total amount of iron oxides occurring in these soils, the most common approach utilized is to determine the amount of total iron element which is present, and accordingly to calculate total iron oxides on the basis of total iron content. To achieve this, a quantitative X-ray fluorescence analysis was developed by similar approach as presented above for the cases of determining the contents of soil minerals. The theory and the application of the method is given below.

The basis of the analysis is the comparison of X-ray fluorescent peak intensities of the element in the sample with intensities of the same element in specimens of the original sample plus known additional amounts of the element in question. In other words, the element to be determined is used as an internal standard. Although use of the element to be determined as an internal standard was suggested by many authors, a linear relationship between the intensity and the concentration of the element was assumed (12,28,1,33). This assumption is true only when the concentration of the element in the soil and the additional known amounts are rather low. Otherwise, due to the effects of absorption and enhancement the relationship between the intensity and the concentration is not linear (12,13,1,17,33,47). The method described here takes both absorption and enhancement into account and is applicable to soil samples containing high concentrations of the element in question.

For a direct quantitative analysis of a sample it is necessary to have a relation between the measured peak intensity of a particular element and its percentage in the sample. Such a relation, however, is usually governed by the matrix effects which include both absorption and enhancement as shown below, therefore a direct correlation is not possible.

Birks (12) gives a complete derivation of the equation for expected fluorescent intensity. Both absorption and enhancement are taken into consideration in that derivation. If an assumption is made that the exciting radiation is monochromatic, the following expression is obtained for intensity:

$$I_{fx} = \frac{Q_x I_{p0} \rho_x}{(\mu_p \csc \phi_p + \mu_f \csc \phi_f) \rho} [1 - e^{-(\mu_p \csc \phi_p + \mu_f \csc \phi_f) \rho l}] \quad (\text{Eq. 10})$$

where I_{fx} = expected fluorescent intensity of some characteristic line of element x

Q_x = excitation constant of element x

I_{p0} = intensity of the primary radiation

ρ_x = density of element x in the layer dl which is shown in Figure 7

ρ = density of the sample

μ_p = mass absorption coefficient of the sample for the primary radiation

μ_f = mass absorption coefficient of the sample for the fluorescent radiation

ϕ_p = angle at which primary radiation strikes the surface of the sample as shown in Figure 7

ϕ_f = angle at which fluorescent radiation emerges, as shown in Figure 7

l = the distance from the surface of the sample to the layer dl as shown in Figure 7

The expression, $(\mu_p \csc \phi_p + \mu_f \csc \phi_f)$, in the Equation 10 accounts for absorption and enhancement, which was verified experimentally by Beattie and Brissey (9).

Now, if l is allowed to go to infinity and ρ_x/ρ is expressed by x , which is the weight fraction of the element to be measured, Equation 10 becomes simply:

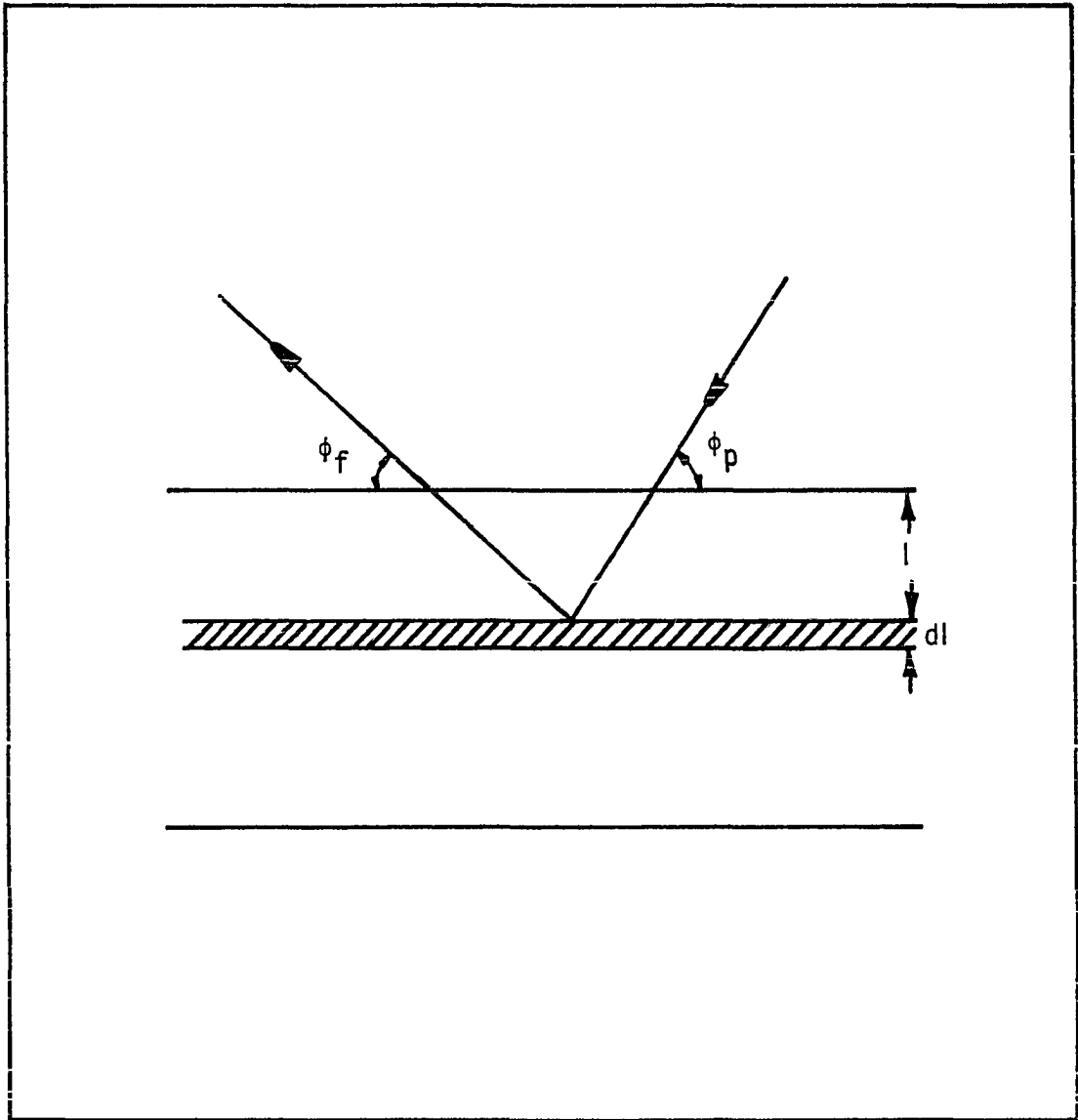


Figure 7. Primary and fluorescent radiation paths through a thick specimen

$$I_{fx} = \frac{Q_x I_{p0} x}{(\mu_p \csc \phi_p + \mu_f \csc \phi_f)} \quad (\text{Eq. 11})$$

By definition, mass absorption coefficients, μ_p and μ_f , can be expressed as:

$$\mu_p = x\mu_{xp} + (1-x)\mu_{mp} = x(\mu_{xp} - \mu_{mp}) + \mu_{mp} \quad (\text{Eq. 12})$$

$$\mu_f = x\mu_{xf} + (1-x)\mu_{mf} = x(\mu_{xf} - \mu_{mf}) + \mu_{mf} \quad (\text{Eq. 13})$$

where μ_{xp} and μ_{mp} are mass absorption coefficients of the element being determined and the matrix material for primary radiation, respectively. Parameters μ_{xf} and μ_{mf} are mass absorption coefficients of the element being determined and the matrix material for fluorescent radiation, respectively.

Substitution of Equations 12 and 13 into Equation 11 gives:

$$I_{fx} = \frac{Q_x I_{p0} x}{x[(\mu_{xp} - \mu_{mp}) \csc \phi_p + (\mu_{xf} - \mu_{mf}) \csc \phi_f] + (\mu_{mp} \csc \phi_p + \mu_{mf} \csc \phi_f)} \quad (\text{Eq. 14})$$

The terms $[(\mu_{xp} - \mu_{mp}) \csc \phi_p + (\mu_{xf} - \mu_{mf}) \csc \phi_f]$ and $(\mu_{mp} \csc \phi_p + \mu_{mf} \csc \phi_f)$ are constants, and can be designated as A and B, respectively. Therefore Equation 14 becomes:

$$I_{fx} = \frac{Q_x I_{p0} x}{Ax + B} \quad (\text{Eq. 15})$$

The matrix effects (i.e., absorption and enhancement) are accounted for in this equation by the parameters Q_x , A, and B. As it is shown by the following analysis, these effects can be eliminated by addition of known quantities of the element being determined to the sample.

When a known quantity of the element being determined is added to the sample, this mixture is referred to as the specimen. However, it is

usually more expedient to add a compound of the element rather than the pure element. Therefore, in addition to the element in question, other elements are added to the sample. Let c be the known added weight fraction of the element in the specimen and k be the weight fraction of the element in the compound added. Then, the weight fraction, c_0 , of the elements other than the element being determined can be obtained from:

$$c_0 = \frac{1-k}{k} c \quad (\text{Eq. 16})$$

Now, the weight fraction of the sample in the specimen is $(1-c-c_0)$ and the unknown weight fraction of the element in the specimen is $(1-c-c_0)x$.

Therefore, the total weight fraction of the element in the specimen is:

$$X = (1-c-c_0)x + c \quad (\text{Eq. 17})$$

Substitution of Equation 16 into Equation 17 gives:

$$X = (1 - \frac{c}{k})x + c \quad (\text{Eq. 18})$$

Obviously, the mass absorption coefficients of the specimen for primary and fluorescent radiations will be different than those of the sample.

These coefficients can be expressed in the following manner:

$$\mu_p' = X\mu_{xp} + (1 - X - \frac{1-k}{k} c)\mu_{mp} + \frac{1-k}{k} c \mu_{op}$$

or

$$\mu_p' = X(\mu_{xp} - \mu_{mp}) + c(\frac{1-k}{k} \mu_{op} - \frac{1-k}{k} \mu_{mp}) + \mu_{mp} \quad (\text{Eq. 19})$$

and

$$\mu_f' = X(\mu_{xf} - \mu_{mf}) + c(\frac{1-k}{k} \mu_{of} - \frac{1-k}{k} \mu_{mf}) + \mu_{mf} \quad (\text{Eq. 20})$$

where μ_p' and μ_f' are mass absorption coefficients of the specimen for primary and fluorescent radiations, respectively; and μ_{op} and μ_{of} are mass

absorption coefficients of the added elements other than the element being measured for primary and fluorescent radiations, respectively.

Now, fluorescent intensity, I_{fc} , produced by the total amount of the element in the specimen can be expressed as:

$$I_{fc} = \frac{Q_x I_{po} X}{(\mu_p' \csc \phi_p + \mu_f' \csc \phi_f)} \quad (\text{Eq. 21})$$

Substitution of Equations 19 and 20 into Equation 21 gives:

$$I_{fc} = \frac{Q_x I_{po} X}{AX + B + c \left[\left(\frac{1-k}{k} \right) (\mu_{op} - \mu_{mp}) \csc \phi_p + \left(\frac{1-k}{k} \right) (\mu_{of} - \mu_{mf}) \csc \phi_f \right]} \quad (\text{Eq. 22})$$

The term $\left[\left(\frac{1-k}{k} \right) (\mu_{op} - \mu_{mp}) \csc \phi_p + \left(\frac{1-k}{k} \right) (\mu_{of} - \mu_{mf}) \csc \phi_f \right]$ is a constant which can be designated as D. Thus Equation 22 takes the following form:

$$I_{fc} = \frac{Q_x I_{po} X}{AX + B + Dc} \quad (\text{Eq. 23})$$

Then, by dividing Equation 23 by Equation 15, the ratio of the peak intensities produced by the specimen and the sample can be expressed as follows:

$$\frac{I_{fc}}{I_{fx}} = \frac{X(Ax + B)}{x(Ax + B + Dc)}$$

The value of X as defined by Equation 18 can be substituted into the above equation to give:

$$\frac{I_{fc}}{I_{fx}} = \frac{\left[\left(1 - \frac{c}{k} \right) x + c \right] (Ax + B)}{x \left\{ A \left[\left(1 - \frac{c}{k} \right) x + c \right] + B + Dc \right\}}$$

or

$$\frac{I_{fc}}{I_{fx}} = \frac{Ax^2 - \frac{Ac}{k} x^2 + Acx + Bx - \frac{Bc}{k} x + Bc}{Ax^2 - \frac{Ac}{k} x^2 + Acx + Bx + Dcx}$$

By subtracting 1 from both sides of the above equation, one can obtain the following equation:

$$\frac{I_{fc}}{I_{fx}} - 1 = \frac{Bkc - Bxc - Dkxc}{Akx^2 - Ax^2c + Akxc + Bkx + Dkxc} \quad (\text{Eq. 24})$$

By letting $\frac{I_{fc}}{I_{fx}} - 1$ be equal to I and grouping the terms, Equation 24 becomes:

$$I = \frac{c(Bk - Bx - Dkx)}{c(Akx + Dkx - Ax^2) + Akx^2 + Bkx}$$

and

$$\frac{c}{I} = c \left[\frac{Akx + Dkx - Ax^2}{Bk - Bx - Dkx} \right] + \left[\frac{Akx^2 + Bkx}{Bk - Bx - Dkx} \right] \quad (\text{Eq. 25})$$

Now letting

$$m = \left[\frac{Akx + Dkx - Ax^2}{Bk - Bx - Dkx} \right]$$

and

$$n = \left[\frac{Akx^2 + Bkx}{Bk - Bx - Dkx} \right]$$

Equation 25 becomes a linear equation:

$$\frac{c}{I} = mc + n \quad (\text{Eq. 26})$$

If c, the concentration of the element added to the sample, is plotted versus c/I, a straight line will be obtained with a slope of m and an intercept of n. From these experimentally determined values it is possible to compute x, the unknown weight fraction of the element in the sample.

By adding 1 to the expression for m and then dividing it by n, all the unknown quantities are eliminated except x, and the following

equation results:

$$\frac{m + 1}{n} = \frac{k - x}{kx} \quad (\text{Eq. 27})$$

solving Equation 27 for x the following expression is obtained:

$$x = \frac{kn}{k(m+1) + n} \quad (\text{Eq. 28})$$

where, once more, m and n are experimentally determined slope and intercept, respectively, and k is the weight fraction of the element in the compound added.

In order to evaluate the reliability of this method, an "artificial soil" sample was prepared with high concentration of iron element. More precisely, it contained 40% hematite and 60% kaolinite. Since the weight fraction of iron in hematite is 0.7, the concentration of iron element in the artificial "soil" was calculated to be 28%. This "soil" sample was then mixed with additional known amounts (5, 8, 12, 15, and 20%) of a chemically pure hematite, to prepare the specimens. Steel rings 4.5 mm thick were used as sample holders to satisfy the assumption of infinite thickness of the sample, which is necessary for Equation 11. Sample holders were made large enough not to intercept the excitation radiation and were checked by blank tests. For consistency of volume and weight percentages, specimens were compressed into the rings at a constant porosity. Tungsten radiation operated at 40 kvp and 10 ma was used for excitation. The fluorescent radiation was analyzed using a flat NaCl single crystal and a gas flow tube detector (10% methane + 90% argon). The diffraction peak corresponding to the $K\alpha$ characteristic radiation of iron, which has a wavelength of 1.9373 Å, and (200) spacing of NaCl

crystal, which has a value of 2.82 \AA , was recorded on a strip chart recorder at a 2θ angle value of 40.14 degrees. Peak intensities, as shown in Figure 8, were determined by measuring the peak areas above the baseline using a planimeter.

Three separate intensity measurements were made on the artificial "soil" sample and each specimen, and the intensity ratios were calculated using the average intensities. The values of c/I were calculated and plotted versus c . The graph is shown in Figure 9 with the regression line and 95% confidence limits. Knowing the slope, m , and the intercept, n , of the resulting line, Equation 28 was used to calculate the amount of iron in the artificial "soil" sample. The result came out to be 27% which compares favorably with the 28% which is the concentration of iron in the artificial "soil" sample. The calculus method of error analysis (67) exhibited that at the 5% significance level the range in calculated iron content is from 25.5% to 28.5%.

The composite samples of each soil series were subjected to the analysis described above for the determination of total iron contents of Hawaiian soils.

Besides X-ray fluorescent analysis, replicates of each soil sample were digested in a mixture of perchloric and phosphoric acid, filtered, diluted to a known volume and analyzed for iron content with an atomic absorption spectrophotometer.

The results of X-ray fluorescent analysis are shown in Table A1 in Appendix A. These values were, again, corrected for hygroscopic moisture

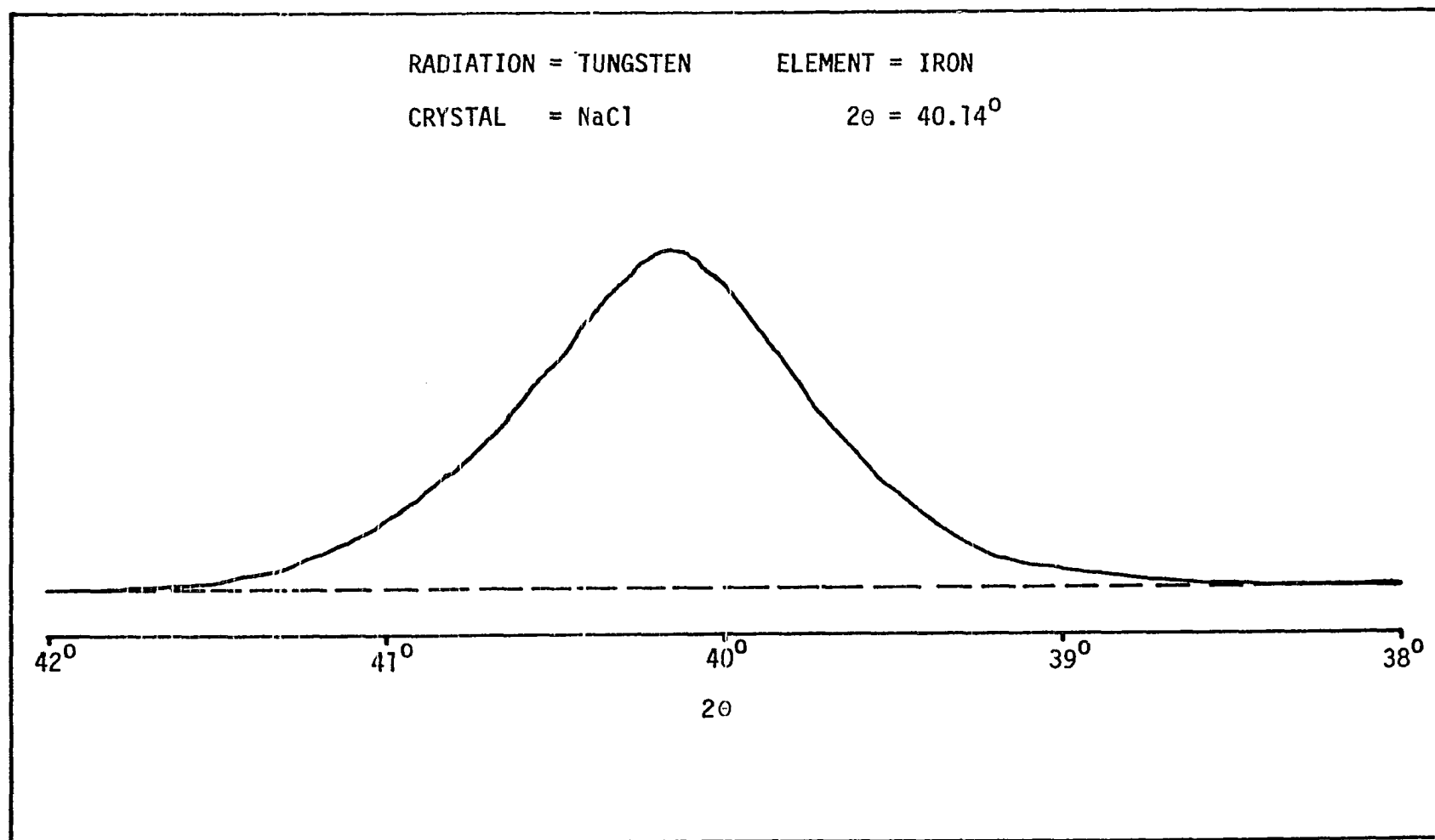


Figure 8. Diffraction peak of fluorescent radiation

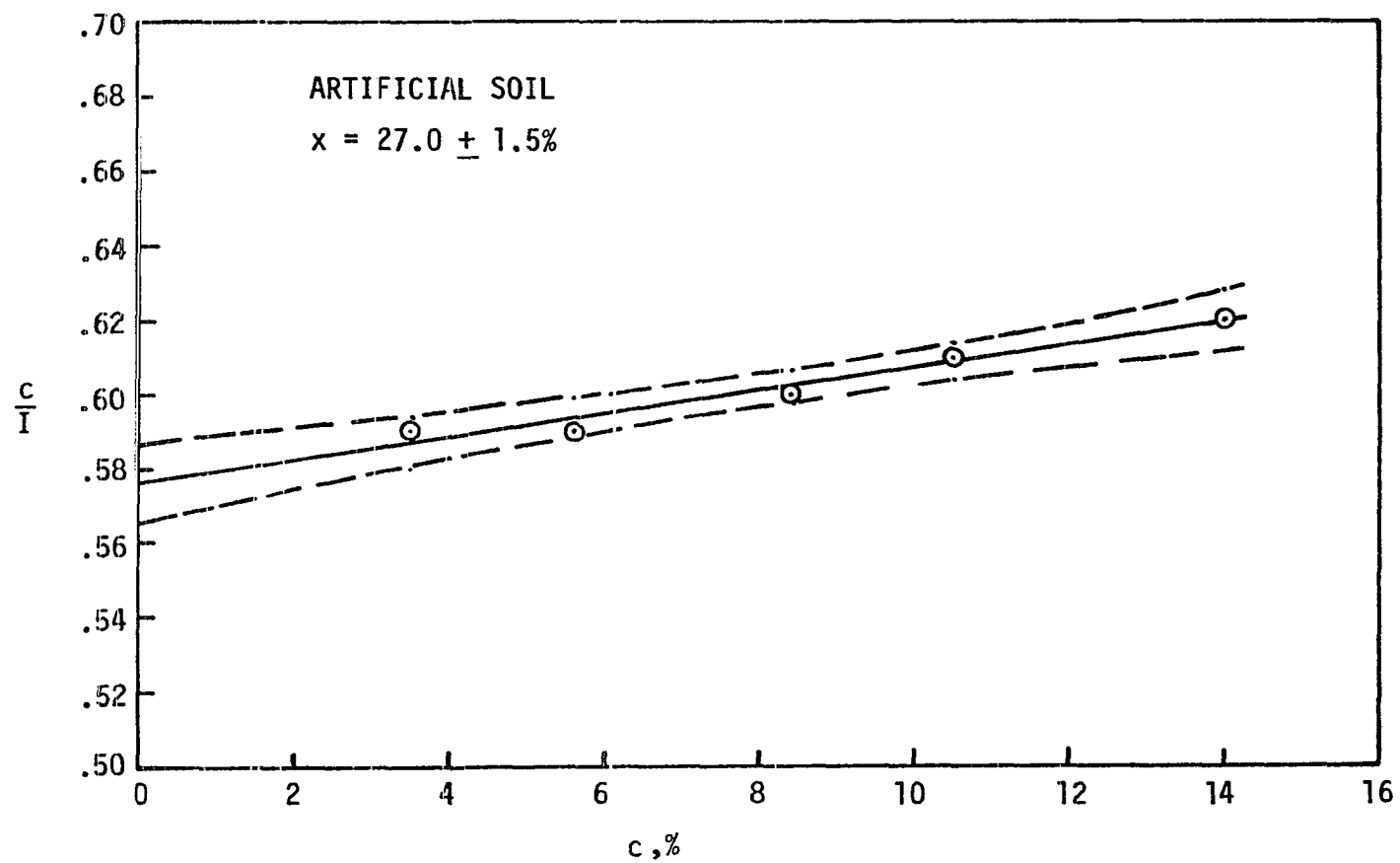


Figure 9. Experimental results of artificial soil containing 28% iron

and listed in Table 4 together with the results obtained from atomic absorption spectrophotometer.

Organic matter contents of the soils were also determined by the dichromate method and are included in Table 4.

Pore size analysis by mercury injection

The usefulness of mercury injection porosimetry to characterize the pore size distribution of soils in order to relate soil structure to engineering properties was introduced by Diamond (20). Since then several studies have been conducted satisfactorily on soils (64,6,2). The technique is based upon the Washburn (76) equation:

$$p = \frac{-2T \cos\theta}{r}$$

where P is pressure, T is surface tension, θ is angle of contact, and r is radius of pore. Prior to being placed in the sample cell of the porosimeter, the soil sample is dried. The sample cell, containing the dry soil, is then placed in the sample chamber of a mercury penetration porosimeter. The porosimeter used in this study is a Micromeritics Model 910 Mercury Penetration Porosimeter. The sample chamber is evacuated with a vacuum pump so that gas will not block the flow of mercury into the pores of the sample. Once the sample chamber is evacuated, mercury is let into the chamber filling the sample cell and immersing the soil sample. By knowing the volume of sample cell and measuring the volume of mercury which flows into the cell, it is possible to calculate the total volume of the sample. As pressure is applied, mercury penetrates the samples. Both the volume of mercury which penetrates the soil and the pressure required to cause this penetration are measured. Using these data in the Washburn

equation, it is possible to compute the radius of pore which is being penetrated at a given pressure. It is then possible to plot a pore size distribution curve.

The instrument used in this study has a pressure range from 1 psi (0.07 kg/cm^2) to 50,000 psi (3500 kg/cm^2). Using a mercury surface tension of 474 dynes per centimeter and a contact angle of 140 degrees, it is possible to measure pore radii between 105.4 micrometers and 0.00211 micrometers. This porosimeter also has the capability to empty the pores by reducing the pressure and eventually applying a vacuum at the end of the penetration phase. This allows measuring the pore size distribution on the "extrusion" cycle and from that data a characterization of the irregularity of the pores or the so-called ink bottle effect.

As it was stated earlier, prior to testing with mercury porosimeter, soil samples need to be dried, in order to remove the moisture from the pores into which the mercury will penetrate. To evaluate the influence of drying on the pore size distribution of all soil series, two or three portions of each soil from the same boring and depth were subjected to freeze drying, oven drying and/or air drying. Among those three drying techniques, freeze drying is accepted as the best, to keep the disturbance that may be caused by drying at a minimum level, if it is performed properly. The most important step in freeze drying technique is to freeze the sample rapidly enough to prevent any formation of ice crystals which cause expansion and disturbance within the sample. To achieve this, isopentane is used as suggested by Tovey and Wong (68). First, a bottle of isopentane is immersed into the liquid nitrogen and then, when the tempera-

ture of isopentane drops down to its freezing point (-160 degrees centigrade), soil sample is immersed into the isopentane and left there for at least three minutes. After that process, the sample is immediately transferred to the freeze dryer for sublimation. The samples were kept in the freeze dryer for at least 48 hours, and sublimated under a vacuum of 0.3 to 0.4 micrometer mercury pressure. The results exhibited that other than three soil series, Puhi, Kapaa, and Halii, all give practically the same pore size distribution curve for three differently dried samples, as shown in Figures B1-B6 in Appendix B.

For each series four to ten samples from various depths and borings were subjected to pore size distribution determinations. Figures B1-B10 show the range of pore size distribution curves for all the soil series. Puhi has different pore size distribution for samples from shallow and deep portions of B-horizon. Halii, on the other hand, has some concretions which give different pore size distribution compared to soil matrix. So these two soil series were investigated as if they were four separate soils. For soils other than Puhi and Halii, it was concluded that the variation in pore size characteristics within a soil series is fairly small, and an average curve was considered to represent the whole soil series.

On the other hand, when the representative pore size distribution of the various soil series are compared, there is a wide range in the curves, as shown in Figures 10-13. From these curves, once more, each of which is representative of a series, it is possible to generate a set of parameters to characterize the pore structure of each series. The parameters

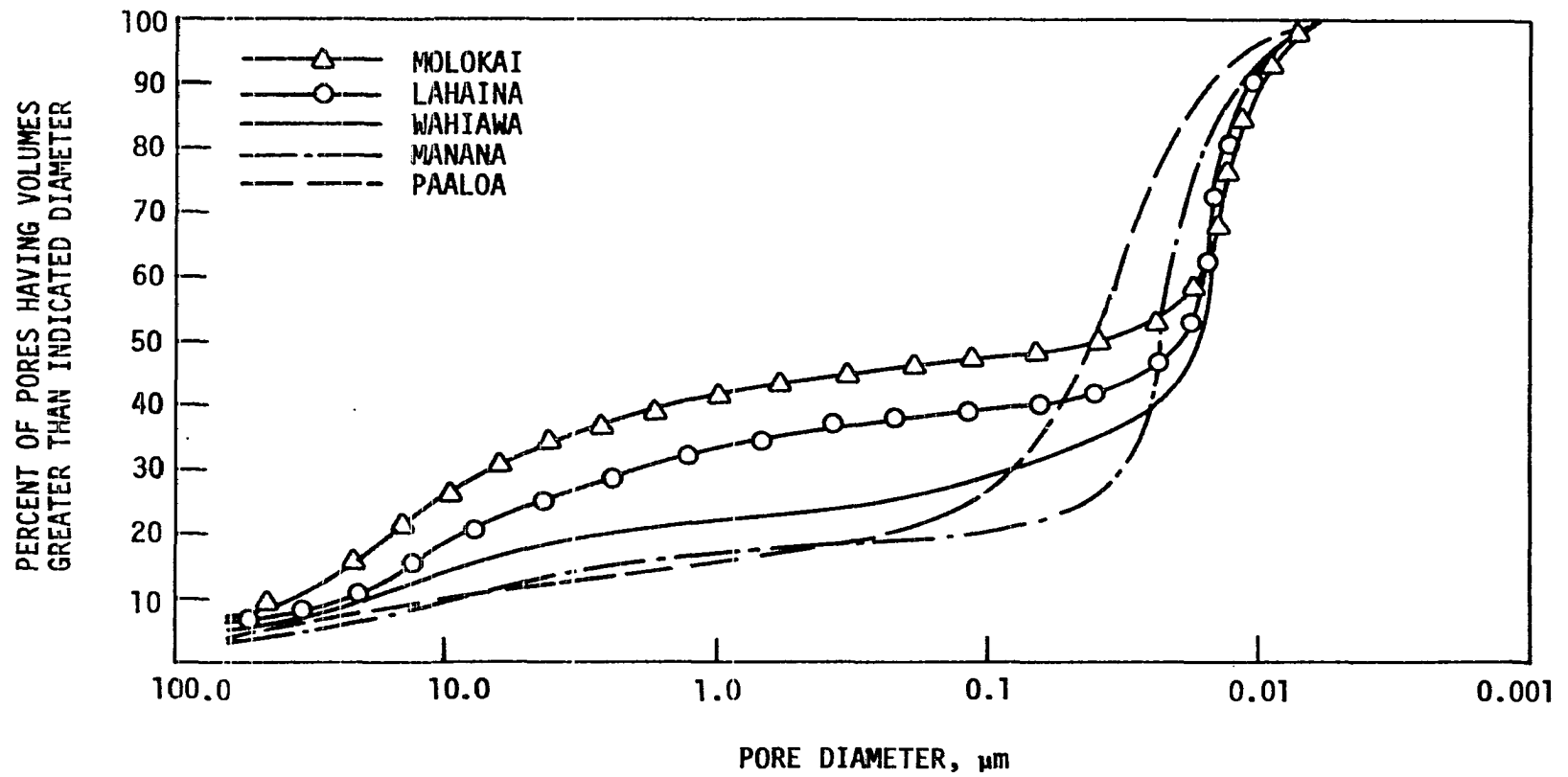


Figure 10. Cumulative plot of pore size distribution curves for the soils from the island of Oahu, Hawaii

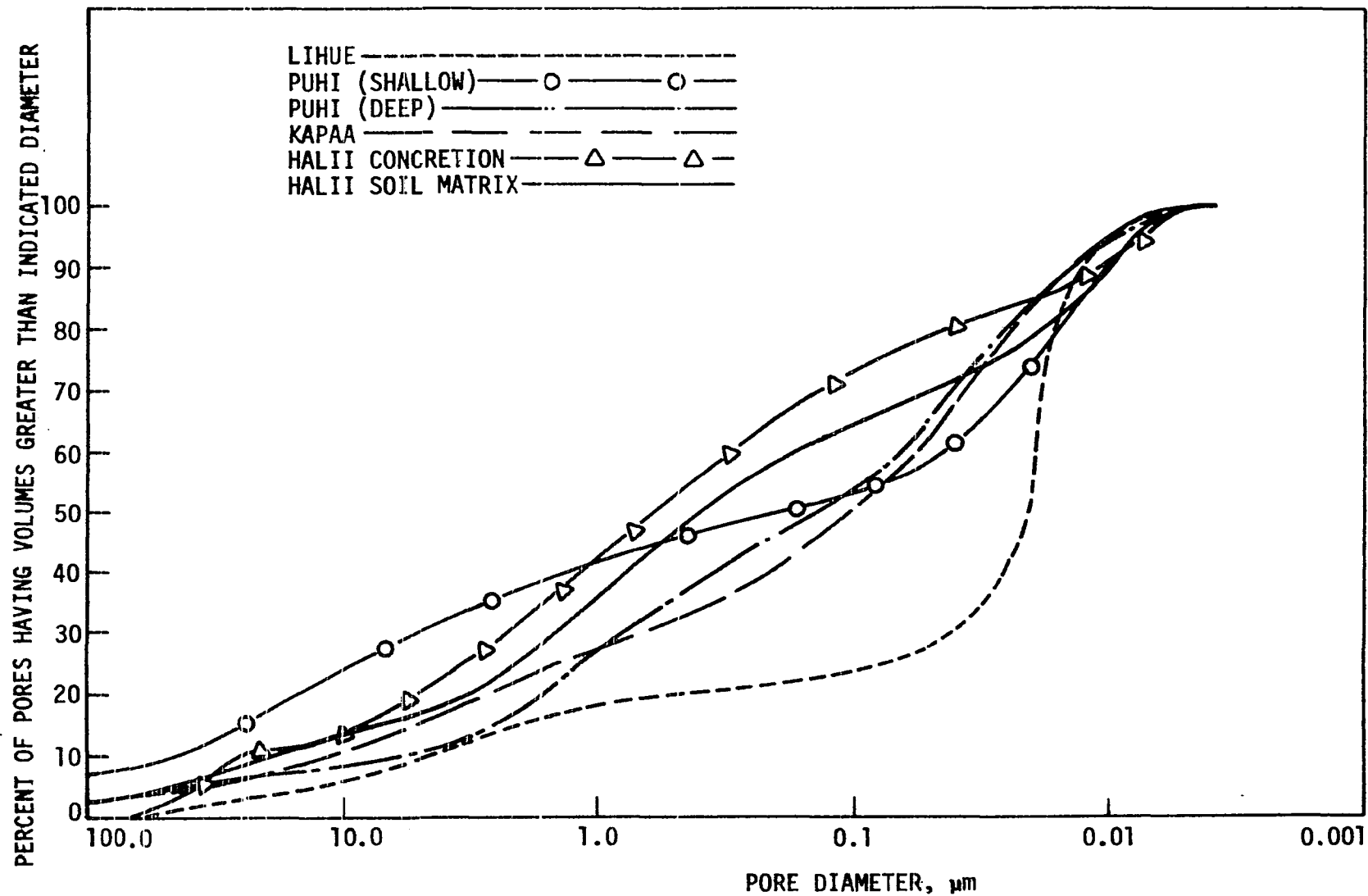


Figure 11. Cumulative plot of pore size distribution curves for the soils from the island of Kauai, Hawaii

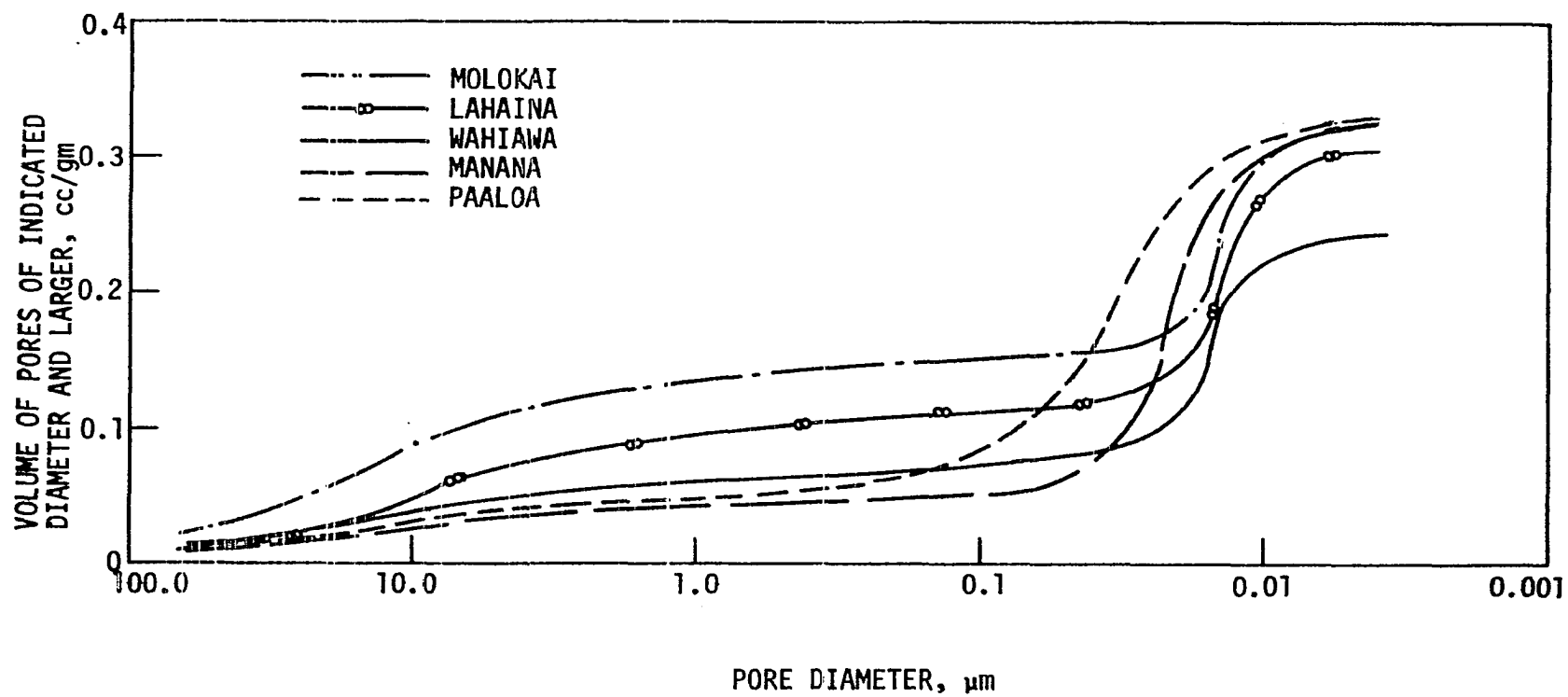


Figure 12. Cumulative plot of pore size distribution curves for the soils from the island of Kauai, Hawaii

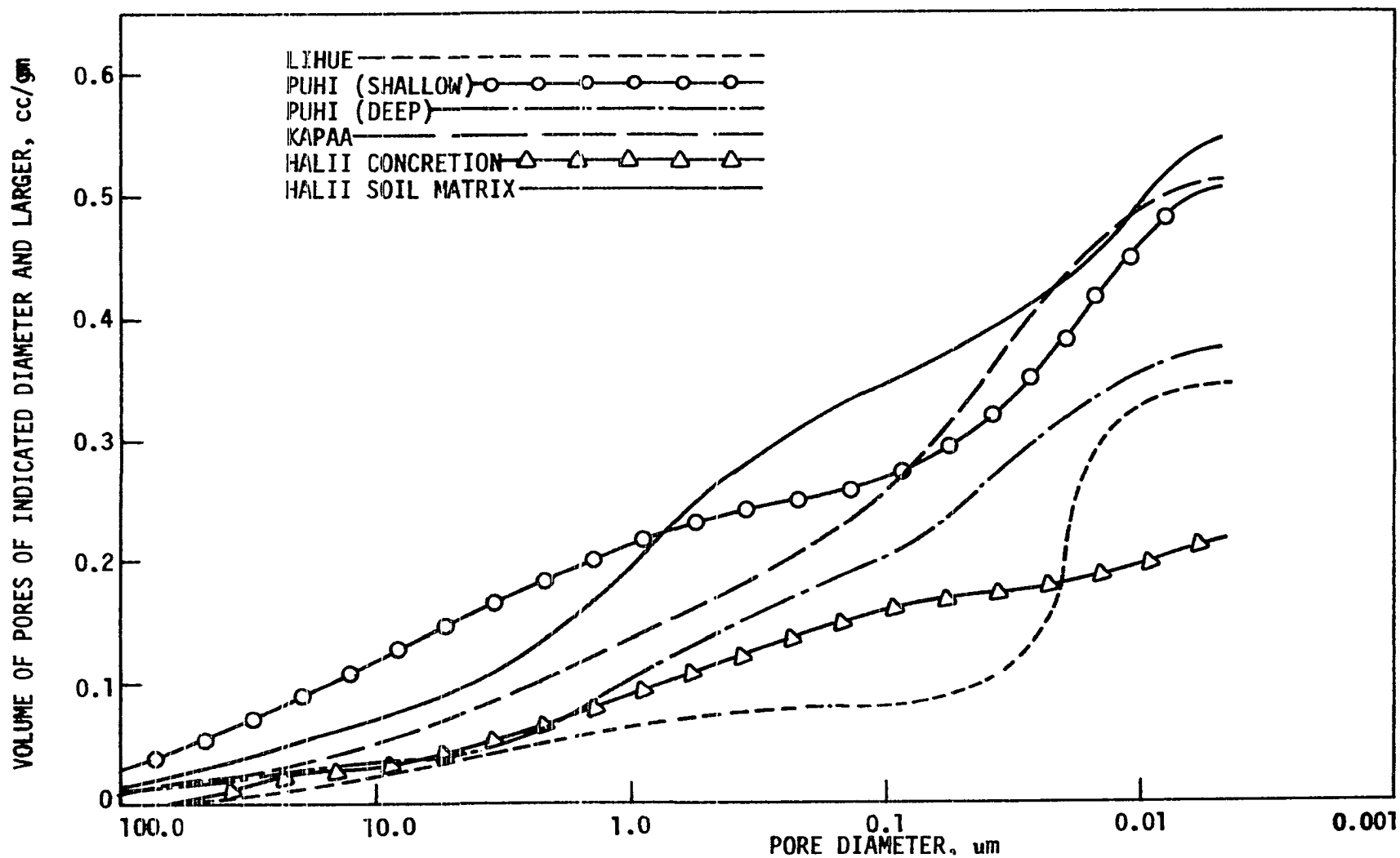


Figure 13. Cumulative plot of pore size distribution curves for the soils from the island of Kauai, Hawaii

generated are the median (50%) and small mode pore diameters, the uniformity coefficient, and the void ratios computed from the mercury injection data as well as from measurements of the bulk geometry of the Shelby tube samples and the dry weight of the samples. The uniformity coefficient is defined, in analogy with the uniformity coefficient calculated from particle size distribution curves, as the ratio of the minimum pore diameters corresponding to 40 and 80 percent of the total pore volume penetrable by mercury, respectively.

In addition to the injection curves, extrusion curves were plotted to describe the pore diameter versus volume relationship as the mercury pulled from the soil, as shown in all the figures in Appendix B. The volume of mercury which remains in the sample at the end of the evacuation is a measure of the necking down of pores. The volume of mercury retained in the soil is expressed as a percentage of the total volume of mercury injected into the sample during the pressurization cycle of the test.

Table 5 outlines all the parameters generated from mercury porosimetry results.

Scanning electron microscopy

Scanning electron microscope, a JEOL 1971 Model U3, was used for visual inspection of the pore structure and aggregate size of selected undisturbed soils. A magnification of 100 was used all through the study in order to have a large scanning area, and consequently to characterize soils better. The samples used were either oven or freeze dried, and coated with carbon and gold before they were studied with the microscope. The micrographs obtained are shown in Figures 14-16.

Table 5. Pore size parameters generated from mercury porosimetry data

Soil series	Void ratio by bulk measurement	Void ratio by Hg-injection	Percent of total pore volume intruded by Hg	Median diameter μm	Small mode pore diameter μm	Mercury retained %	Uniformity coefficient d_{40}/d_{80}
Molokai	1.088	0.960	88.5	0.037	0.015	55.2	107.9
Lahaina	1.174	0.919	78.3	0.019	0.014	47.6	5.2
Wahiawa	1.020	0.723	70.9	0.017	0.015	50.0	1.8
Manana	1.137	0.978	86.0	0.023	0.022	36.1	1.6
Paaloa	1.347	1.029	76.4	0.038	0.031	40.4	2.2
Lihue	1.342	1.075	80.1	0.021	0.020	38.6	1.6
Puhi (deep)	1.463	1.255	85.8	0.135	0.032	31.3	13.9
Puhi (shallow)	1.660	1.660	100.0	0.190	0.025	30.2	82.0
Kapaa	1.899	1.739	91.6	0.102	0.040	28.9	9.0
Halii (soil matrix)	1.905	1.902	99.8	0.380	-	25.1	41.2
Halii (concretion)	0.802	0.609	75.9	0.590	-	36.9	27.4

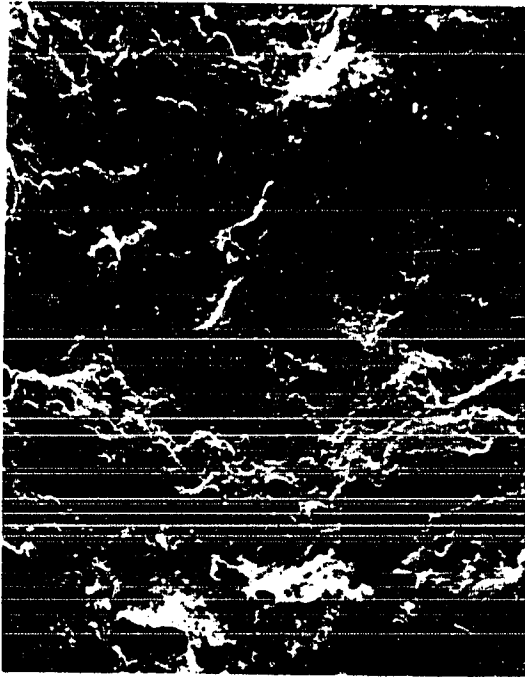


Figure 14. Wahiawa soil series

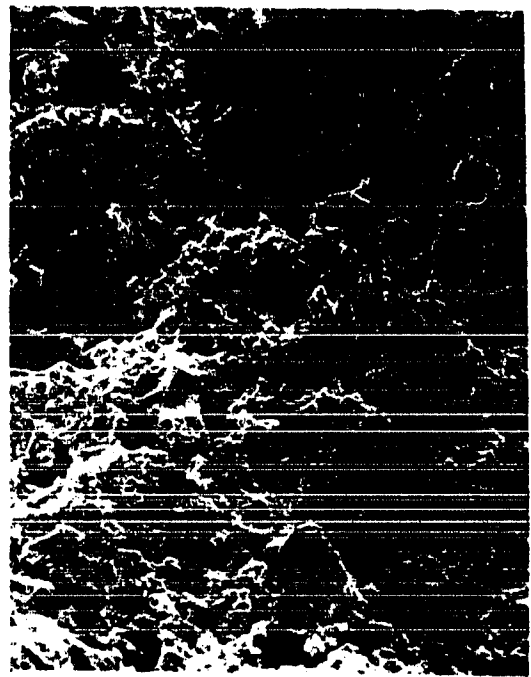


Figure 15. Lihue soil series

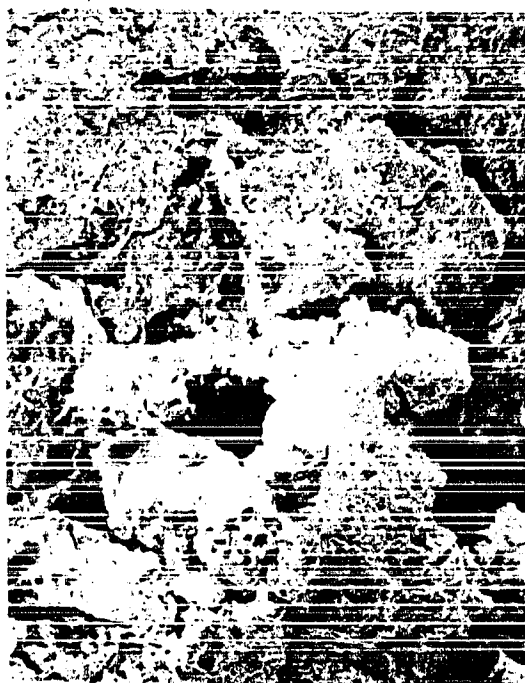



Figure 16. Halii soil series

Scale:  0.1 mm

Slaking tests

Two undisturbed samples from each soil series were subjected to slaking tests in order to measure stability and size of soil aggregates. One of the two samples of each soil series was oven dried at 105 degrees centigrade for 24 hours, before the test. The other sample was tested at its natural moisture content. Each soil sample weighing about 12 grams was immersed into the water and observed carefully for 24 hours. The rate of slaking, the amount of slaking at the end of the test, and relative sizes of the aggregates at the end of disintegration, were recorded. The results are given in Table 6.

Strength tests

Strength characteristics of the soils were analyzed by Paulson (49). Direct shear testing was used as a means of determining laboratory undisturbed soil strength. This method was considered to be the best for the purpose of characterizing several soils, with limited undisturbed samples. The method of preparation of undisturbed samples for direct shear and the method of testing are explained and discussed in detail in Paulson's thesis (49).

The strain rate utilized was 0.05 inches per minute and normal pressures used had a range of 6-210 psi. Prior to shearing, each soil sample was consolidated under a normal pressure which is equal to in situ overburden pressure. Paulson states that it is very difficult to obtain a completely drained or completely undrained condition with direct shear testing as is possible with triaxial testing. Therefore, the procedure

Table 6. Slaking test results

Soil series	Moisture condition of the sample tested	Rate of slaking	Slaking at the end of 24 hours	Relative size of aggregates
Molokai	Oven dried	Fast	Complete	Small
	Natural moisture	Fast	Complete	Small
Lahaina	Oven dried	Very fast	Complete	Small
	Natural moisture	Very fast	Complete	Small
Wahiawa	Oven dried	Fast	Complete	Small
	Natural moisture	Fast	Complete	Small
Manana	Oven dried	Slow	Complete	Large
	Natural moisture	Slow	Complete	Large
Paaloa	Oven dried	Slow	Complete	Large
	Natural moisture	Medium	Complete	Large
Lihue	Oven dried	Fast	Complete	Medium
	Natural moisture	Slow	Complete	Medium
Puhi	Oven dried	Almost zero	Some cracks	-
	Natural moisture	Very slow	Complete	Large
Kapaa	Oven dried	Almost zero	Some cracks	-
	Natural moisture	Very slow	Complete	Large
Halii	Oven dried	Zero	-	-
	Natural moisture	Almost zero	Some cracks	-

used by Paulson in the determination of strength parameters can be referred to as "consolidated-partially drained" type.

Table 7 outlines the representative strength parameters of the soils, tested undisturbed, at room temperature, and under the natural moisture conditions.

Table 7. Strength parameters of undisturbed soils

Soil series	Cohesion psi	Internal friction angle degree
Molokai	40	34
Lahaina	50	52
Wahiawa	25	27
Manana	30	57
Paaloa	22	38
Lihue	17	41
Puhi	12	52
Kapaa	10	44
Halii	7	35

ANALYSIS AND DISCUSSION OF TEST RESULTS

In this section of the thesis, the data will be analyzed, in order to evaluate the significance of degree of weathering on the engineering behavior of lateritic soils derived from basalt. Other studies, performed on basalt derived tropical soils, will be included in the analysis, to widen the spectrum and to improve the understanding of such soils from an engineering point of view.

Engineering Properties of the Soils

Specific gravity of lateritic soils appears to be a very useful parameter in relating these soils to the degree of weathering. The possibility of specific gravity as a classification parameter for predicting the engineering behavior of lateritic soils was first introduced by Lohnes and Demirel (37). As stated previously, by definition, the specific gravity of a soil sample is the weighted average of the specific gravities of the minerals which comprise the soil. The specific gravities of common rock-forming minerals and secondary minerals observed in laterites and lateritic soils are shown in Table 8. According to Alexander and Cady (3), primary feldspars are reduced to kaolinite and primary ferromagnesian minerals are converted to sesquioxides, even the kaolinite is converted to gibbsite, as weathering proceeds. Higher specific gravity indicates the presence of relatively larger amounts of high specific gravity minerals in the soil, and suggests a more weathered soil. Lohnes and Demirel (37) observed a good correlation between the specific gravity and extractable iron content of some selected Puerto Rican lateritic soils. Trow and

Table 8. Specific gravities of common minerals in lateritic soils

Primary minerals	Specific gravities	Secondary minerals	Specific gravities
Quartz	2.65	Kaolinite	2.2-2.6
Orthoclase feldspars	2.5-2.6	Gibbsite	2.4
Plagioclase feldspars	2.61-2.75	Hematite	4.9-5.3
Augite	3.3-3.6	Goethite	3.3-3.5
Hornblende	2.9-3.3		
Serpentine	2.5-2.8		

Morton (70) reported some engineering data on selected lateritic soils from the Dominican Republic, showing that the specific gravity is closely related to goethite content. The Hawaiian soils investigated in this study also exhibit a good correlation between specific gravity and total iron content, measured by X-ray fluorescence analysis, as shown in Figure 17. Therefore, it was concluded that specific gravity could be considered as a measure of degree of weathering. In the following analyses, specific gravity will be taken as a parameter reflecting the degree of weathering, and the other properties of the soils will be examined versus specific gravity, to observe whether there exists a correlation between those properties and the weathering or not.

The relationship between dry density of the soils and specific gravity is shown in Figure 18, which also includes some basalt derived soils from Puerto Rico, studied by Lohnes and Demirel (37). The relation-

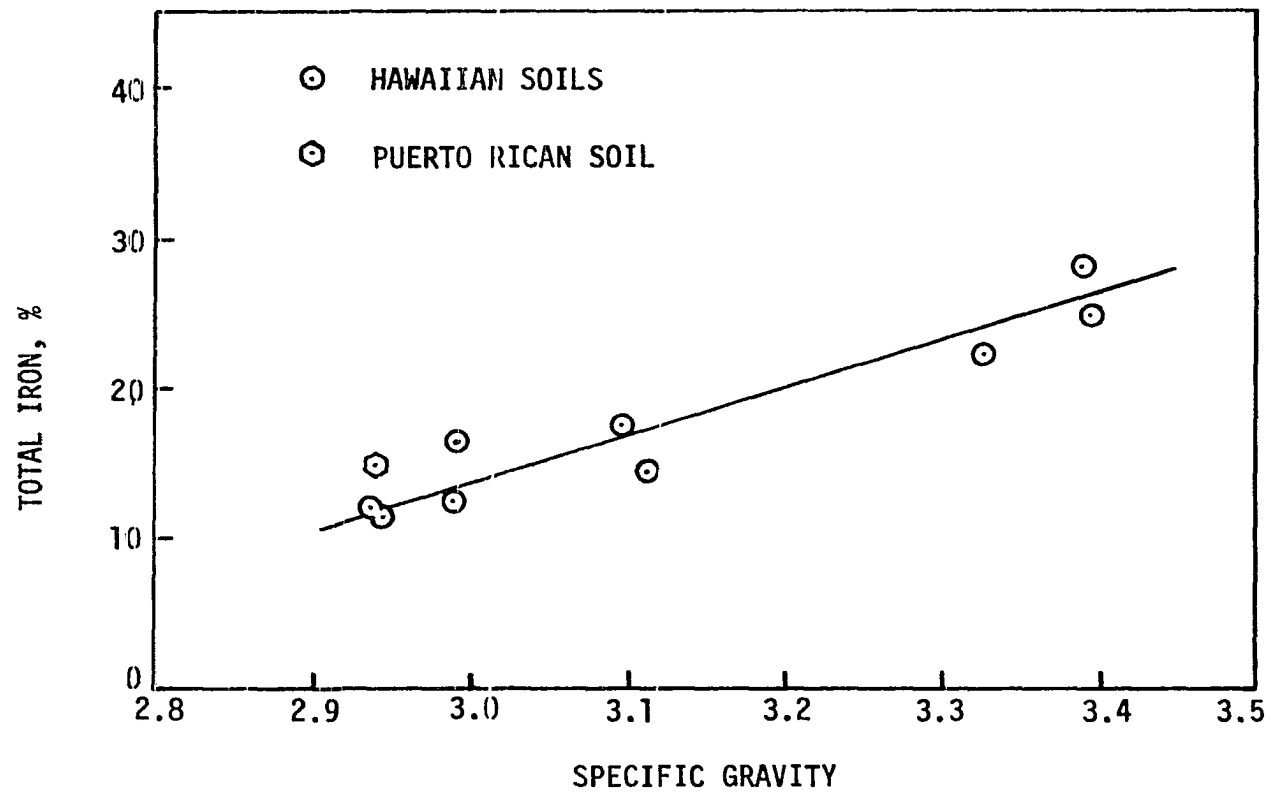


Figure 17. Relationship between total iron content and specific gravity

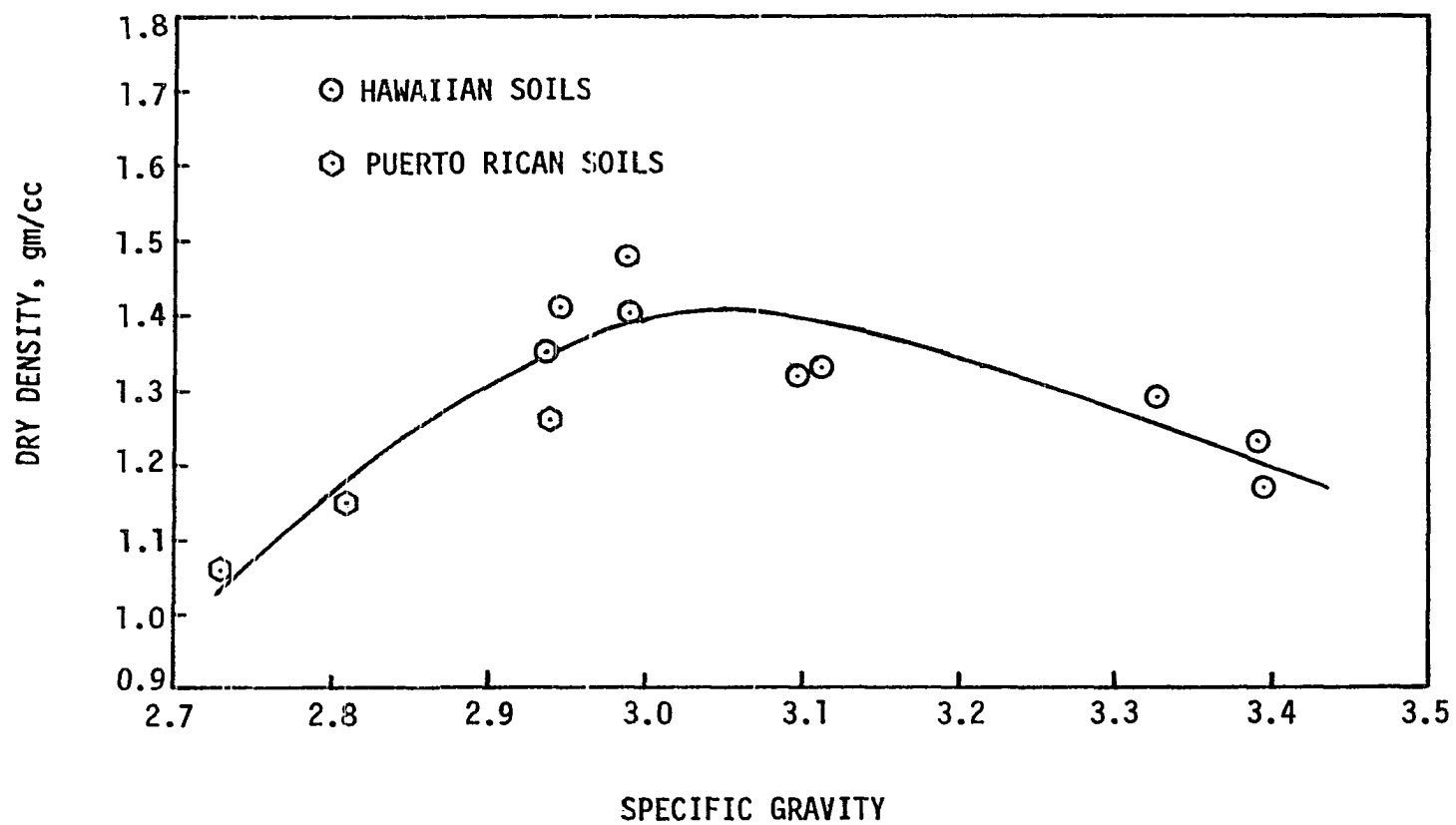


Figure 18. Relationship between dry densities and specific gravity

ship indicates that dry density increases first as specific gravity increases, and then it starts to decrease with further increasing in specific gravity. The void ratio, on the other hand, first decreases and then increases with increasing specific gravity as shown in Figure 19. These relationships of dry density and void ratio with specific gravity are interpreted as follows. In relatively less weathered soils the formation of clay minerals is the major event taking place in the course of weathering. During this stage the voids of the B-horizon are filled with the accumulation of fine clay particles, so void ratio decreases and dry density increases. Further weathering, however, causes an increase in the content of sesquioxides and diminishes the active role of clay content. At this stage, the accumulation of secondary minerals is almost over, and the sesquioxides start to play an important role within the body of the soil. Sesquioxides of iron and aluminum are known as very active binding agents to cause aggregation (40,5,8). This effect plus increasing specific gravity which means less volume of solids in the unit volume of soil, cause an increase in the void volume, and accordingly void ratio increases and dry density decreases.

The plasticity and gradation data are given in Table 3. Although, as previously noted, these data for lateritic soils have limited usefulness, attempts were made to correlate these data with the weathering and with other data obtained by measurements on undisturbed samples and mineralogical analysis. No correlations were found. All the soils show very low activities, and according to Skempton's (61) classification they are rated as inactive. Since kaolinite, which has a low activity of 0.38, is

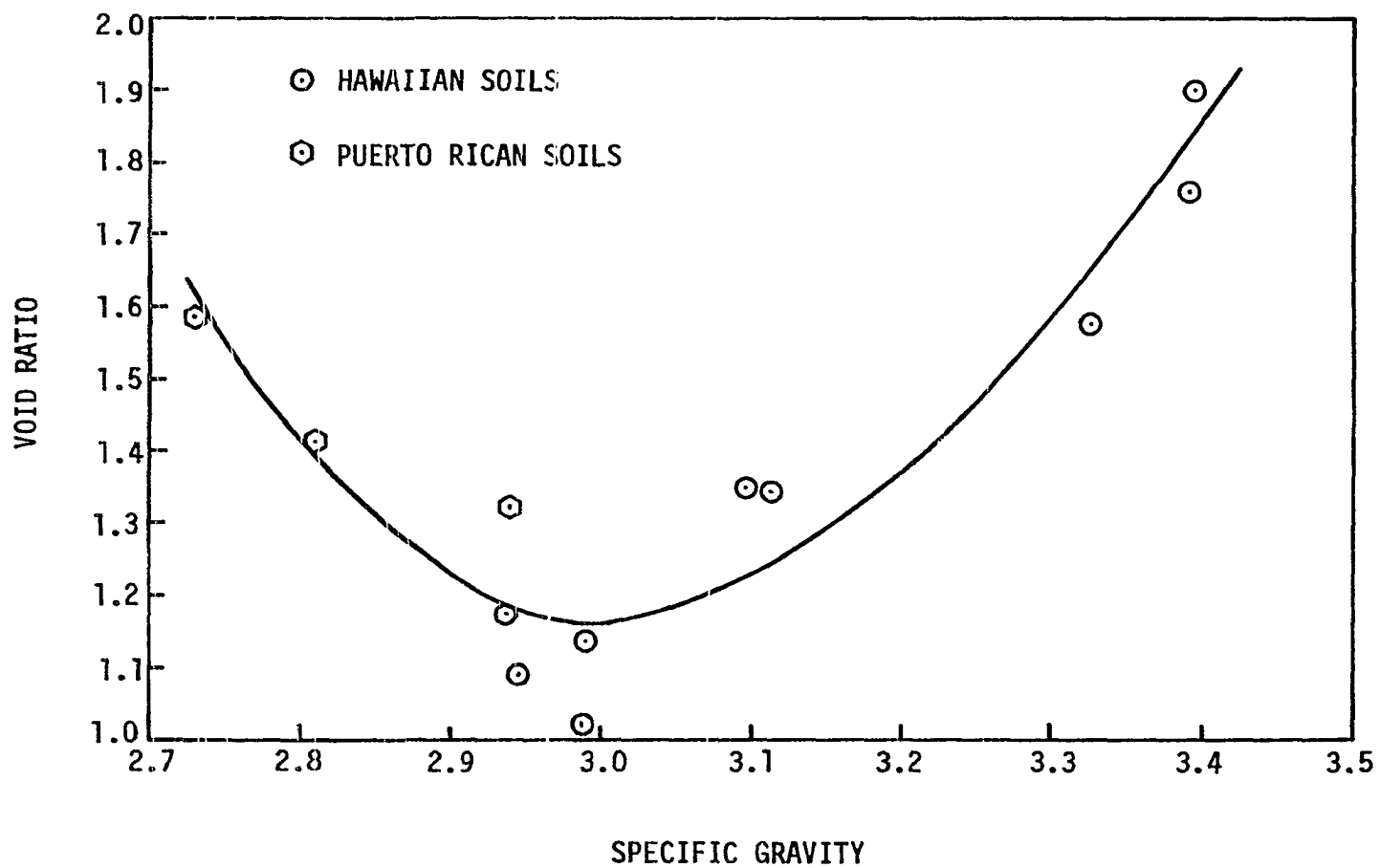


Figure 19. Relationship between void ratio and specific gravity

the main clay mineral encountered in these soils, one should not expect high activity in such soils.

These results support the idea which eliminates plasticity and gradation properties of lateritic soils in characterizing these soils from an engineering behavior point of view. As discussed previously, the inadequacy of plasticity and grain-size distribution data for the prediction of engineering behavior of lateritic soils is generally attributed to the difficulty to disperse the individual soil grains, which are cemented together by sesquioxides, prior to testing.

Mineralogical and Chemical Analyses

The predominant materials in the Hawaiian soils studied are kaolinite, gibbsite and iron oxides. Quantitative mineralogical and chemical analyses of soils were performed by making use of X-ray diffraction, X-ray fluorescence, differential thermal analysis, and thermal gravimetric analysis. The results are shown in Table 4.

If the constituents are considered in relation to weathering, it will be observed that sesquioxide content, which is obtained by gibbsite content plus total Fe_2O_3 content, increases as the degree of weathering, or specific gravity, increases as shown in Figure 20. Kaolinite, on the other hand, decreases with increased weathering. Figure 21 which also includes three basalt derived Puerto Rican soils studied by Lohnes and Demirel (37) shows the relationship between kaolinite and specific gravity. Note that the trend for Puerto Rican soils is the opposite compared

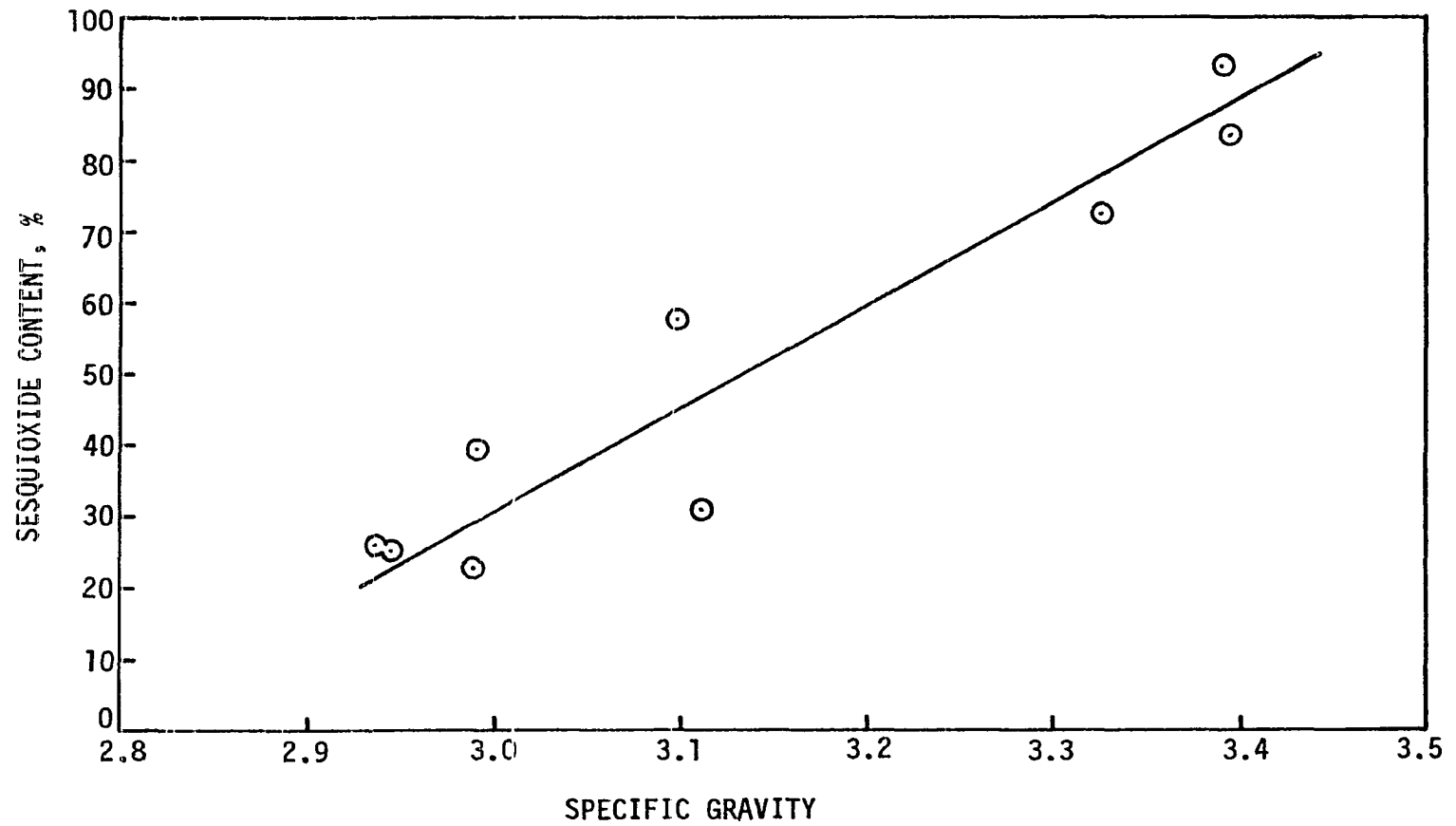


Figure 20. Relationship between sesquioxide content and specific gravity for Hawaiian soils

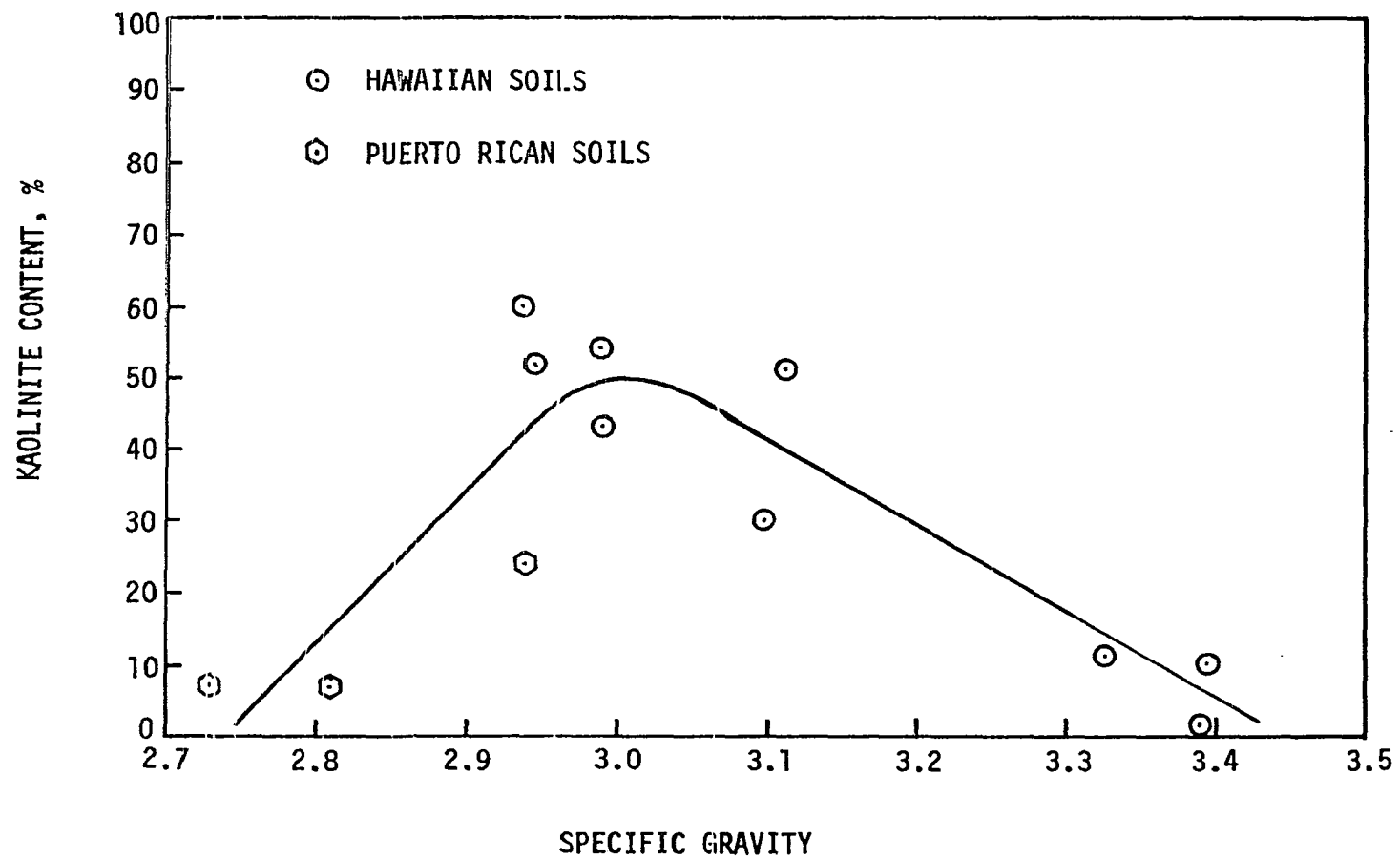


Figure 21. Relationship between kaolinite content and specific gravity

to the one of Hawaiian soils, that is, kaolinite increases with increasing specific gravity for Puerto Rican soils.

These observations agree with the model of weathering proposed by Alexander and Cady (3), and by Hamilton (27). In the early stages of weathering, the formation of clay minerals is significant, but as weathering proceeds, clay content starts to decrease, and sesquioxides of aluminum and iron constitute the major portion of the minerals. This can be shown further by plotting kaolinite content versus sesquioxide content of Hawaiian soils, as shown in Figure 22, which indicates a gradual decrease in kaolinite content while sesquioxides are increasing in amount.

As previously noted, Halii soil series which is the most weathered of all soils studied contains some concretions. Those concretions were subjected to quantitative mineralogical analysis, and it was observed that about 75% of the sample is composed of gibbsite. The rest are iron oxides as measured by total analysis. This explains the low specific gravity of concretions. On the other hand, soil matrix of Halii has lower gibbsite content and higher specific gravity.

Besides mineralogical analysis, organic matter content of each soil series was also determined and shown in Table 4. The organic matter content increases with increasing weathering as shown in Figure 23. Organic matter also is known as a binding agent in soils leading to soil aggregation. In tropical soils, however, this effect of organic matter is not that important, because mainly sesquioxides are responsible for stable aggregate formation (8).

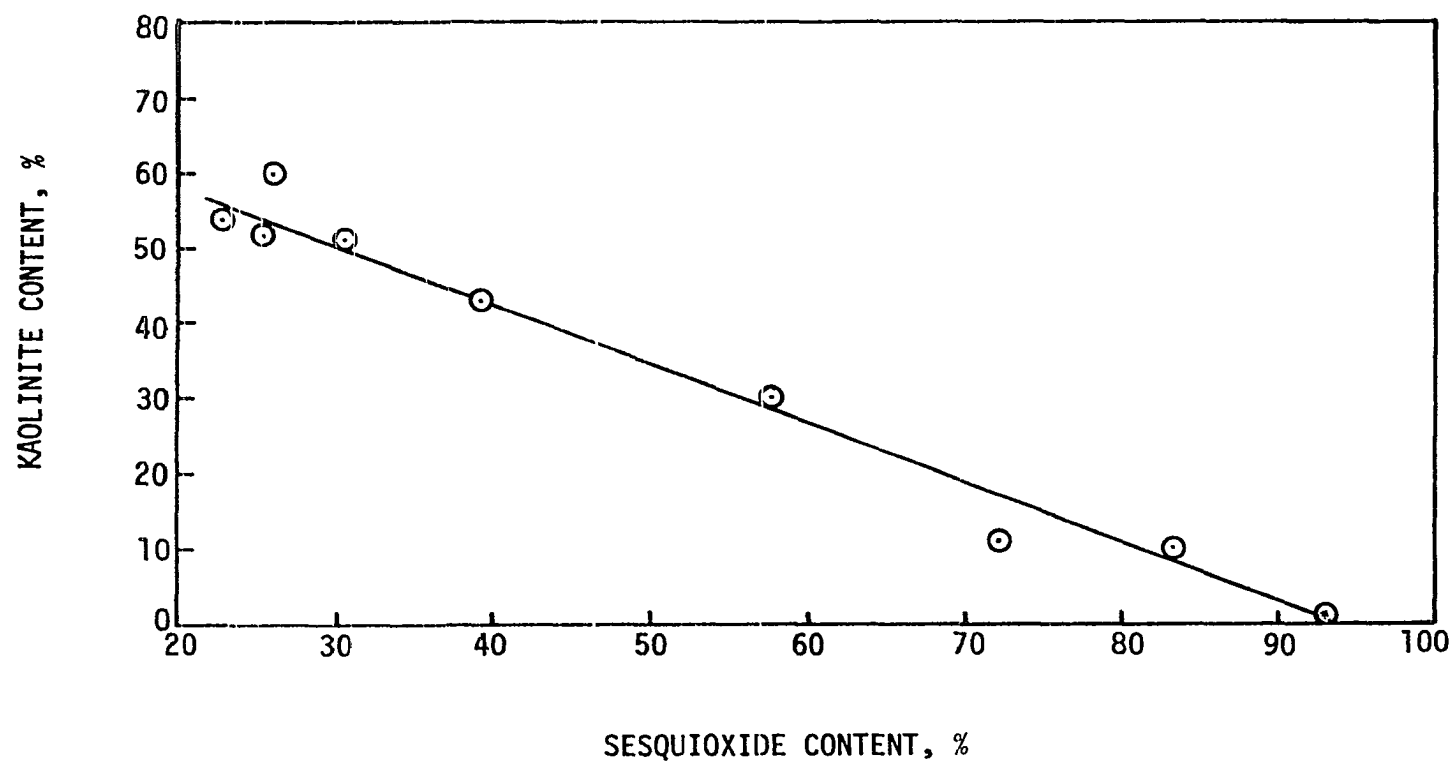


Figure 22. Relationship between kaolinite and sesquioxide contents of Hawaiian soils

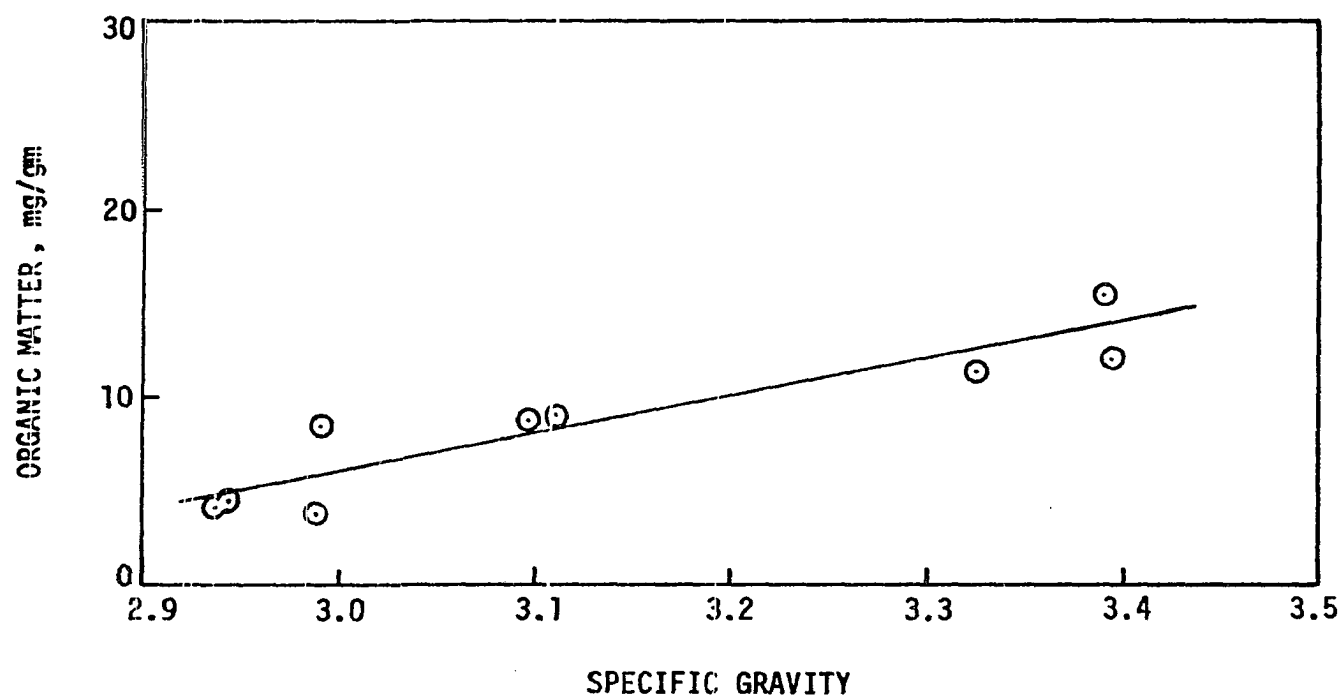


Figure 23. Relationship between organic matter and specific gravity for Hawaiian soils

Although the presence of halloysite and montmorillonite in Hawaiian lateritic soils was reported occasionally in the literature (21), they were not observed in the soils studied. These two minerals are known as being formed in the very early stages of weathering and they are not stable. So, under the influence of favorable environmental conditions present in the tropical regions, the weathering proceeds quite rapidly, and these unstable minerals are converted to more stable minerals in a relatively short period of time. The soils studied here appear to be weathered enough not to contain any such unstable minerals.

Titanium is another element which is encountered in lateritic soils (16,56), mostly in the form of ilmenite as primary mineral, or anatase as secondary mineral. The highest concentration of titanium oxides, though, usually takes place at the surface of the soil. In other words, if titanium exists in a lateritic soil profile, it is generally concentrated in the A-horizon (56). Since in this study only the B-horizons of the soils were investigated, the possibility of observing high amount of titanium was quite low. No titanium compound was detected by X-ray and differential thermal analysis. An elemental analysis by scanning electron microscope performed on the same soils by Paulson (49) exhibited some titanium in trace amounts.

Pore Size Analysis

The importance of soil structure in understanding the engineering behavior of lateritic soils is well-recognized (29,43,62,6). The most common methods utilized in studying the structure of lateritic soils are

microscopic methods, such as scanning electron microscopy, and analyzing thin sections by light microscopy. Mercury injection technique which has been recently applied to soils promises to be another useful tool to analyze the soil structure, and to quantify, at least, the pore structure of soils.

Here, an attempt was made to analyze the pore structure of selected lateritic soils with mercury injection technique. Various parameters were generated from the pore size distribution curves to characterize the pore structure of the soils and they are listed in Table 5.

At this step, the first thing to be observed is to plot various pore size parameters versus specific gravity and see how these parameters vary with proceeding weathering. Figure 24 shows median diameter versus specific gravity plot, indicating that pore sizes are getting larger as the soils get more weathered. The very same thing is indicated in small mode pore diameter versus specific gravity plot, shown in Figure 25. Figure 26 shows a decrease in volume of mercury retained in the sample, at the end of the test, as weathering proceeds, and this was interpreted as another indication for enlargement of pores in more weathered soils, because larger the pore sizes, the less possibility of necking down of pores. The uniformity coefficient versus specific gravity plot shown in Figure 27 exhibits that in the cases of more severely weathered soils the distribution gets less uniform, that is, instead of having a narrow range of pore size to contain the major portion of the pore volume, there are all sizes of pores distributed more evenly within the soil domain.

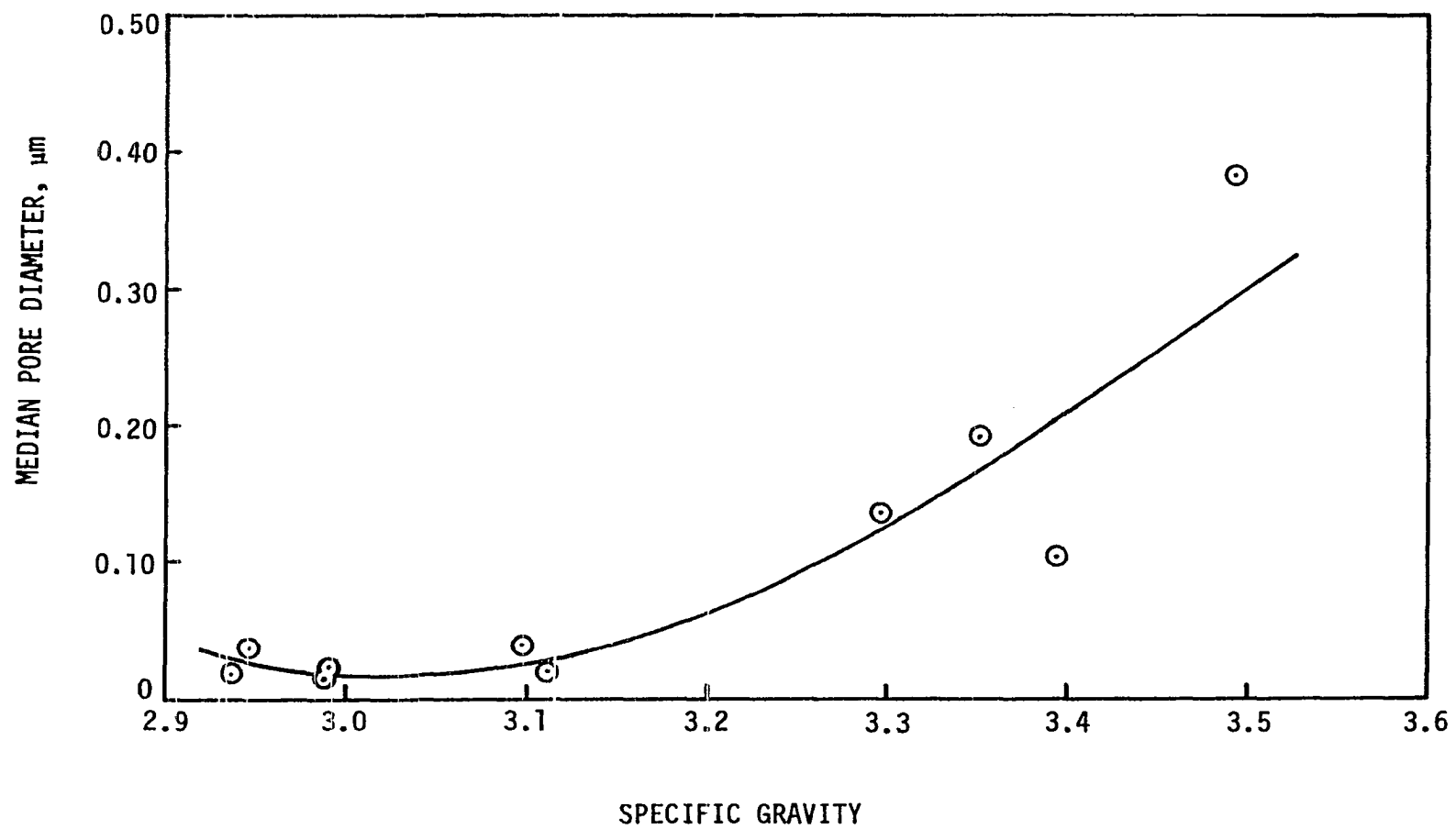


Figure 24. Relationship between median pore diameter and specific gravity for Hawaiian soils

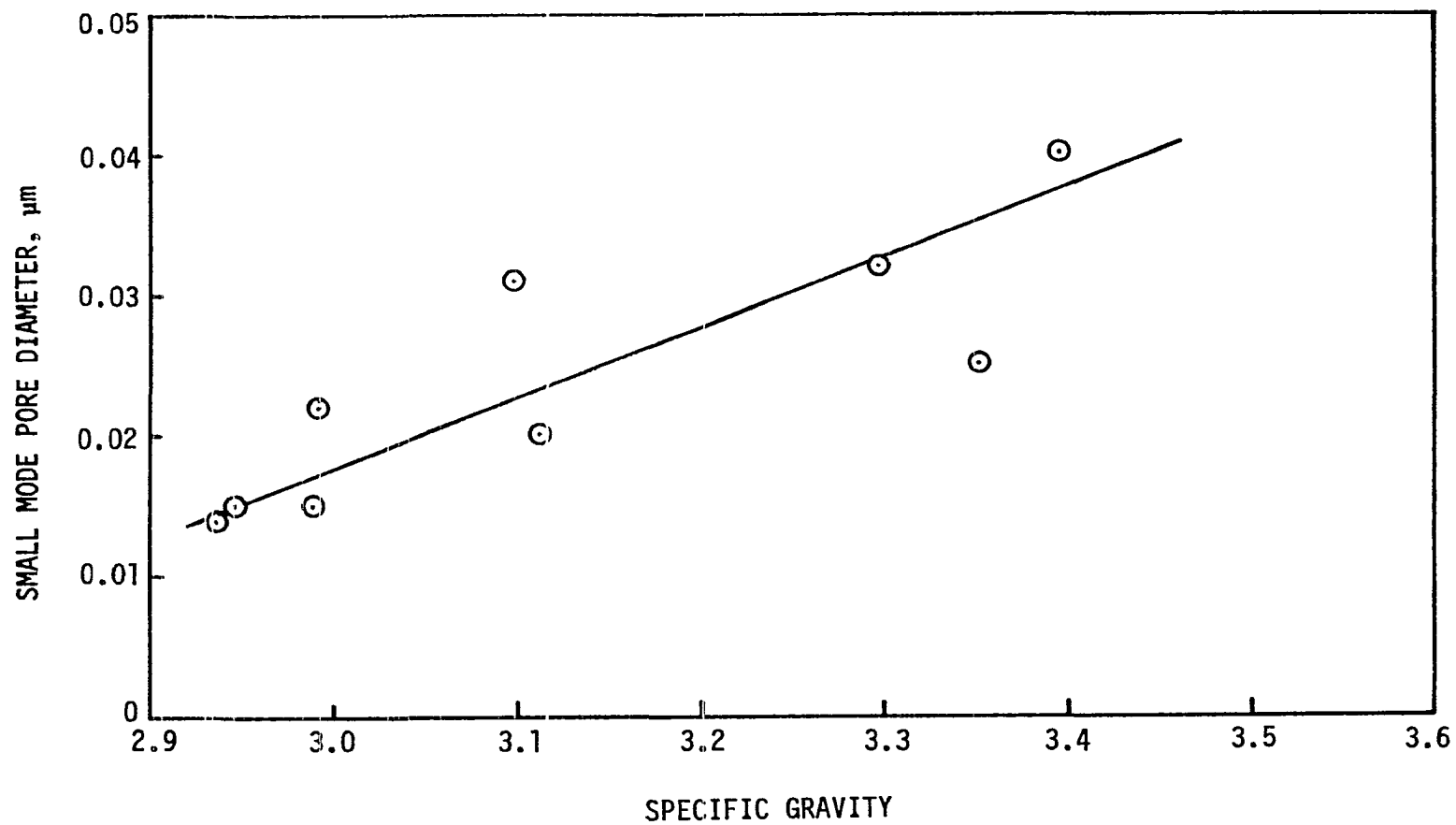


Figure 25. Relationship between small mode pore diameter and specific gravity for Hawaiian soils

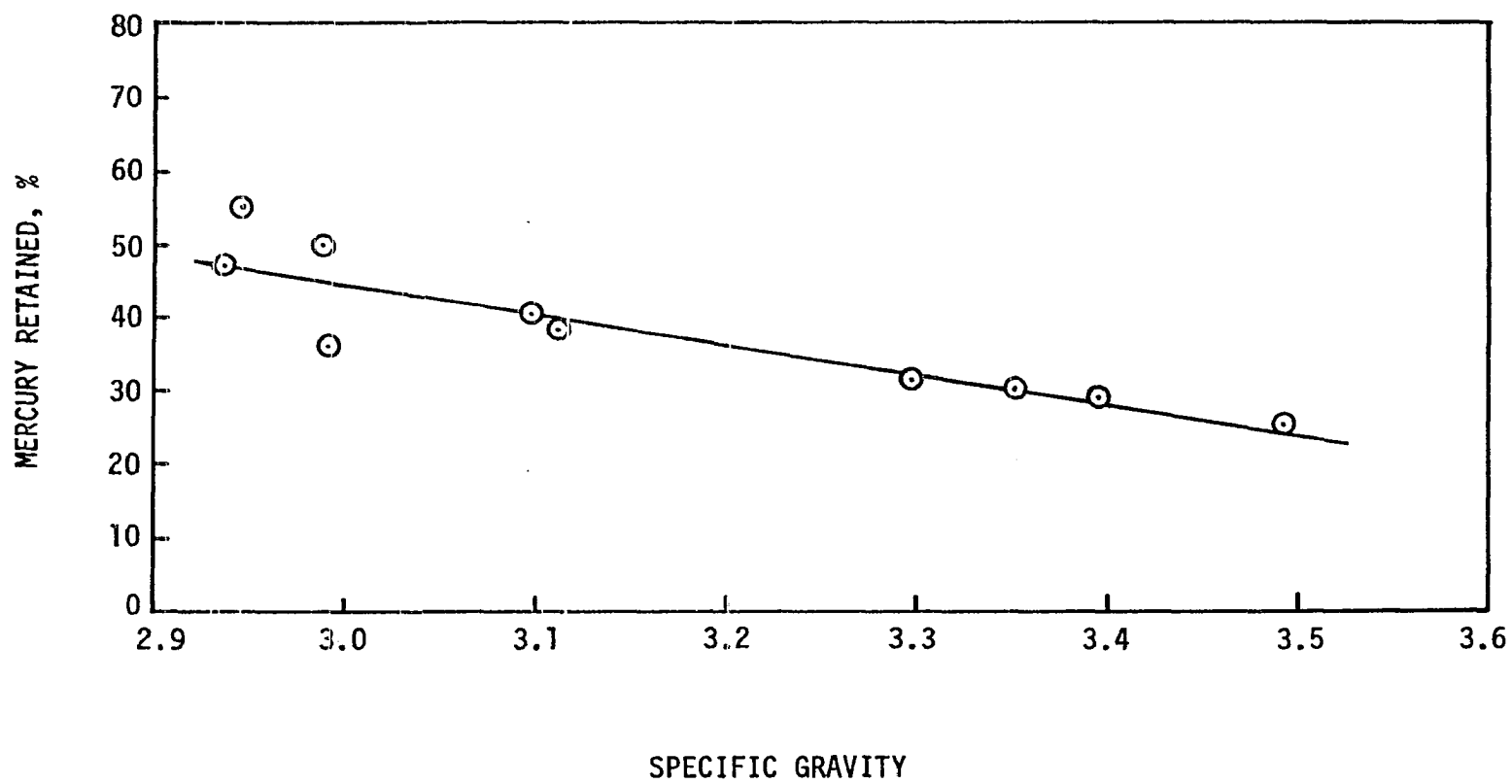


Figure 26. Relationship between retained mercury and specific gravity for Hawaiian soils

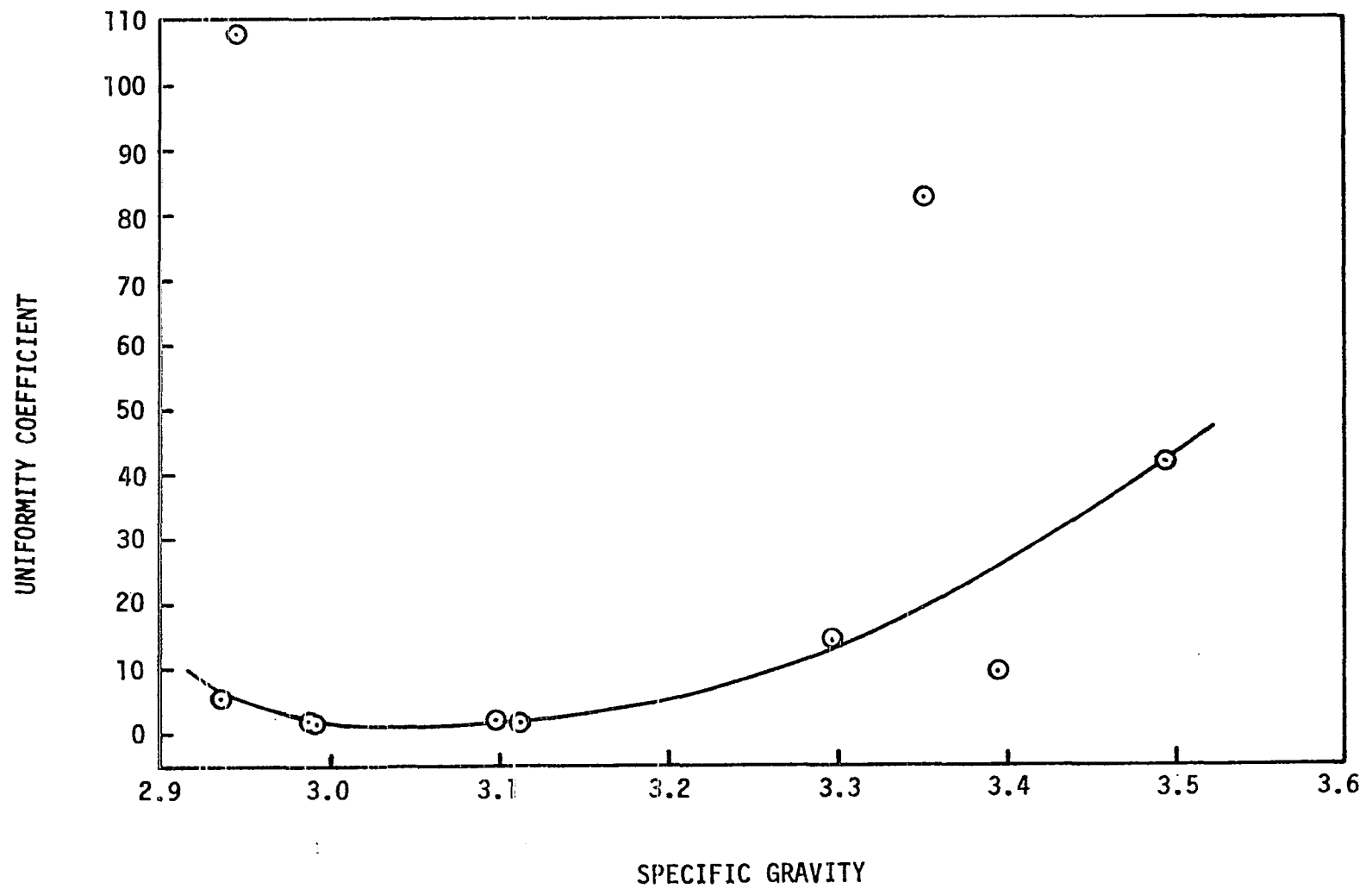


Figure 27. Relationship between uniformity coefficient and specific gravity for Hawaiian soils

A comparison of void ratios calculated from mercury injection with void ratios determined from bulk density measurements reveals that, in majority of the soils, not all the voids have been intruded by the mercury. In other words, a portion of the total pore volume is occupied by pores which have diameters smaller than 0.0042 micrometers. The percent of total pore volume, intruded by mercury, listed in Table 5, indicates that the amount of these very small pores gets smaller as the soils get more weathered.

In order to show further experimental evidences of the enlargement of pores with increasing weathering, the absolute volume of pores per gram of dry soil for different ranges of pore size as determined from Figures 12 and 13 is plotted versus specific gravity. The results, shown in Figures 28-31, indicate that small size pores decrease while medium, large and very large size pores increase in amount with increasing weathering. Very large, large, medium, and small pores correspond to the size ranges of larger than 10.0, 10.0-1.0, 1.0-0.1, and 0.1-0.01 micrometer pore diameter, respectively. Figures 32-35, on the other hand, show the percentage of each pore size range based on total pore volume intruded by mercury versus specific gravity plots, again indicating that the percentage of small pores decreases, and of medium, large, and very large pores increases with proceeding weathering.

To have large size pores in more weathered soils can be interpreted as having larger soil aggregates in such soils. To have a soil composed of fine grains with large size pores among them, is not very likely. When this observation is considered together with the results of mineralogical

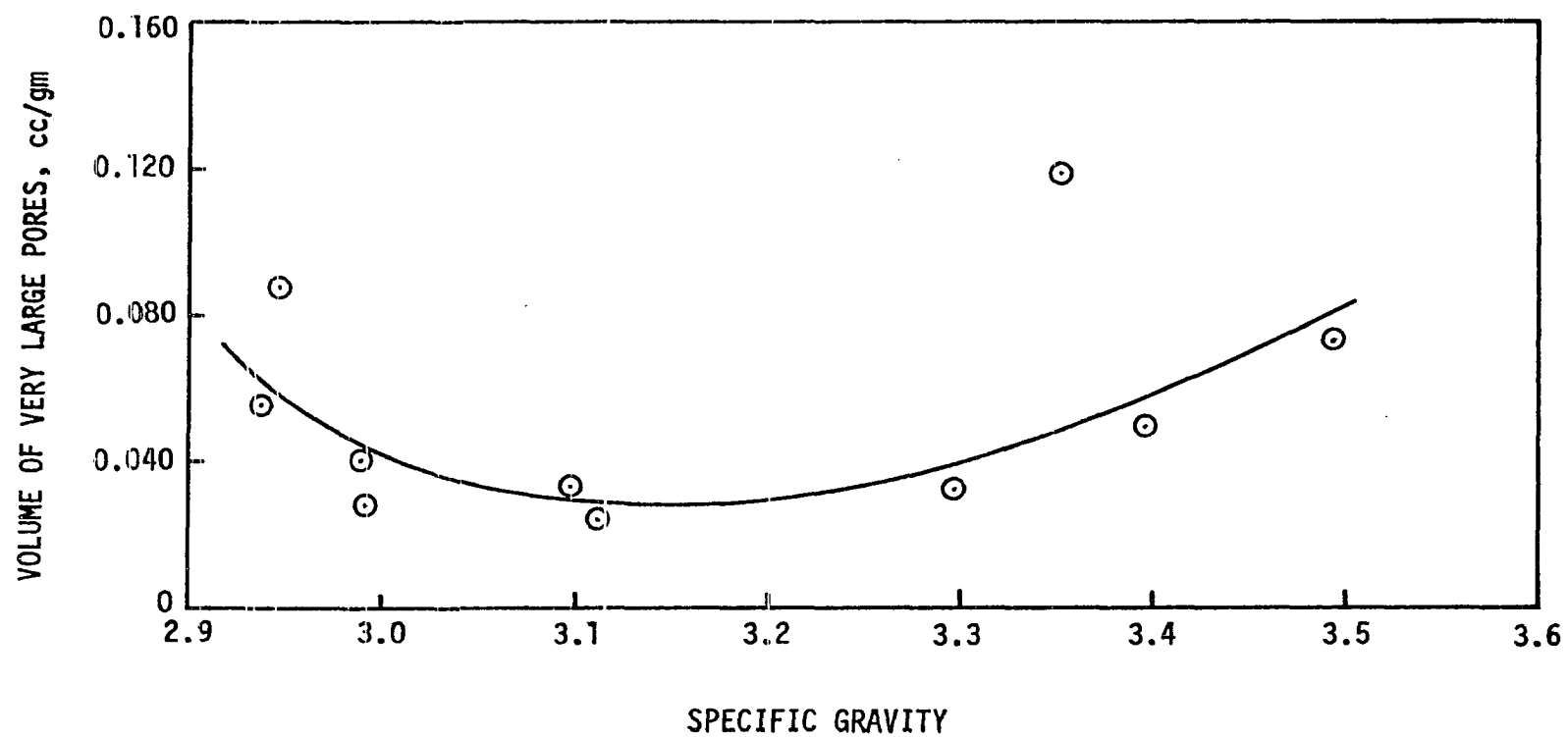


Figure 28. Relationship between volume of very large pores and specific gravity for Hawaiian soils

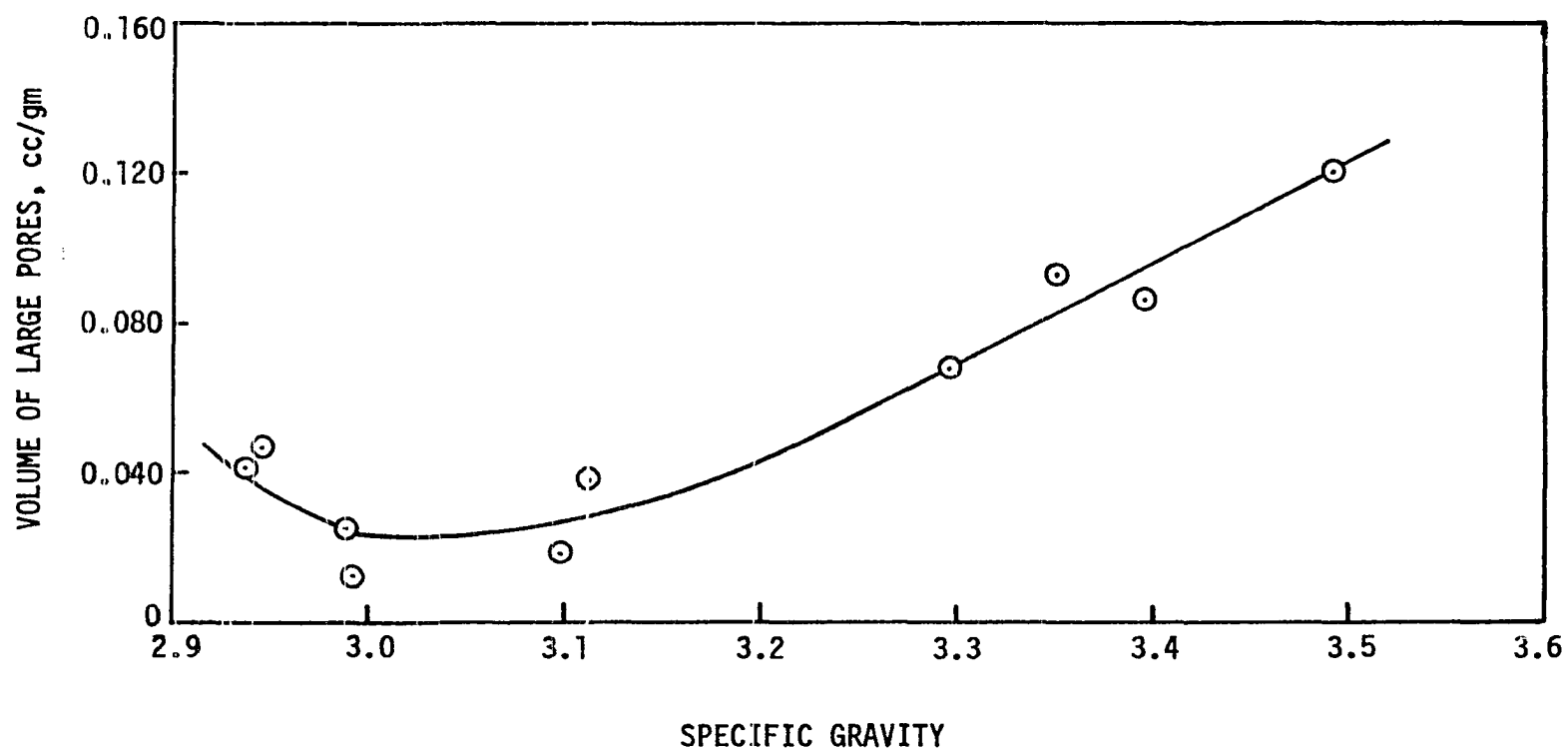


Figure 29. Relationship between volume of large pores and specific gravity and Hawaiian soils

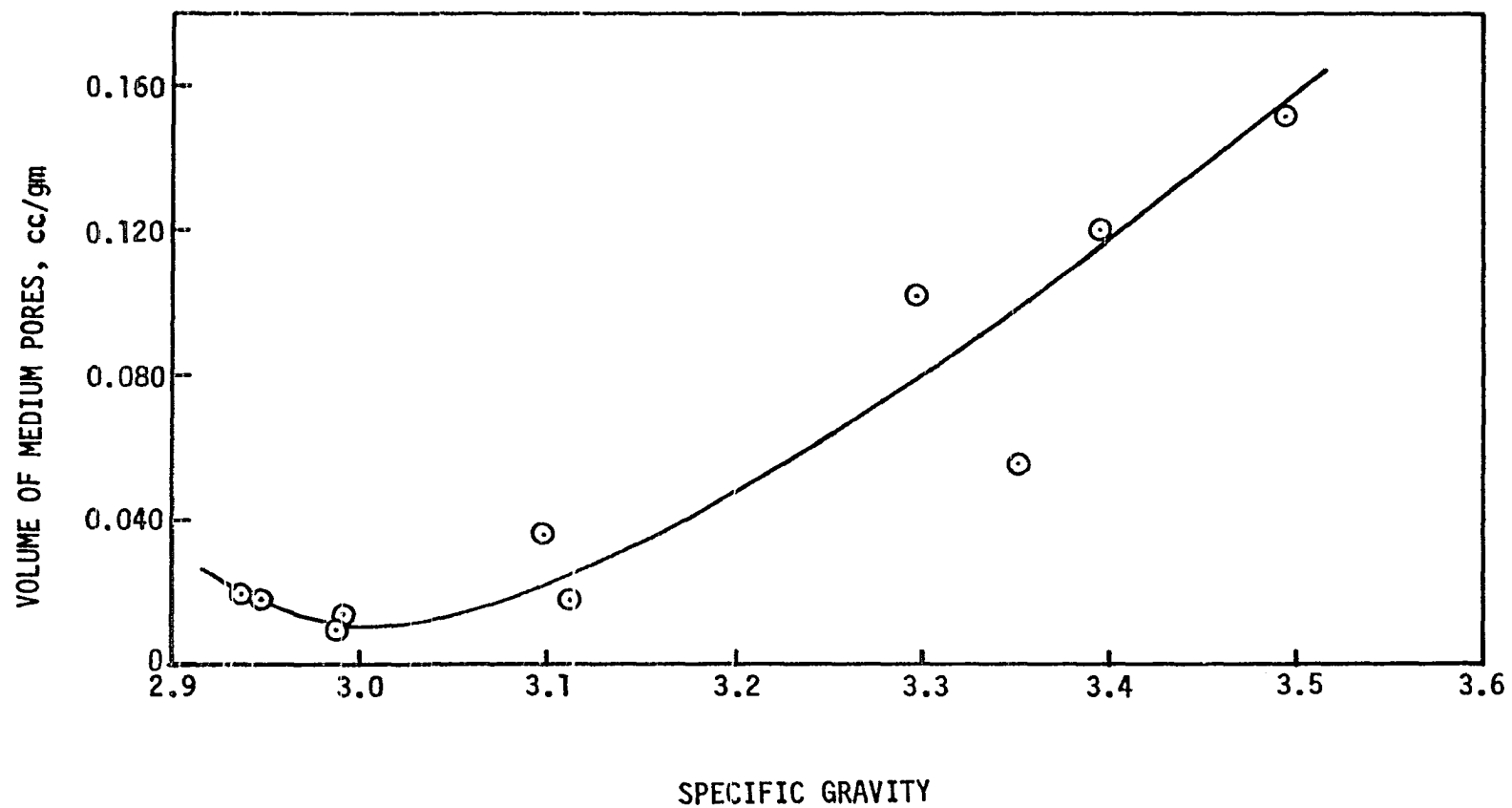


Figure 30. Relationship between volume of medium pores and specific gravity for Hawaiian soils

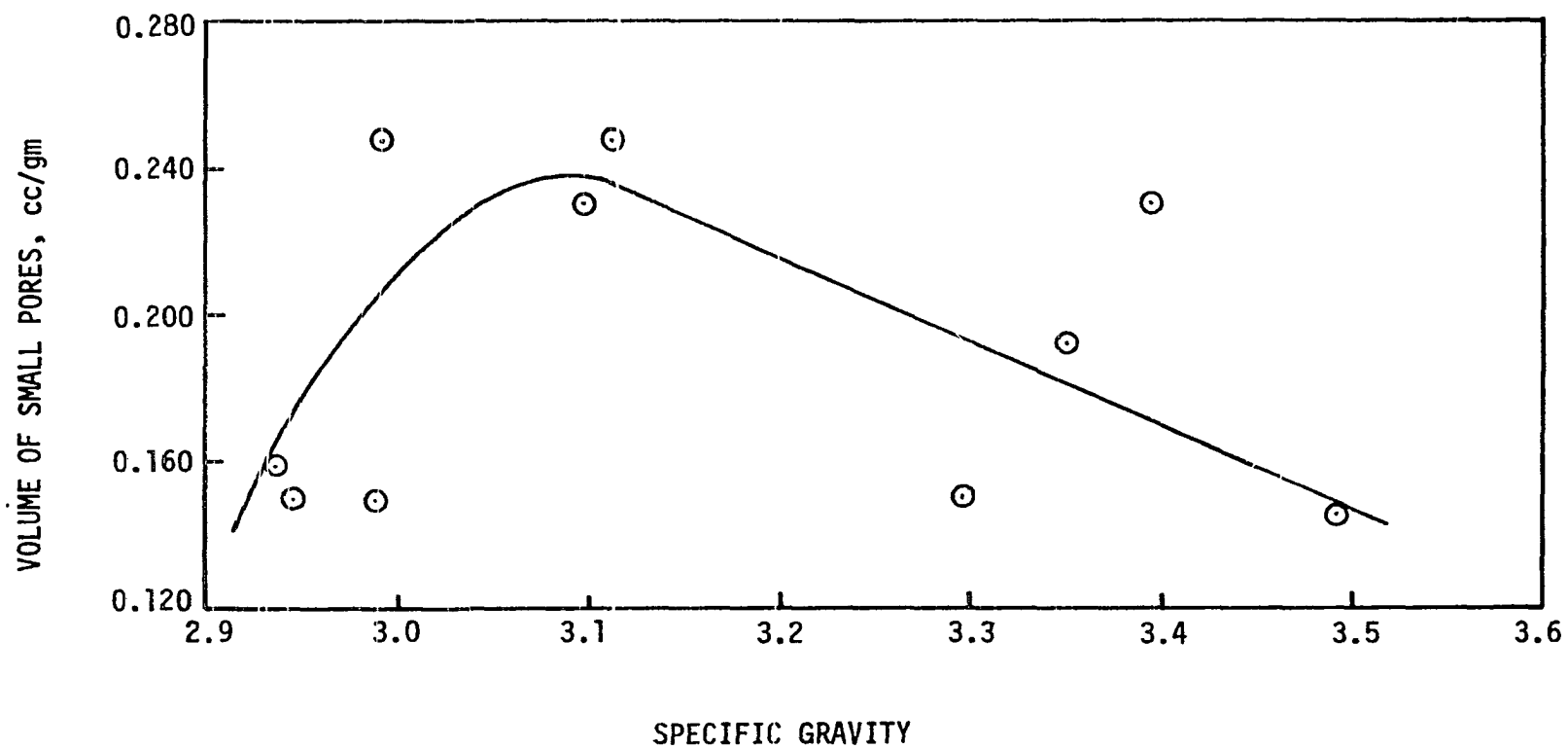


Figure 31. Relationship between volume of small pores and specific gravity for Hawaiian soils

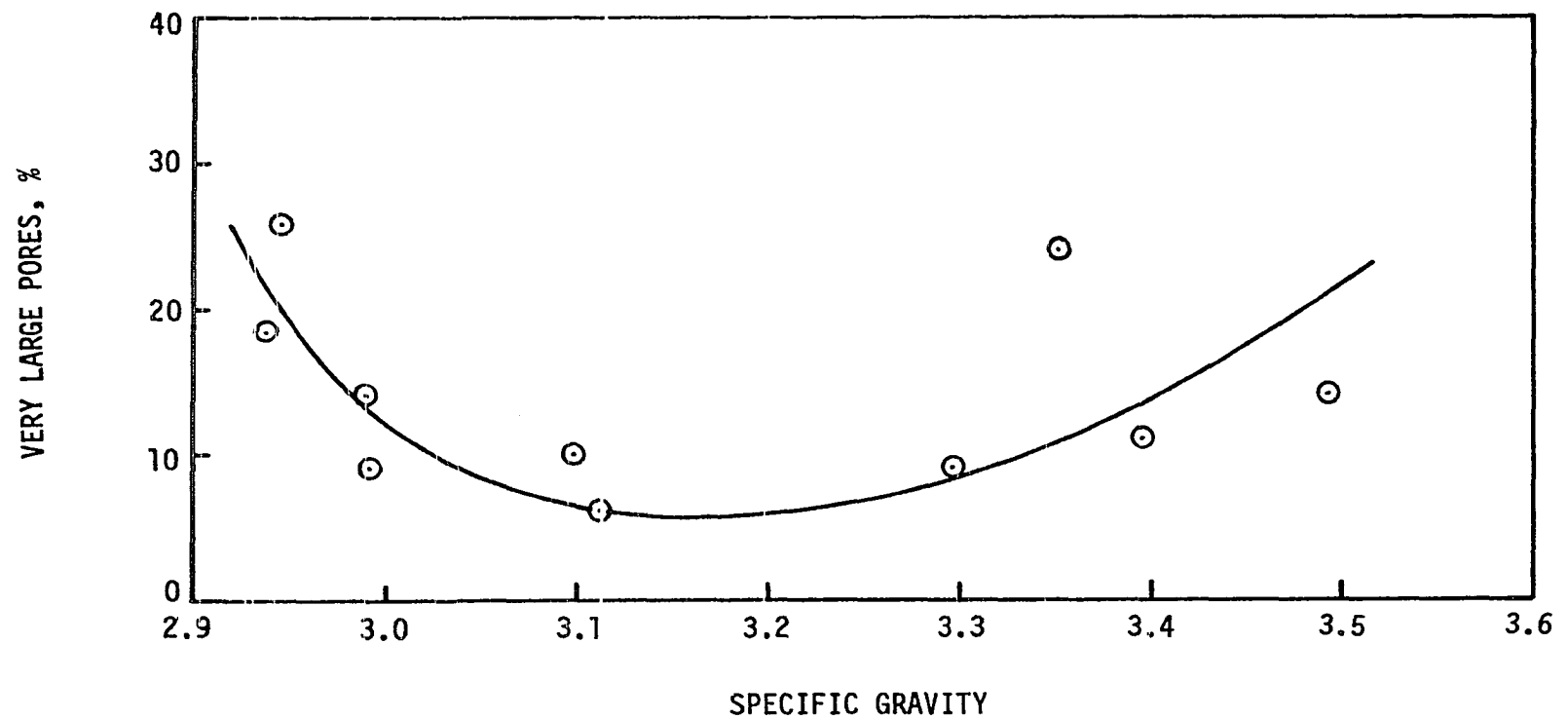


Figure 32. Relationship between percentage of very large pores and specific gravity for Hawaiian soils

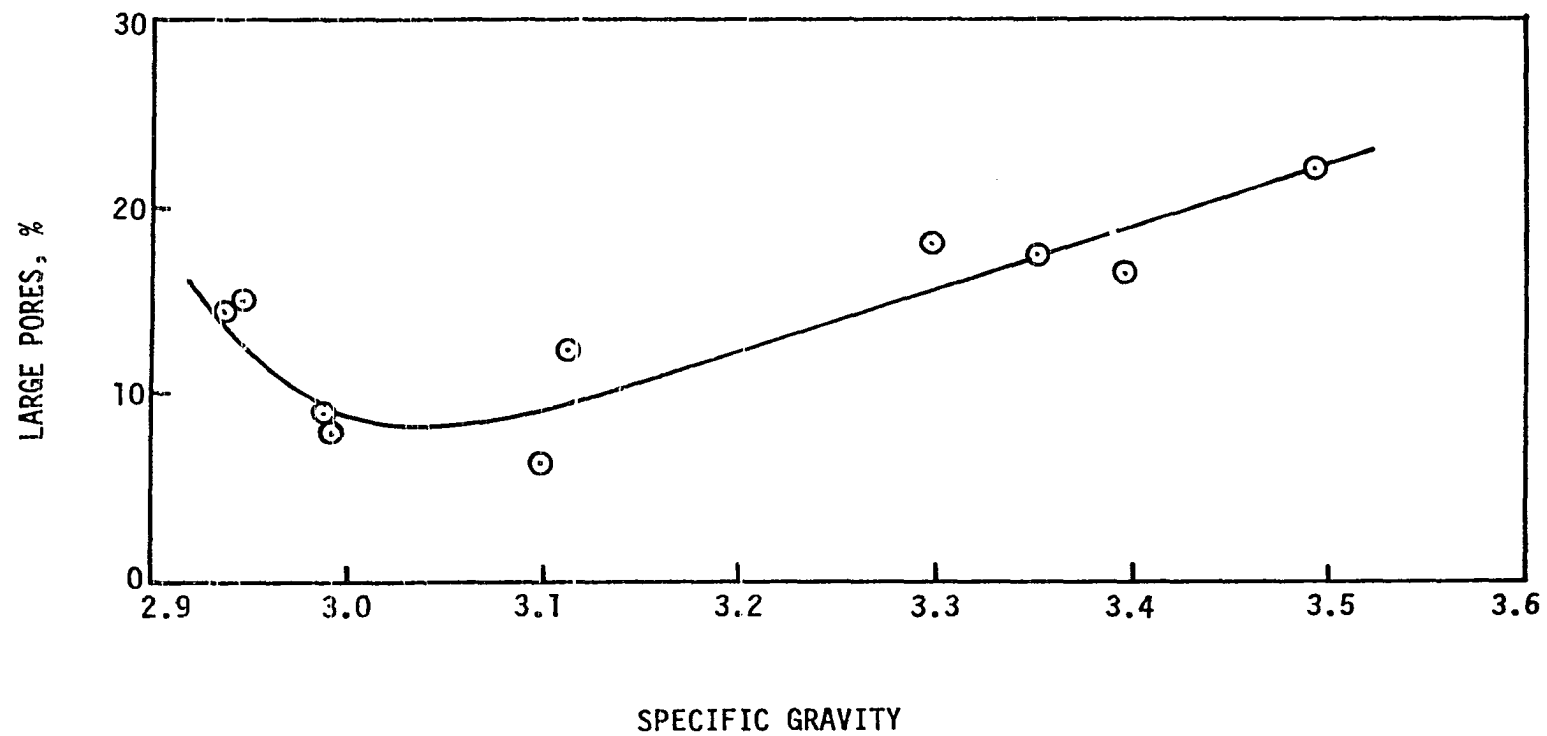


Figure 33. Relationship between percentage of large pores and specific gravity for Hawaiian soils

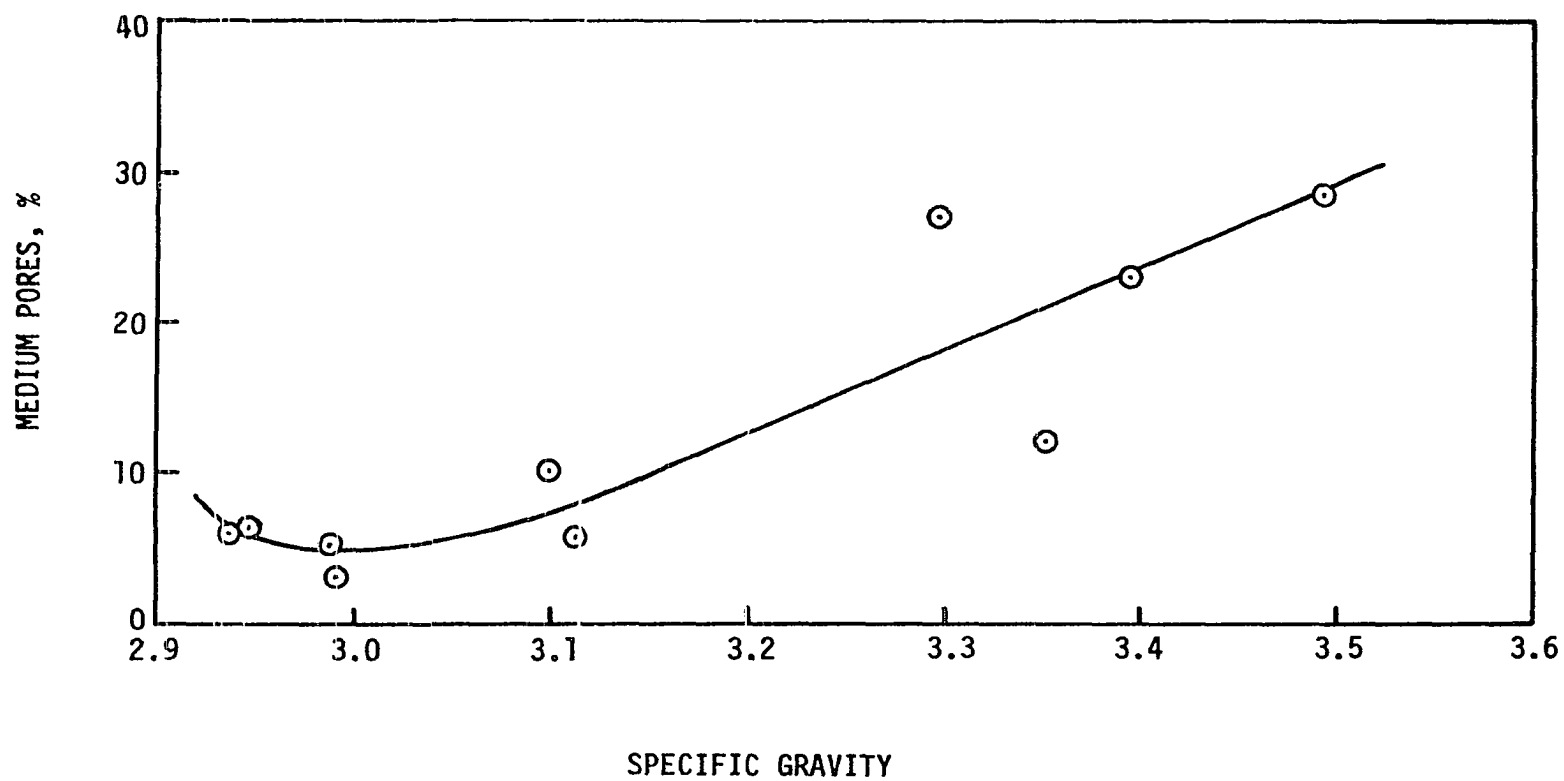


Figure 34. Relationship between percentage of medium pores and specific gravity for Hawaiian soils

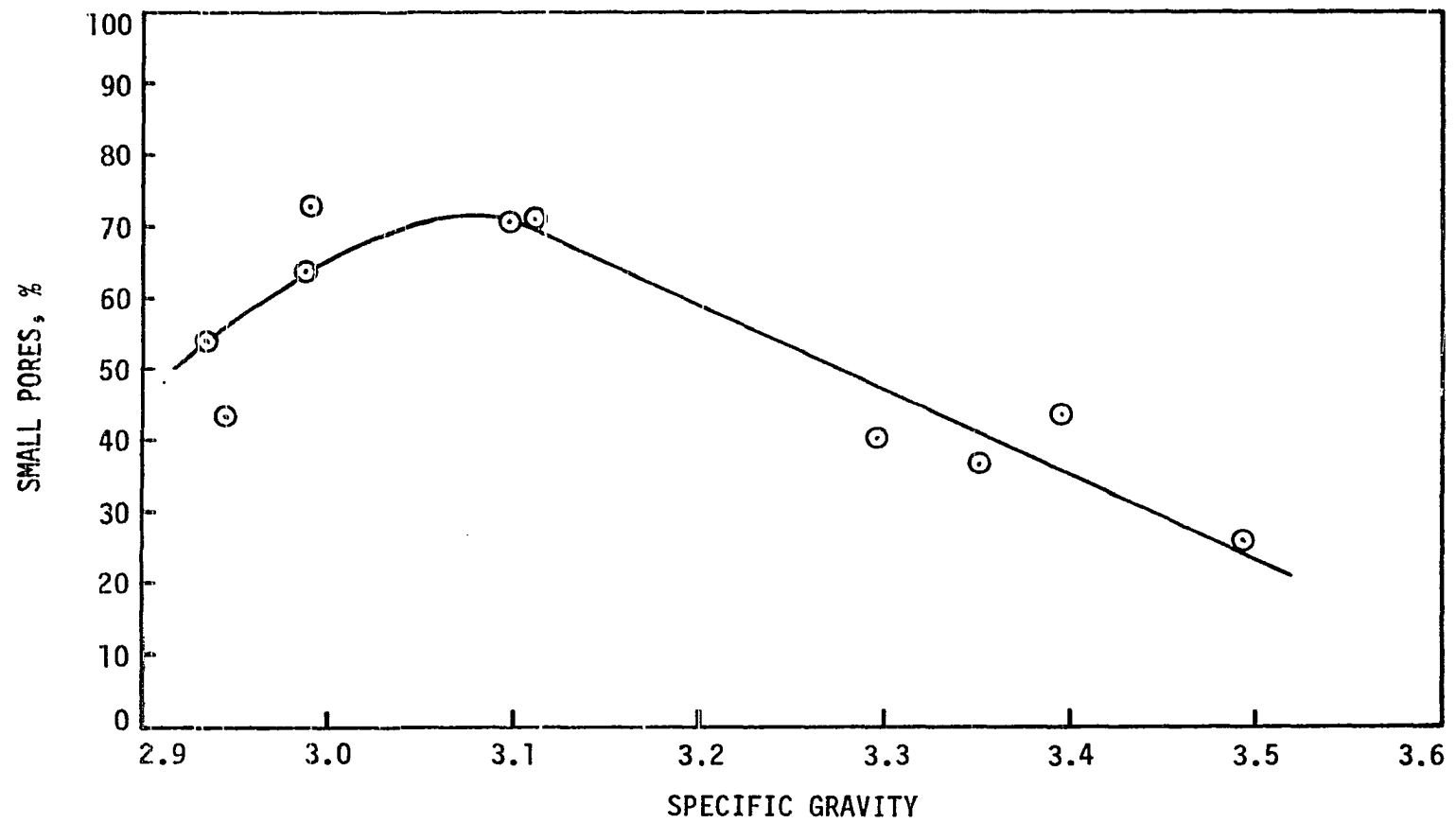


Figure 35. Relationship between percentage of small pores and specific gravity for Hawaiian soils

analysis, the situation might be understood better. As stated previously, in the course of weathering at one stage, kaolinite is the major mineral component in the soil. In the further stages of weathering, kaolinite content starts to decrease while sesquioxides of iron and aluminum increase in amount. Kaolinite is known to be very inert as a binding agent and has very little effect on aggregation (50). Sesquioxides, on the other hand, have the capability of cementing the small grains together and forming larger, water stable soil aggregates (40,5,8). As long as there is available sesquioxides in the soil, aggregation proceeds in the direction of forming larger and larger aggregates (5). As weathering proceeds further, sesquioxide content keeps on increasing, leading to the formation of larger soil aggregates. As a result of this discussion, it might be said that toward the last stages of weathering, lateritic soils possess a granular quality due to the aggregation taking place.

The influence of drying on the structure of lateritic soils was investigated by taking two or three portions of an undisturbed soil sample obtained from the same boring and depth of a soil series and subjecting them to freeze drying, oven drying, and/or air drying. Then each sample was tested in the mercury porosimeter and the results were compared to see if there is any difference in the pore structure of those differently dried samples. Six of the nine soil series gave essentially the same kind of pore size distribution for all differently dried samples. Three naturally wet soils, Puhi, Kapaa and Hali soil matrix, exhibit some shrinkage in oven dried samples, that is, absolute volume of pores per gram of dry soil are less in oven dried samples compared to freeze dried

samples as shown in Figures B7-B10 in Appendix B. The shrinkage in these three soils was caused by high natural moisture contents which are well above the shrinkage limits of these soils. The rest six soil series have either lower or little above moisture contents compared to their shrinkage limits. In a soil which has a moisture content less than its shrinkage limit, one should not expect any shrinkage after drying. This observation, in a sense, is in contrast with what is reported in the literature. Many investigators suggest that lateritic residual soils have a cemented structure, forming a continuous three-dimensional framework, resulting from the binding action of sesquioxides (75,37). The results obtained in this study, however, do not support this concept for all soils. If that were the situation, there would not be any shrinkage in the soil body.

The shrinkage observed in those three soils suggests that instead of having a continuous three-dimensional framework, the soil grains are coated by the sesquioxides and cemented together by iron and aluminum gels to form larger individual particles as described by Baver et al. (8). Alternate wetting and drying dehydrates irreversibly these gels and water stable soil aggregates are formed. There might be, of course, some cementation among individual soil aggregates too, but to consider the whole body of soil as being a continuous, stable, three-dimensional framework cannot be justified. Such a structure of continuous three-dimensional framework most probably occurs in laterite crusts or within the individual concretions which have rock-like or gravel-like intact structures.

Slaking Tests

Oven dried and naturally moist samples of each soil series were subjected to slaking test and the results are listed in Table 6. The general trends observed are as follows. Relatively less weathered soils slake faster and into smaller aggregates. More weathered soils, on the other hand, slake very slowly or do not slake at all; the ones which slake disintegrate into relatively larger aggregates. By comparing the slaking test results obtained from oven dried and naturally moist samples, it was concluded that oven dried ones are more resistant against slaking. This latter observation is one of the characteristics of lateritic soils. In the case of temperate soils, dry samples slake more rapidly than naturally moist samples, because in such soils, dry state leads to a rapid moisture intake and swelling accompanied by compression of contained air which may ultimately cause an explosive-like effect (80). The larger resistance of lateritic soils to slaking in dry state is attributed to the cementation caused by dehydration of hydrated iron and aluminum oxides (80).

If the slaking test results of those three wet soils, Puhi, Kapaa and Halii, which exhibit considerable volume changes after oven drying are considered, it will be observed that in naturally moist state, they are either completely disintegrated or cracked. This can be considered as a further verification of a soil structure which has a particulate nature, rather than being a continuous three-dimensional framework. It appears that in the state of natural moisture, the voids among individual soil aggregates are filled with water, and as the soils dry out the moisture

evaporates, and this brings the soil aggregates closer to cause a shrinkage.

The larger aggregates in more weathered soils can be explained, once more, by the presence of larger amounts of sesquioxides which lead to soil aggregation. In less weathered soils, kaolinite which is quite inactive as a binding agent is the predominant mineral, so the formation of soil aggregates is at a quite low level, and as a result of that, soils slake fast and into relatively small particles.

Scanning Electron Microscopy

Scanning electron microscopy was utilized in order to get some more supporting data showing the differences in the structure of the soils weathered to different degrees. To achieve this, three soil series were selected, one being relatively less weathered, one intermediately weathered, and one heavily weathered, and subjected to microscopic studies. The micrographs taken are shown in Figures 14-16. If these micrographs are examined carefully, it will be observed that the relatively less weathered soil, Wahiawa, has the smallest soil aggregates accompanied with small size pores. The heavily weathered soil, Halii, on the other hand, clearly exhibits the aggregation, and the size of pores among those aggregates are larger compared to those of Wahiawa soil. Intermediately weathered soil, Lihue, can be placed in between those two, from the pore and aggregate sizes point of view.

The samples belonging to those soil series which do not show any shrinkage, i.e., Wahiawa and Lihue, were examined oven dried. Halii was freeze dried to keep the in situ structure undisturbed.

Strength Tests

Strength parameters, cohesion and internal friction angle of the undisturbed soils tested at their natural moisture content were determined by direct shear testing. The results are listed in Table 7.

The variation in these parameters as degree of weathering varies is shown in Figures 36 and 37. Puerto Rican basalt derived lateritic soils are again included in those plots to have a wider spectrum. Cohesion versus specific gravity plot, Figure 36, shows that cohesion first increases and then decreases with increasing degree of weathering. Examination of the other properties of soils versus cohesion reveals that the void ratio can be considered as the controlling factor of cohesion. This is a similar observation obtained by Lohnes and Demirel (37) for Puerto Rican soils. To show this better, void ratio is plotted against cohesion as shown in Figure 38. It appears that cohesion increases with decreasing void ratio.

Internal friction angle, on the other hand, keeps on increasing all the way through as weathering proceeds, as shown in Figure 37. This behavior is interpreted in the following manner. During the stage of clay formation, although clay content increases, the void ratio decreases due to the accumulation of clays in the B-horizon and filling the large voids. This process apparently leads to a well-graded soil and improves the value

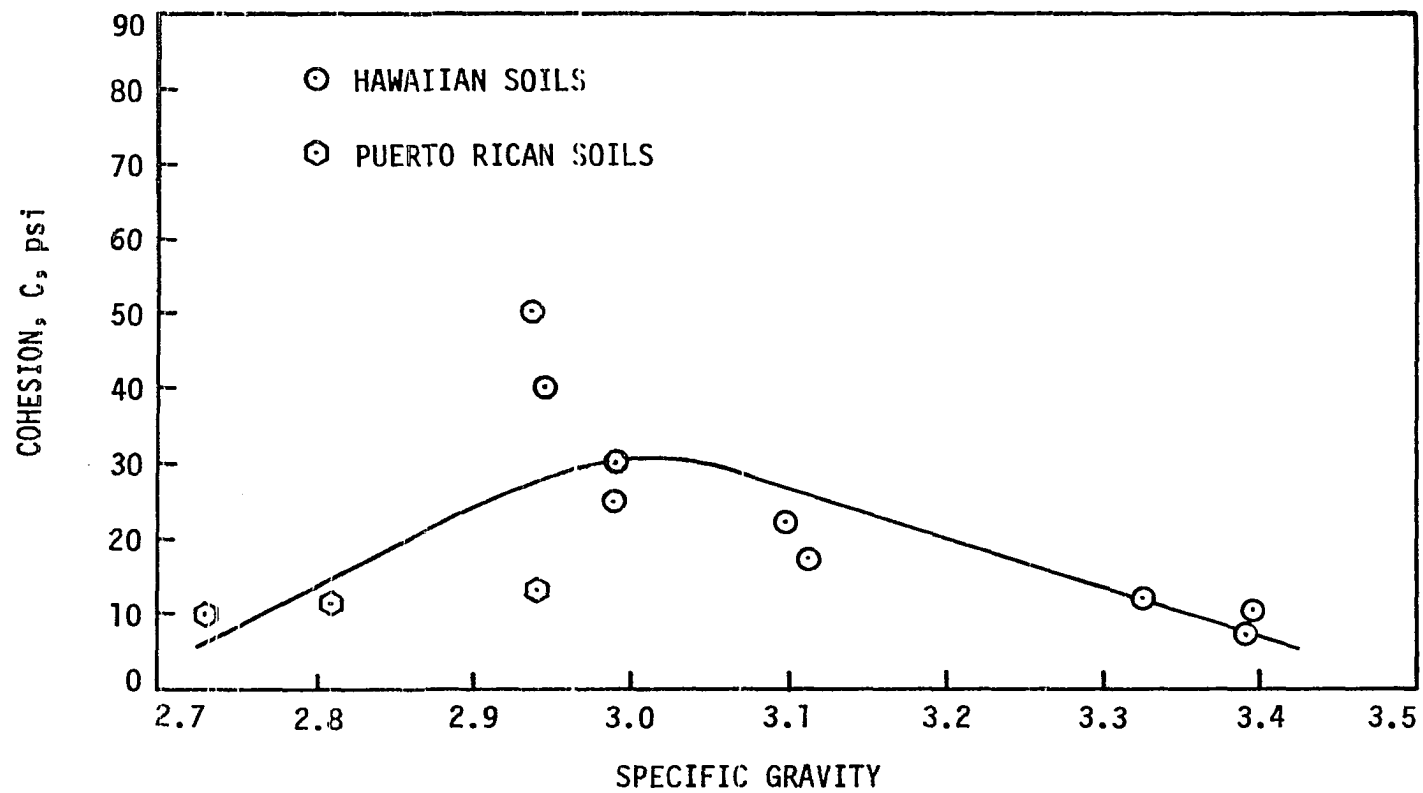


Figure 36. Relationship between cohesion and specific gravity

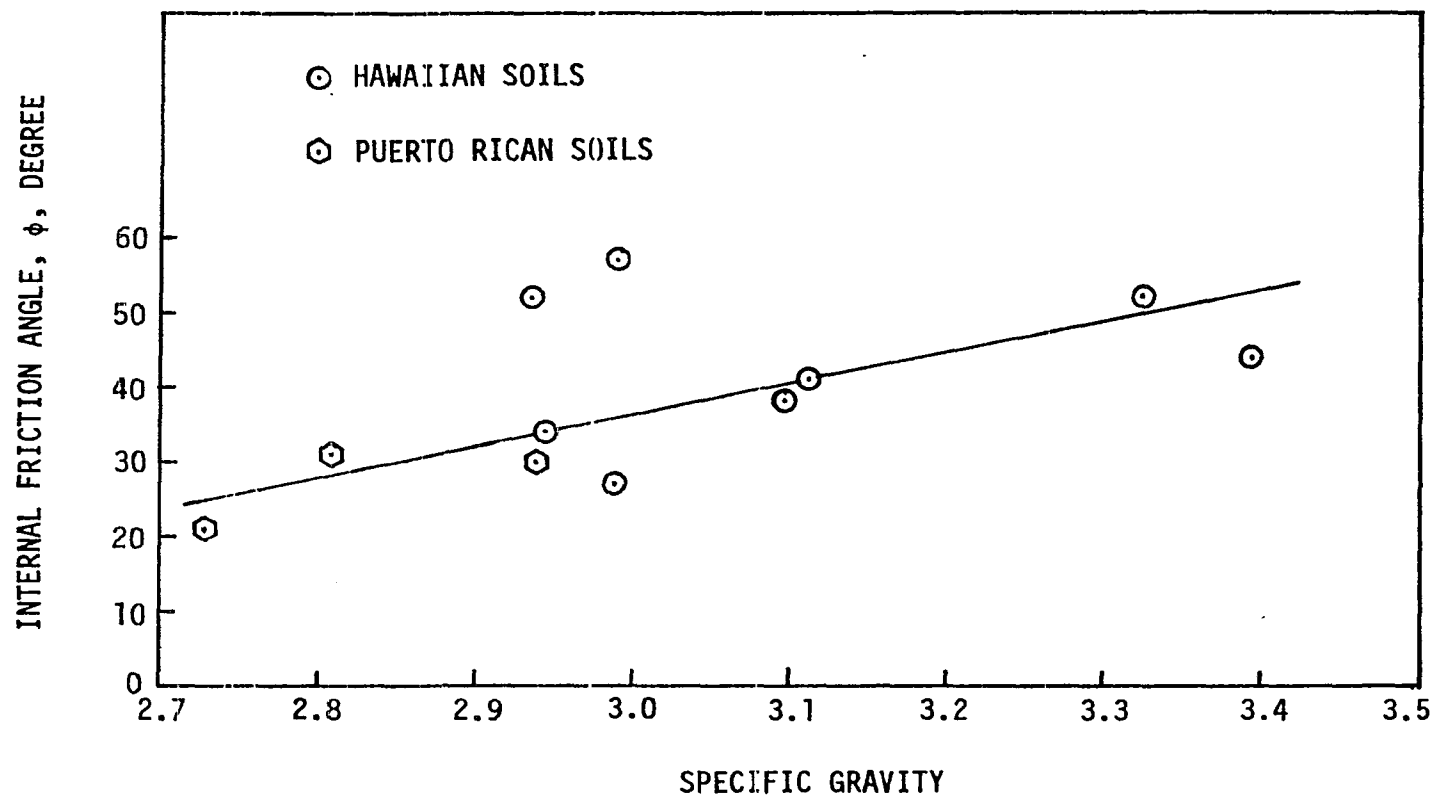


Figure 37. Relationship between internal friction angle and specific gravity

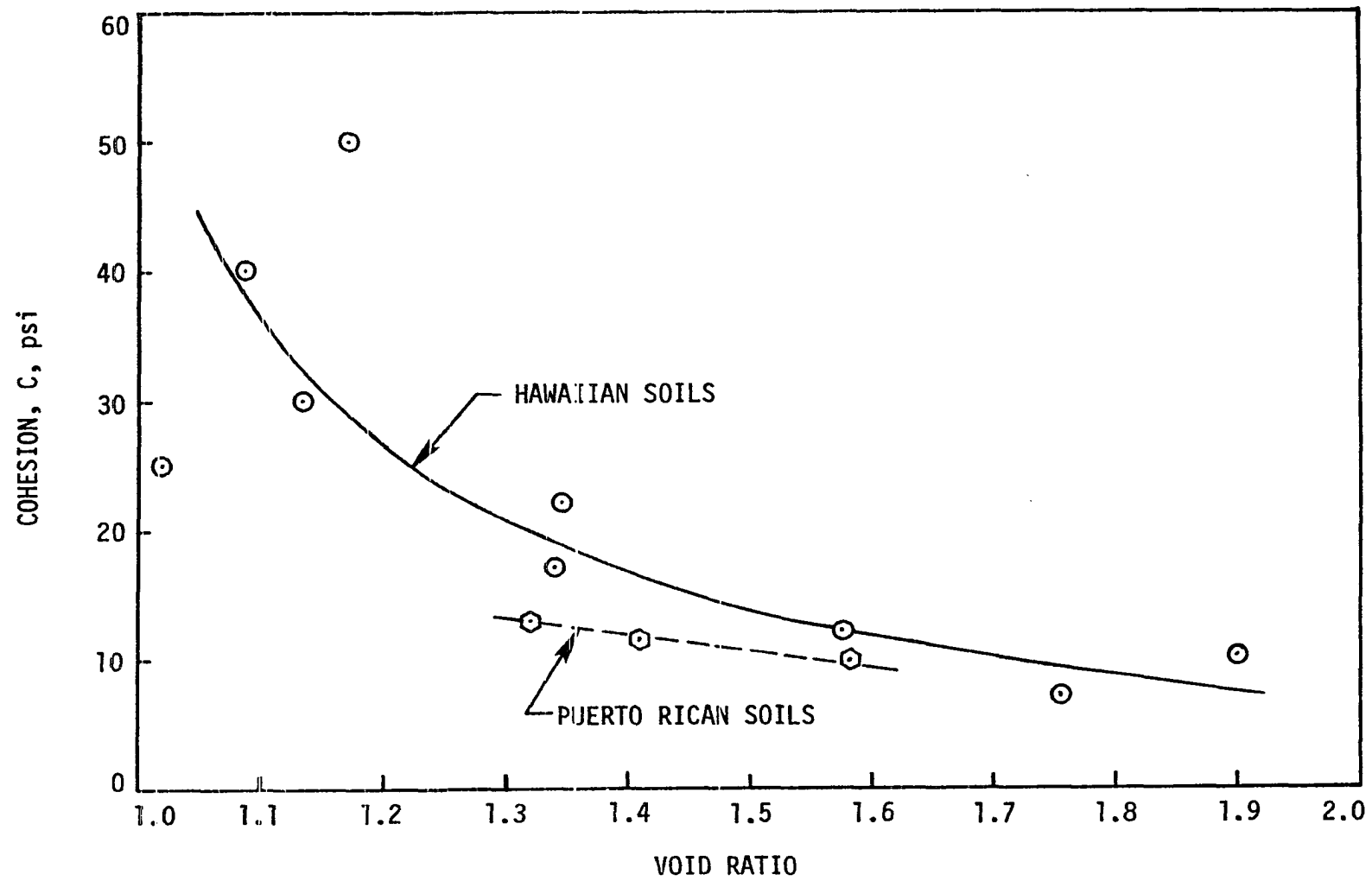


Figure 38. Relationship between cohesion and void ratio

of the internal friction angle. In the further stages of weathering, due to the increasing amount of sesquioxides, the formation of large, water stable soil aggregates takes place and this yields a soil which is granular in nature. This improves the internal friction angle even further.

A question that is worthwhile to be answered is: What is the relationship between the mineralogy and the shear strength of the soils studied? At the first glance, it will be observed that cohesion varies in accordance with varying kaolinite content, that is, larger the kaolinite content, larger the cohesion of the soil as shown in Figure 39. This is what one should expect; the cohesion of a soil increases with increasing clay content.

Internal friction angle, on the other hand, has the tendency to increase with increasing amount of sesquioxides. This is again due to the formation of large, water stable soil aggregates with the binding action of sesquioxides.

From the preceding discussion, one may conclude that mineralogy of lateritic soils is the governing factor of almost all the other soil properties. Engineering properties of the soils, such as natural dry density, void ratio, and specific gravity, have been found to be closely related to the minerals present in the soils. Pore structure and grain size are again directly related to the mineralogy. Finally, shear strength of the soils is found to be controlled by the mineralogy.

The influence of moisture on the strength parameters of lateritic soils has been investigated by many investigators (7,49). The strength parameters were found to vary with the varying moisture content, even

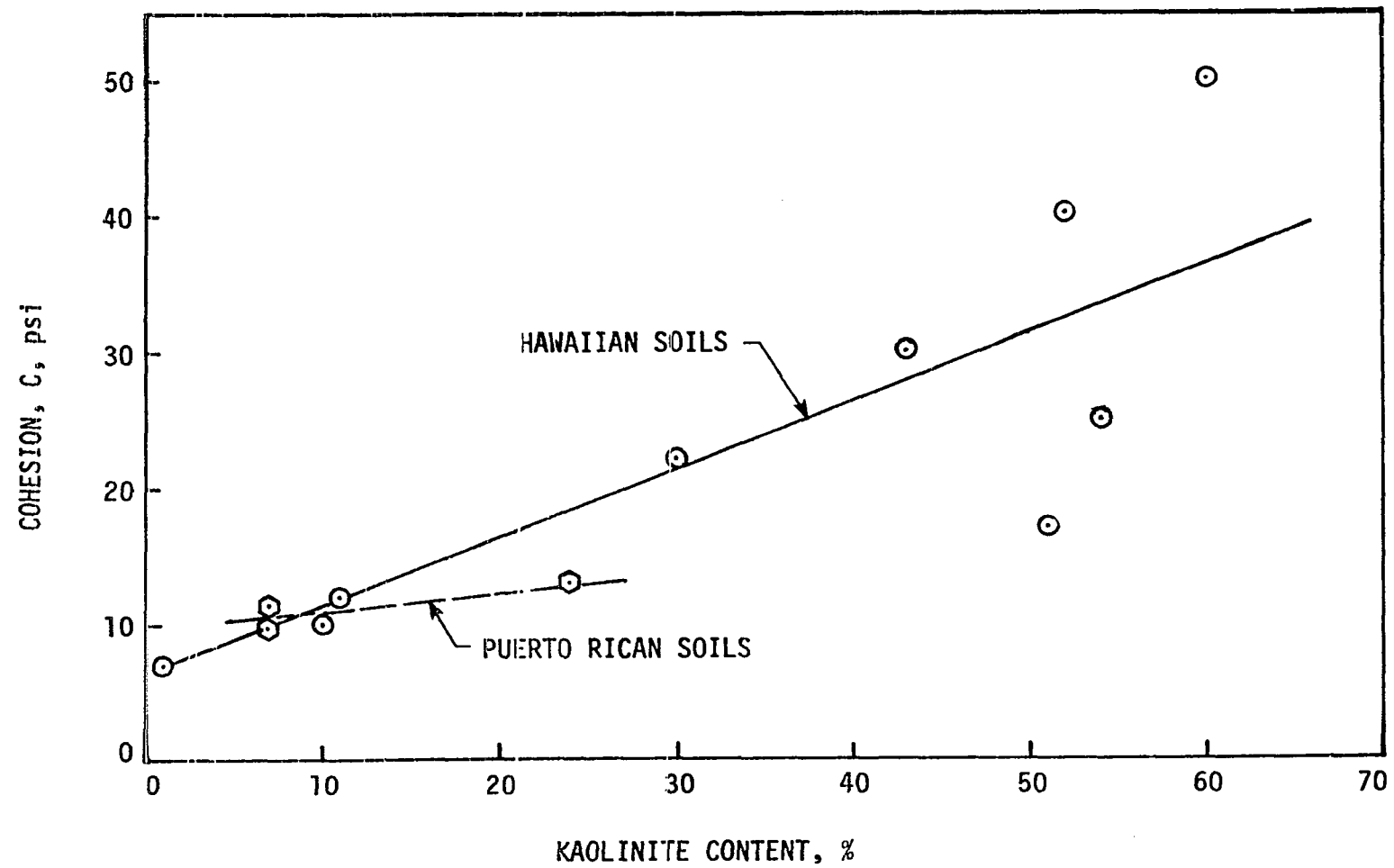


Figure 39. Relationship between cohesion and kaolinite content

within the same soil series (49), such that, the less moisture content, the stronger the soils become. This aspect was investigated here by comparing the cohesion values of the Hawaiian soils studied with their natural moisture contents. Figure 40 shows the variation in cohesion with varying natural moisture content, indicating that the cohesion reduces as the natural moisture increases.

Environmental Considerations

As stated previously, there are five main factors influencing the soil formation. They are parent material, climate, topography, vegetation, and time. The soils investigated in this study have more or less the same parent material, vegetation, and time. Even topography does not differ drastically from one soil series to another. Therefore, climate can be considered as the governing soil forming factor of the soils studied. Furthermore, rainfall intensity is the only major climatic factor varying from soil to soil. In a sense, rainfall here, reflects the degree of weathering of the soils. This fact can be observed readily by relating the other soil properties to rainfall. Good correlations exist between them, similar to those obtained between other soil properties and specific gravity. Mineralogy, for example, is highly related to rainfall in these soils. Figures 41-43 show the relationships of kaolinite, gibbsite and total iron with varying rainfall, respectively. Gibbsite and total iron increase, kaolinite decreases very systematically with increasing rainfall intensity indicating that more weathered soils occur in high rainfall regions. This is not always the case, though, there are

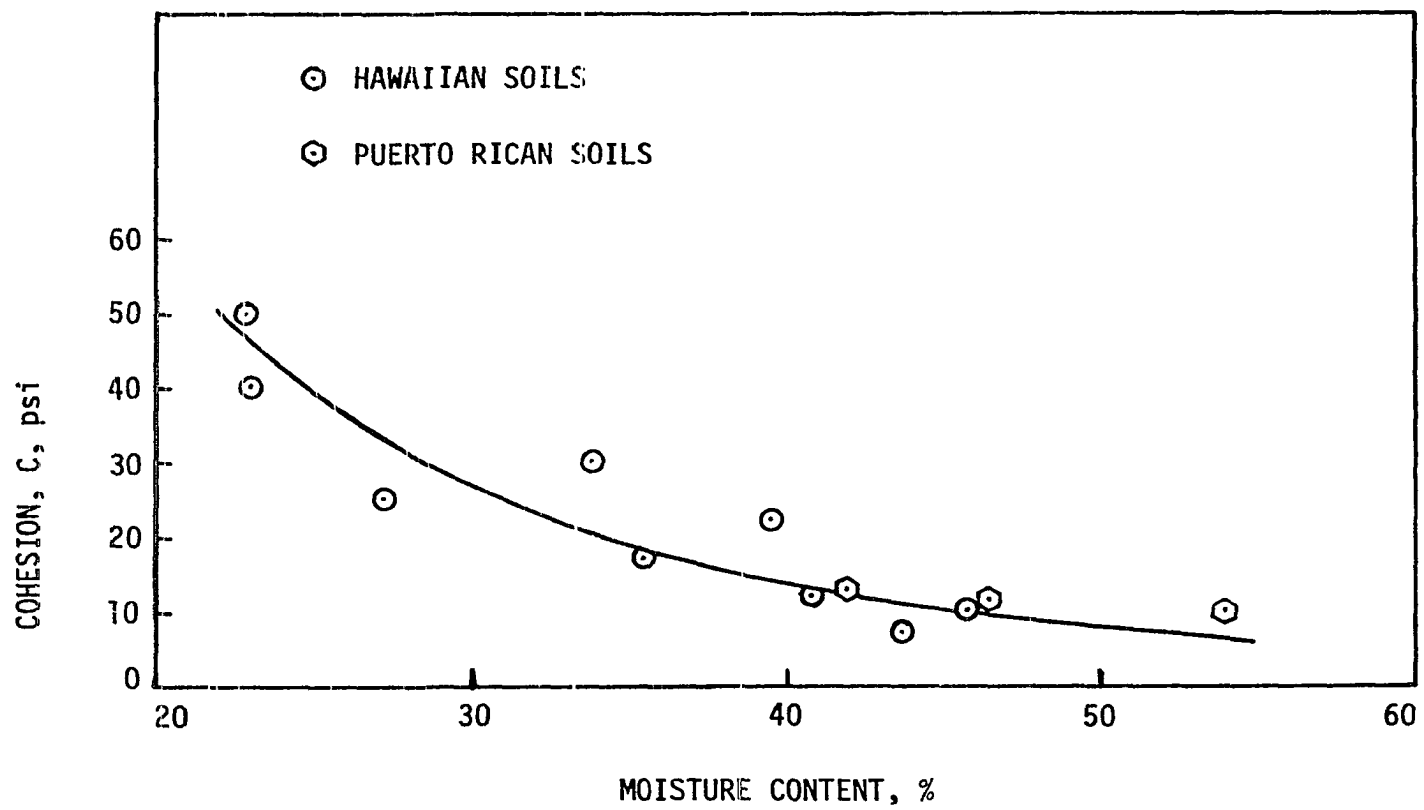


Figure 40. Relationship between cohesion and moisture content

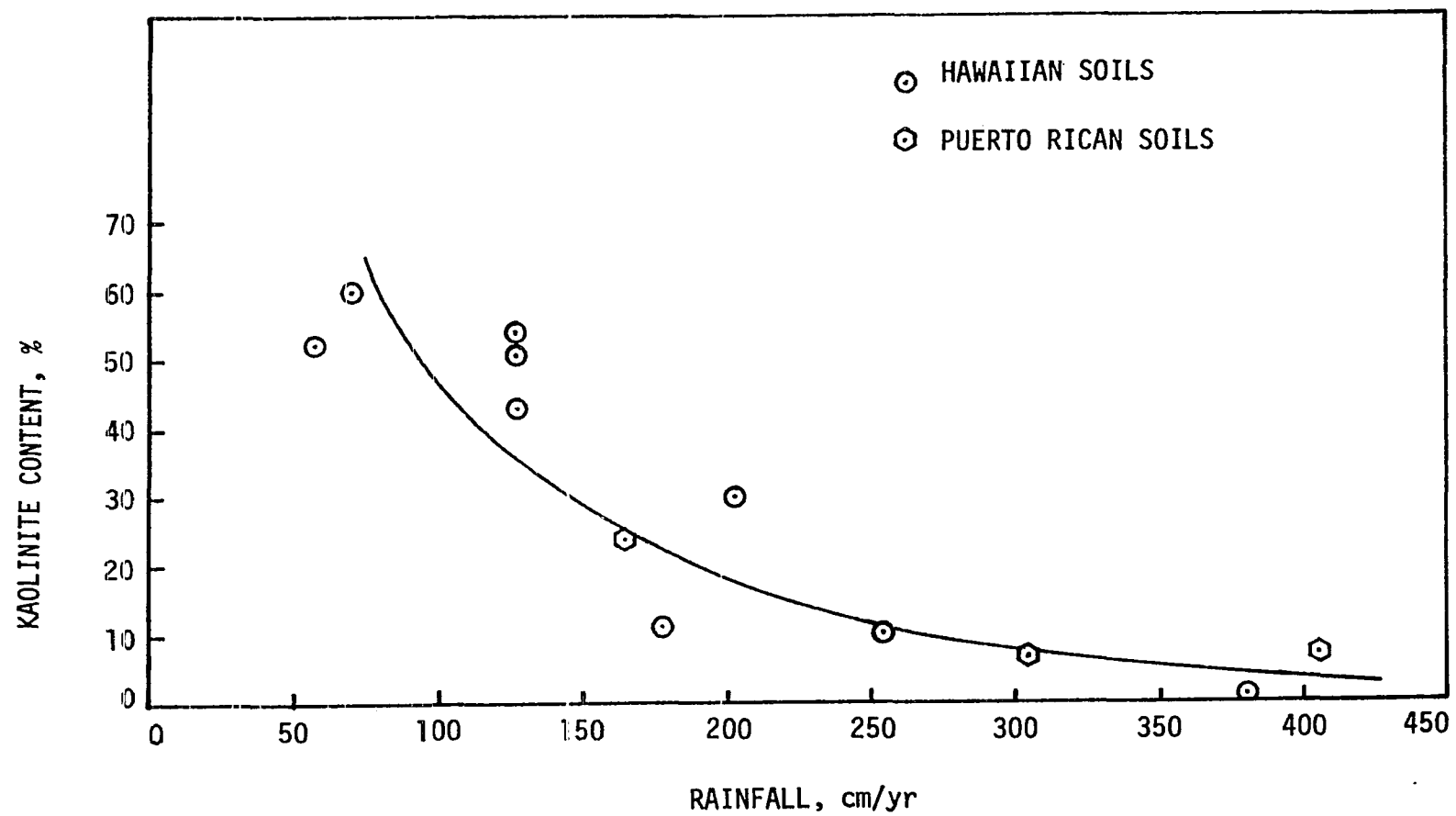


Figure 41. Relationship between kaolinite content and rainfall

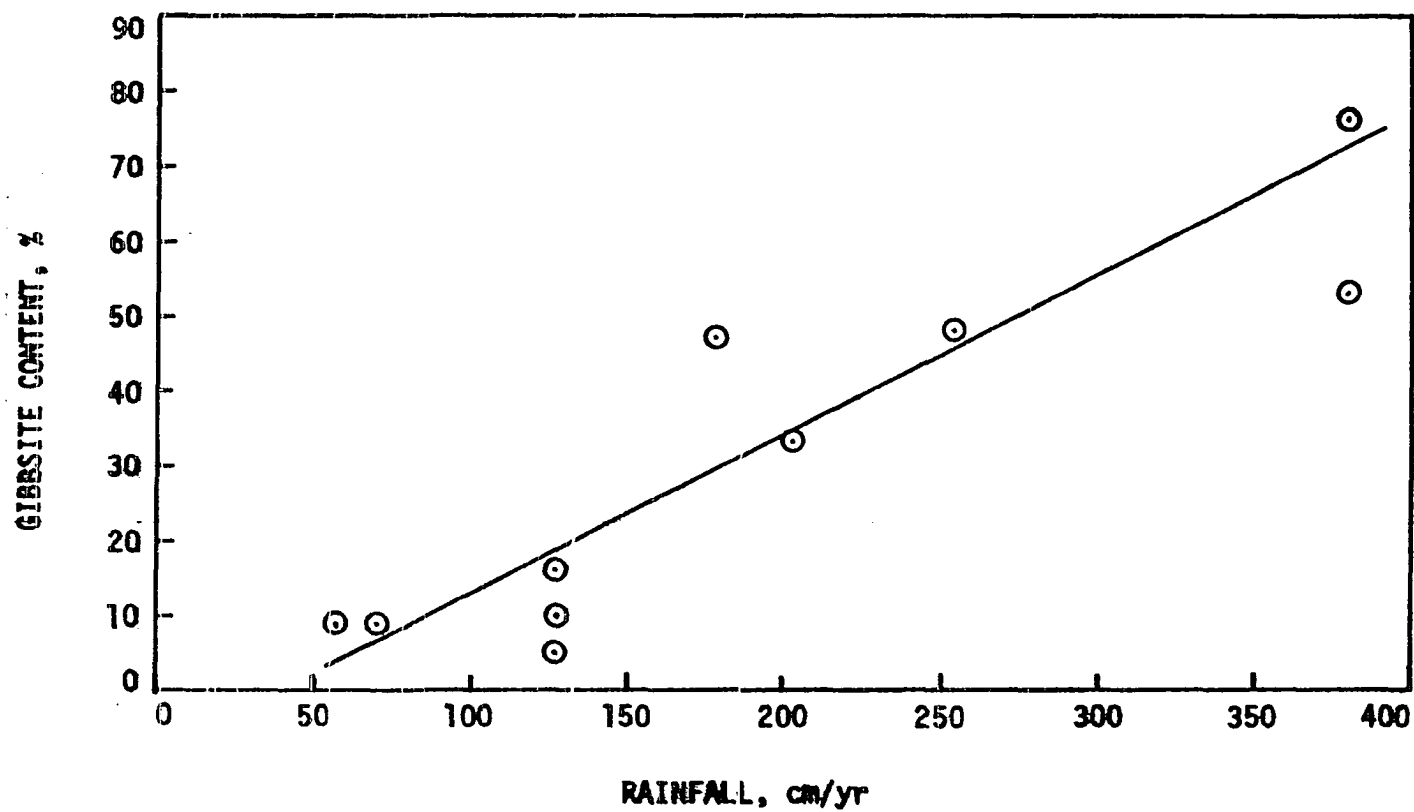


Figure 42. Relationship between gibbsite content and rainfall

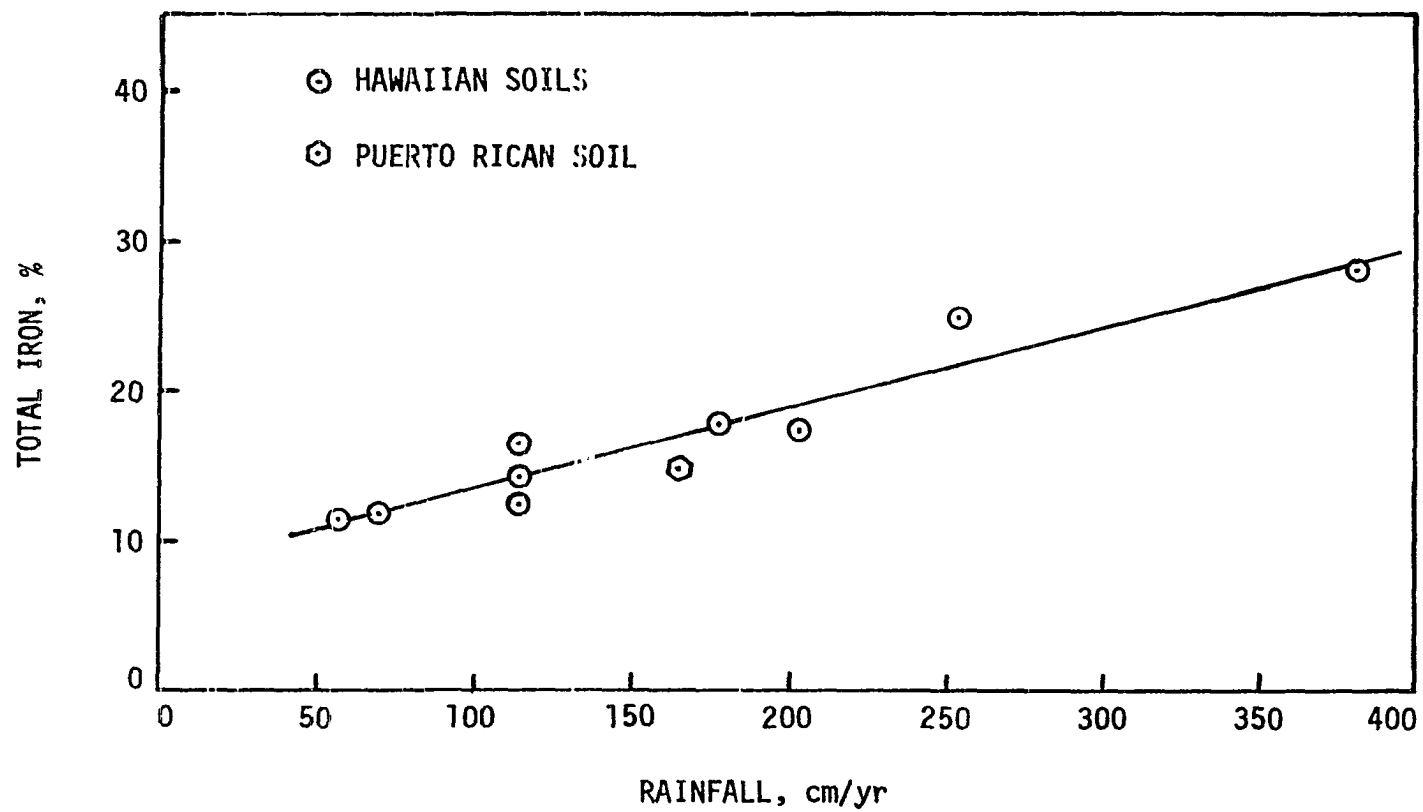


Figure 43. Relationship between total iron and rainfall

some cases in which the influence of some other soil factors outweigh that of climate. In their study on some selected lateritic soils from Puerto Rico, Lohnes and Demirel (37) found that for some soil series topography has much more influence on weathering than rainfall does. To show this better, specific gravity is plotted versus rainfall for Hawaiian and Puerto Rican soils as shown in Figure 44. As this figure exhibits specific gravity increases with increasing rainfall for Hawaiian soils, indicating that the rainfall is the major environmental factor influencing the weathering. In the case of Puerto Rican soils, however, specific gravity decreases with increasing rainfall showing that rainfall, as a soil forming factor, is not as effective as in the case of Hawaiian soils.

Natural moisture content and void ratio, which were found to influence the strength behavior of the soils, have tendencies to increase with increasing rainfall. Figure 45 shows the relationship between natural moisture content and rainfall intensity for Hawaiian and Puerto Rican soils.

A Model for Engineering Classification of Lateritic Soils Derived from Basalt

In the light of the previous discussions, an attempt is made here to establish a model which relates engineering properties, mineralogy, and strength characteristics of lateritic soils to weathering. The proposed model is shown schematically in Figure 46 and expands on an earlier proposal by Lohnes and Demirel (37). The model can be explained as follows.

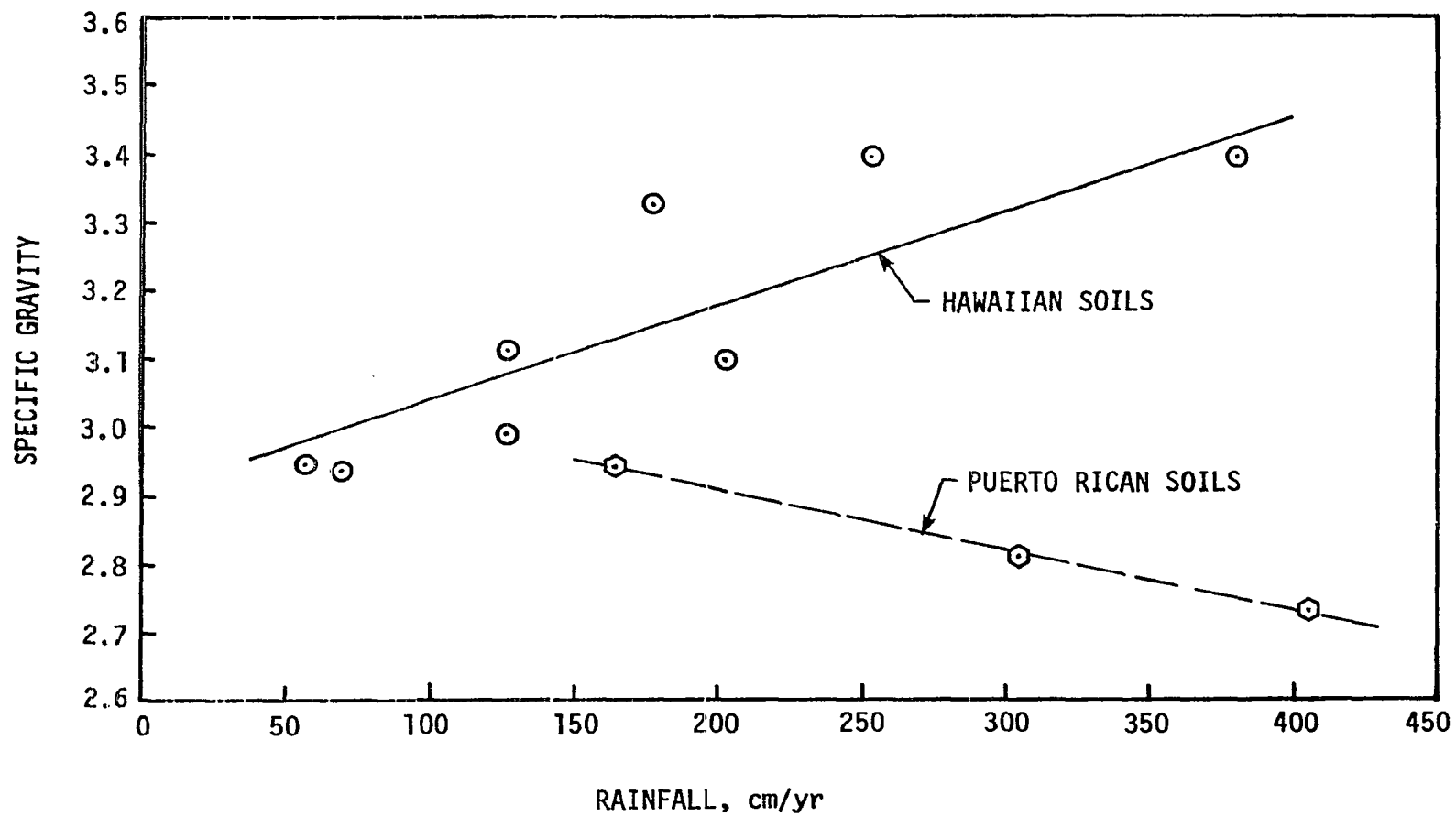


Figure 44. Relationship between specific gravity and rainfall

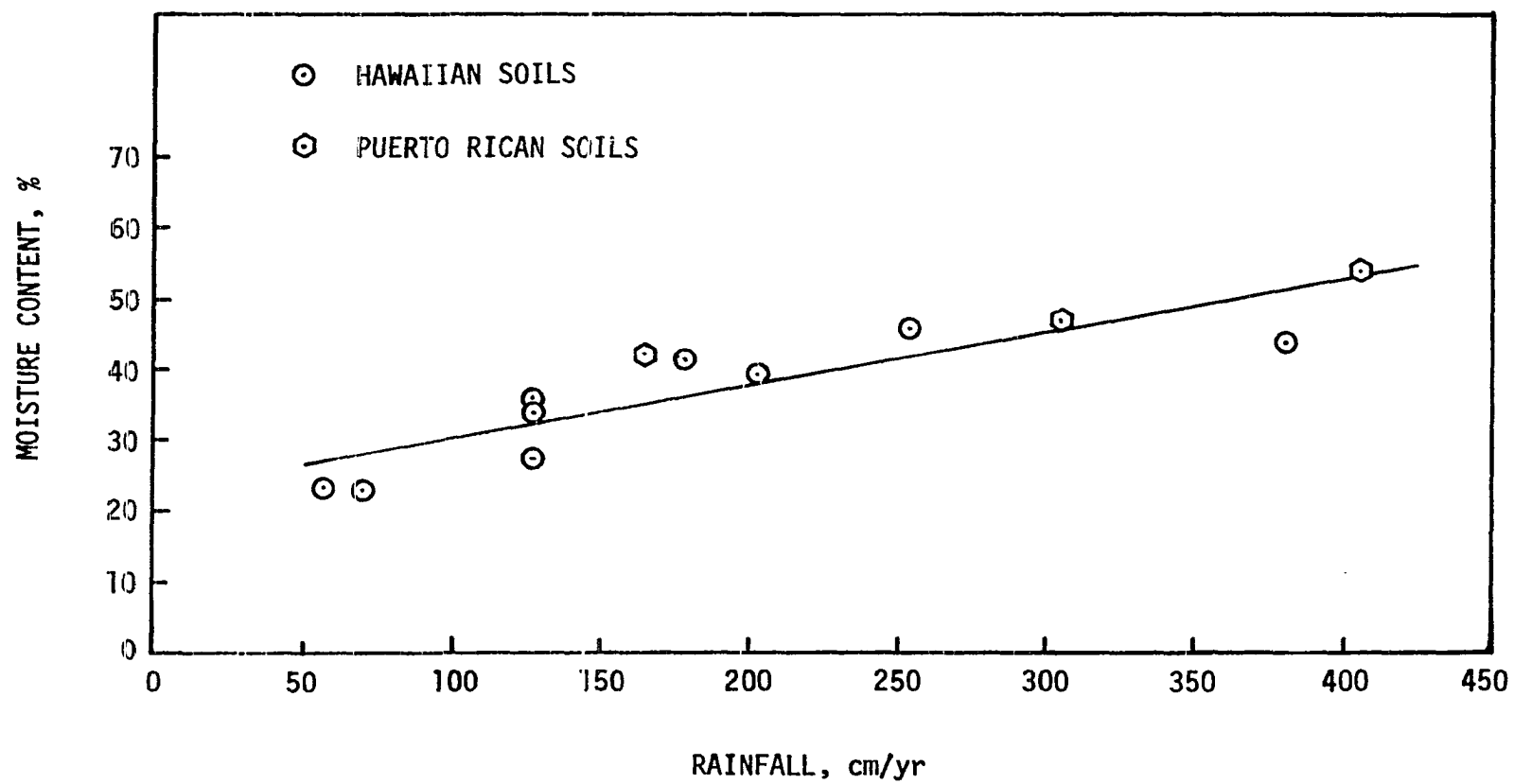


Figure 45. Relationship between moisture content and rainfall

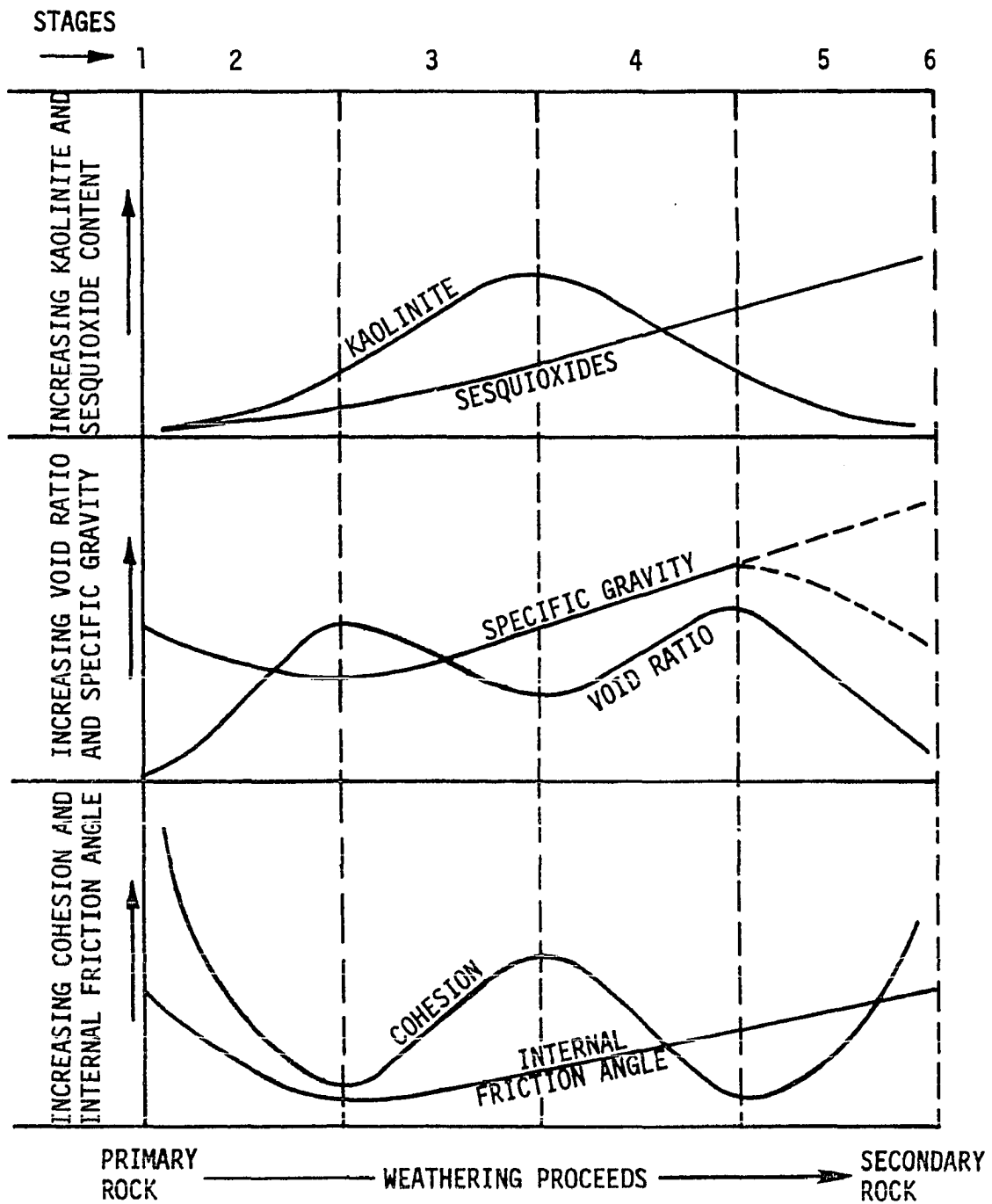


Figure 46. A model for variation in engineering properties of basalt derived lateritic soils resulting from weathering

The parent rock, shown as Stage 1 in Figure 46, has very low void ratio and quite high cohesion and internal friction angle. The characteristic values of these parameters and of specific gravity for basalts can be found in literature on rock mechanics (52,22,32,31) and they are listed below:

Specific gravity = 2.80-2.90

Void ratio = 0.01-0.03

Cohesion = 2800-8600 psi

Internal friction angle = 50-55 degrees

In Stage 2, the weathering starts to work on the rock, and the rock begins to disintegrate. This process causes a decrease in the cohesion and the internal friction angle, and an increase in void ratio. The specific gravity of the material, on the other hand, tends to decrease during this stage, because of the eventual formation of secondary minerals which have lower specific gravities than those of primary minerals.

During Stage 3, clay content continues to increase and becomes the major constituent of the soils. This leads to higher cohesion values. The internal friction angle also starts to increase in this stage as the clays fill the voids and produce a well-graded soil. As clays are formed, the voids are filled and consequently, the void ratio starts to decrease. The slow increase in sesquioxide content during Stage 3 influences the specific gravity of the material and it begins to increase especially due to high specific gravity values of iron compounds.

Further weathering brings the soil to Stage 4, in which while sesquioxide content keeps on increasing, kaolinite content starts to

decrease. As Alexander and Cady (3) point out, the kaolinite is probably converted to gibbsite at this stage of the weathering. Since sesquioxides are very active as binding agents, they cement clay particles together and form water stable soil aggregates. Although such stable aggregates have quite high internal cohesion within themselves, the cohesion of the whole soil domain starts to decrease due to the granular nature of the soil resulted from aggregation. The internal friction angle continues to increase due to the formation of large stable aggregates which, in turn, yield a higher degree of interlocking during shear. Specific gravity increases due to the increasing amount of iron oxides. Void ratio, on the other hand, starts to increase in this stage due to the increasing specific gravity which means less volume for solid phase in the soil domain, and due to the formation of larger aggregates which yield to larger pores among them.

In Stage 5, advanced weathering causes a further increase in the amount of sesquioxides and further cementation among the soil aggregates. This leads to the formation of larger concretions of gravel size, and consequently the void ratio starts to decrease. As cementation among larger particles goes on taking place, cohesion starts to increase, as well as internal friction angle. The variation in specific gravity during this stage depends on whether the sesquioxides of iron or aluminum are abundant in the soil. If iron is dominating, the specific gravity keeps on increasing, if aluminum is dominating, specific gravity decreases.

The formation of concretions is then followed by coalescence of concretions and their cementation by iron and/or aluminum colloids, until the

entire system is a continuous iron and/or aluminum oxide cemented crust. This end product of weathering is indicated as "secondary rock" in Figure 46. One may intuitively say that this end product will have high cohesion and internal friction angle, low void ratio, and either high or low specific gravity depending upon whether the laterite is ferruginous or aluminous, respectively.

The Hawaiian soils studied here cover Stage 4 and part of Stage 3 and 5. The Puerto Rican soils studied by Lohnes et al. (38,37) provide some data for Stage 3. Stage 1 is known from the studies performed on basalts and Stage 6 should be very close in properties to Stage 1. So, the only stage without any experimental evidence is Stage 2.

An Engineering Classification Scheme for Basalt Derived Lateritic Soils

The model described above indicates some very interesting correlations between the strength parameters and other properties of lateritic soils, in the course of weathering process.

The cohesion, for example, seems to be closely related to void ratio, such that it increases as void ratio decreases. The internal friction angle, on the other hand, has a good correlation with the specific gravity. More specifically, internal friction angle increases with increasing specific gravity.

The strength characteristics of lateritic soils can also be related to the mineralogy. Kaolinite content, for example, appears to be controlling the cohesion, such that as it increases, cohesion also increases.

Sesquioxide content appears to be controlling the internal friction angle; larger the sesquioxide content, higher the internal friction angle.

A common problem facing the field engineer in the tropics is how to predict the behavior of lateritic soils without doing extensive measurements on soils. The relationships mentioned above suggest an engineering classification scheme for basalt derived lateritic soils in order to meet that need. The specific gravity and the void ratio are two easily determined soil properties which can be used for classification purposes. Figure 47 shows the proposed classification system for basalt derived lateritic soils. Mineralogy is left out from the classification system, since it needs special instruments and time consuming approaches to be determined.

According to the classification system proposed, a specific gravity value of 3.05 is considered to be critical from the engineering point of view. Most of the relationships between any soil properties and specific gravity show differing trends above and below that value of specific gravity. Due to the granular nature of the soils which have specific gravities larger than 3.05, the internal friction angle is quite high, more specifically, higher than 35 degrees.

The data also suggest some critical values for void ratio. As stated previously, cohesion increases with decreasing void ratio. Therefore, void ratios of 1.25 and 0.90 are chosen as being the critical void ratios. Soils having void ratios larger than 1.25 have low cohesion values, lower than 20 psi. Soils which have void ratios between 1.25-0.90 have higher cohesion values, higher than 20 psi. In cases where void ratio is lower than 0.90, the cohesion gets considerably higher.

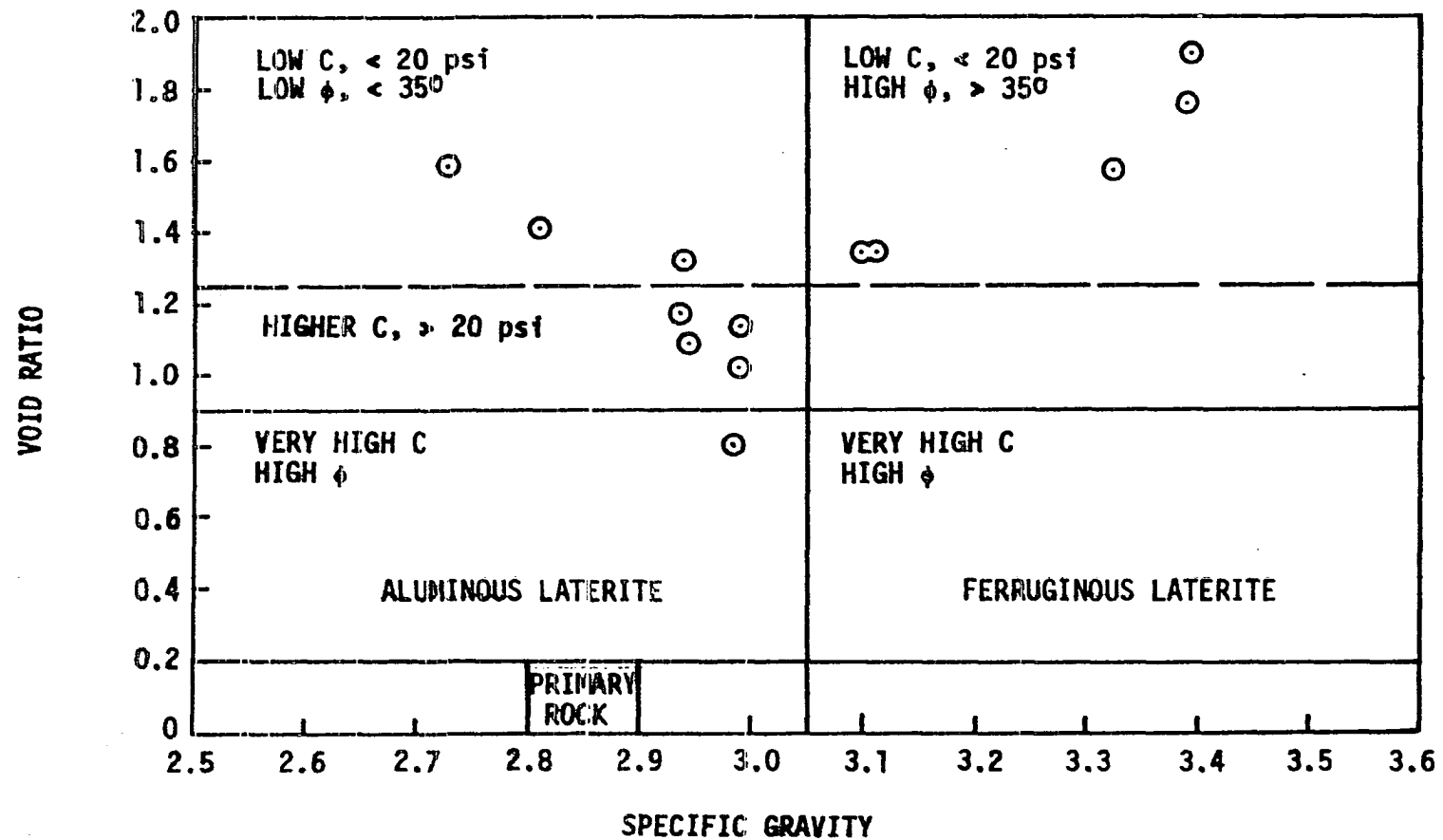


Figure 47. Engineering classification of basalt derived lateritic soils

The classification system shown in Figure 47 contains several regions corresponding to different values of specific gravity and void ratio, and each region indicates a range for strength parameters of the soils which fall in that region.

In any case, mineralogical analysis can be used as further information to find out the stage of weathering at which the soil is occurring and have additional data for predicting the engineering behavior of soils.

CONCLUSIONS

Based upon the results of this study, the following conclusions can be made regarding the engineering behavior of the Hawaiian basalt derived lateritic soils:

1. Plasticity and gradation data of the soils studied do not show any appreciable correlations with the degree of weathering or with other properties of soils. This supports the idea that they cannot be satisfactorily used for classification of lateritic soils.

2. Mineralogy has very good correlation with the degree of weathering. Kaolinite content first increases and then decreases with increasing weathering, whereas, sesquioxides of aluminum and iron keep on increasing in amount all the way through, as weathering proceeds.

Organic matter was found to be increasing with proceeding weathering.

3. Specific gravity of lateritic soils can be utilized as a parameter that reflects the degree of weathering. This can be justified by the definition of specific gravity which reads as the weighted average of the specific gravities of the minerals comprising the soil. Since in the course of weathering the content of heavy minerals keeps on increasing all the way through, the specific gravity should also increase as the weathering proceeds.

4. Pore size analysis with mercury injection technique, slaking tests, and scanning electron microscopy studies revealed that soil aggregation increases with increasing weathering due to the increasing amount of sesquioxides which act as binding agents to cement the soil particles together. This yields a soil which is granular in nature.

5. Strength parameters, cohesion and internal friction angle, as determined by direct shear testing, have systematic trends with increasing degree of weathering. Cohesion and internal friction angle appear to be controlled by void ratio and specific gravity, respectively. More specifically, cohesion increases with decreasing void ratio, and internal friction angle keeps on increasing as the specific gravity increases.

6. Strength parameters can also be related to mineralogy. Kaolinite content and sesquioxide content control the cohesion and the internal friction angle, respectively. The cohesion increases with increasing kaolinite content, and the internal friction angle increases with increasing sesquioxide content.

7. For the particular group of soils investigated in this study, rainfall intensity appears to be the only varying soil forming factor from one soil series to another. The rest of the soil forming factors are more or less the same for all the soil series.

8. The conclusive remarks made above suggest a model for relating engineering properties, mineralogy, and strength characteristics of basalt derived lateritic soils to weathering in the manner as shown schematically in Figure 46. Hawaiian and Puerto Rican lateritic soils derived from basalt provide some experimental evidences to justify this suggested model.

9. Specific gravity and void ratio are the two easily determined parameters which classify basalt derived lateritic soils. The classification scheme is shown in Figure 47. In general, void ratio controls the cohesion and specific gravity controls the internal friction angle. More

specifically, larger the void ratio lower the cohesion, and larger the specific gravity higher the internal friction angle.

LITERATURE CITED

1. Adler, I. 1966. X-ray emission spectrography in geology. Methods in geochemistry and geophysics 4. Elsevier Publishing Company, New York.
2. Ahmed, S., C. W. Lovell, Jr. and S. Diamond. 1974. Pore sizes and strength of compacted clay. Journal of the Geotechnical Engineering Division, ASCE 100:407-425.
3. Alexander, L. T. and J. G. Cady. 1962. Genesis and hardening of laterite in soils. U.S. Department of Agriculture Tech. Bull. 1282.
4. American Association of State Highway Officials. 1971. Standard specifications for highway materials and methods of sampling and testing: Part II. 10th ed. Washington, D.C.
5. Arca, M. N. and S. B. Weed. 1966. Soil aggregation and porosity in relation to contents of free iron oxide and clay. Soil Science 101: 164-170.
6. Badger, W. W. and R. A. Lohnes. 1973. Pore structure of friable loess. Highway Research Record 429:14-23.
7. Baldovin, G. 1969. The shear strength of lateritic soils. Proc. of Specialty Session of Engineering Properties of Lateritic Soils, 7th Int. Conf. Soil Mech. Found. Eng., Mexico City 1:129-142.
8. Baver, L. D., W. H. Gardner and W. R. Gardner. 1972. Soil physics. 4th ed. John Wiley and Sons, Inc., New York.
9. Beattie, H. J. and R. M. Brissey. 1954. Calibration method for X-ray fluorescence spectrometry. Anal. Chem. 26:980.
10. Beinroth, F. H., G. Uehara and H. Ikawa. 1974. Geomorphic relationships of oxisols and ultisols on Kauai, Hawaii. Soil Science Soc. Am. 38:128-131.
11. Bhatia, H. S. 1970. Discussion of engineering characteristics of laterites. Proc. of Specialty Session on Engineering Properties of Lateritic Soils, 7th Int. Conf. Soil Mech. Found. Eng., Mexico City 1:75-80.
12. Birks, L. S. 1959. X-ray spectrochemical analysis. Interscience Publishers, Inc., New York.
13. Blokhin, M. A. 1965. Methods of X-ray spectroscopic research. Pergamon Press, Elmsford, New York...

14. Buringh, P. 1970. Introduction to the study of soils in tropical and subtropical regions. 2nd ed. Centre for Agricultural Publishing and Documentation, Wageningen, the Netherlands.
15. Carroll, D. 1970. Clay minerals: A guide to their X-ray identification. Geological Society of America (Boulder, Colorado) Special paper 126.
16. Carroll, D. and M. Woof. 1951. Laterite developed on basalt at Inverell, New South Wales. Soil Science 72(2):87-99.
17. Cullity, B. D. 1967. Elements of X-ray diffraction. Addison-Wesley Publishing Company, Inc., Reading, Mass.
18. Dean, L. A. 1947. Differential thermal analysis of Hawaiian soils. Soil Science 63:95-105.
19. DeGraft-Johnson, J. W. S., H. S. Bhatia and D. M. Gidigas. 1969. The engineering characteristics of the laterite gravels of Ghana. Proc. of Specialty Session on Engineering Properties of Lateritic Soils, 7th Int. Conf. Soil Mech. Found. Eng., Mexico City 1:117-129.
20. Diamond, S. 1970. Pore size distribution in clays. Clays and Clay Miner. 18:7-23.
21. Dumbleton, M. J., G. West and D. Newill. 1966. The mode of formation, mineralogy and properties of some Jamaican soils. Eng. Geol. 1(3):235-249.
22. Farmer, I. W. 1968. Engineering properties of rocks. E. & F. N. Spon Ltd., London.
23. Fish, R. O. 1971. Shear strength and related engineering properties of selected Puerto Rican oxisols and ultisols. Unpublished M.S. thesis, Iowa State University, Ames, Iowa.
24. Foote, D. E., E. L. Hill, S. Nakamura and F. Stevens. 1972. Soil survey of the Islands of Kauai, Oahu, Maui, Molokai, and Lanai, State of Hawaii. Soil Conservation Service, USDA, in cooperation with University of Hawaii Agr. Exp. Sta., U.S. Gov. Printing Office, Washington, D.C.
25. Fruhauf, B. 1946. A study of lateritic soils. Highway Research Board Proceeding. pp. 579-589.
26. Gidigas, M. D. 1971. The importance of soil genesis in the engineering classification of Ghana soils. Eng. Geol. 5:117-161.

27. Hamilton, R. 1964. Microscopic studies of laterite formations. Pages 269-276 in A. Jongerius, ed. Soil micromorphology. Elsevier Publishing Company, New York.
28. Handy, R. L. and E. A. Rosauer. 1959. X-ray fluorescence analysis of total iron and manganese in soils. Proc. Iowa Academy of Science 66:237-247.
29. Henkle, D. J. 1956. The effect of overconsolidation on the behavior of clays during shear. Geotechnique 6:139-150.
30. Humbert, R. P. 1948. The genesis of laterite. Soil Science 65(4): 281-290.
31. Jaeger, C. 1972. Rock mechanics and Engineering. Cambridge University Press, New York.
32. Jaeger, J. C. and N. G. W. Cook. 1969. Fundamentals of rock mechanics. Methuen & Co., Ltd., London.
33. Jenkins, R. and J. L. deVries. 1967. Practical X-ray spectrometry. Philips Technical Library.
34. Klug, H. P. and L. E. Alexander. 1954. X-ray diffraction procedures. John Wiley and Sons, Inc., New York.
35. Little, A. L. 1969. The engineering classification of residual tropical soils. Proc. of Specialty Session on Engineering Properties of Lateritic Soils, 7th Int. Conf. Soil Mech. Found. Eng., Mexico City 1:1-10.
36. Lohnes, R. A. and R. L. Handy. 1968. Shear strength of some Hawaiian latosols. Proc. 6th Annual Symposium on Eng. Geol. and Soil Eng., Boise, Idaho.
37. Lohnes, R. A. and T. Demirel. 1973. Strength and structure of laterities and lateritic soils. Eng. Geol. 7:13-33.
38. Lohnes, R. A., R. O. Fish and T. Demirel. 1971. Geotechnical properties of selected Puerto Rican soils in relation to climate and parent rock. Geol. Soc. Am. 82:2617-2624.
39. Lohnes, R. A., E. R. Tuncer and T. Demirel. 1975. Pore structure of selected Hawaiian soils. Transportation Research Board. (To be published)
40. Lutz, J. F. 1936. The relation of free iron in the soil to aggregation. Soil Science Soc. Am. Proc. 1:43-45.

41. Mackenzie, R. C. 1957. The differential thermal investigation of clays. Mineralogical Society (Clay Minerals Group), London.
42. Maignien, R. 1966. Review of research on laterites. UNESCO Natural Resources Research IV.
43. Mitchell, J. K. 1956. The fabric of natural clays and its relation to engineering properties. Highway Research Board 35:693-713.
44. Moh, Z. C. and F. M. Mazhar. 1969. Effects of method of preparation on index properties of lateritic soils. Proc. of Specialty Session on Engineering Properties of Lateritic Soils, 7th Int. Conf. Soil Mech. Found. Eng., Mexico City 1:23-25.
45. Mohr, E. C. J. and F. A. Van Baren. 1954. Tropical soils. Under the auspices of the Royal Tropical Institute, Amsterdam. Interscience Publishers, New York.
46. Moye, D. G. 1955. Engineering geology for the Snowy Mountains scheme. Institution of Engineers, Australia, Vol. 27.
47. Müller, R. O. 1972. Spectrochemical analysis by X-ray fluorescence. Plenum Press, New York.
48. Norrish, K. and R. M. Taylor. 1962. Quantitative analysis by X-ray diffraction. Clay Minerals Bull 5(28):98-109.
49. Paulson, S. K. 1975. The strength, structure, and mineralogy of selected Hawaiian lateritic soils. Unpublished M.S. thesis, Iowa State University, Ames, Iowa.
50. Peterson, J. B. 1946. The role of clay minerals in the formation of soil structure. Soil Science 61:247-256.
51. Prescott, J. A. and R. L. Pendleton. 1952. Laterite and lateritic soils. Commonwealth Bureau of Soil Science, Technical Communication No. 47.
52. Reynolds, H. R. 1961. Rock mechanics. Ungar Publishing Company, New York.
53. Ruddock, E. C. 1969. Properties and position in lateritic ground: Some statistical relationships. Proc. of Specialty Session on Engineering Properties of Lateritic Soils, 7th Int. Conf. Soil Mech. Found. Eng., Mexico City 1:11-21.
54. Sherman, G. D. 1949. Factors influencing the development of lateritic and laterite soils in the Hawaiian Islands. Pacific Science 3(4):307-314.

55. Sherman, G. D. 1950. The genesis and morphology of Hawaiian ferruginous laterite crusts. *Pacific Science* 4:315-322.
56. Sherman, G. D. 1952. The titanium content of Hawaiian soils and its significance. *Soil. Sci. Soc. Am. Proc.* 16(1):15-18.
57. Sherman, G. D. and Y. Kanehiro. 1954. Origin and development of ferruginous concretions in Hawaiian latosols. *Soil Science* 77(1): 1-8.
58. Sherman, G. D., Z. C. Foster and C. K. Fujimoto. 1949. Some of the properties of the ferruginous humic latosols of the Hawaiian Islands. *Soil Sci. Soc. Am. Proc.* 13:471-476.
59. Sherman, G. D., Y. Kanehiro and Y. Matsusaka. 1953. The role of dehydration in the development of laterite. *Pacific Science* 7(4): 438-446.
60. Sivarajasingham, S., L. T. Alexander, C. G. Cady and M. G. Cline. 1962. Laterite: In advances in agronomy. Academic Press, New York.
61. Skempton, A. W. 1953. The colloidal activity of clays. *Proc. 3rd Int. Conf. Soil Mech. Found. Eng., Zurich* 1:57-62.
62. Skempton, A. W. 1964. Long-term stability of clay slopes. *Geo-technique* 14:75-102.
63. Smothers, W. J. and Y. Chiang. 1966. Handbook of differential thermal analysis. Chemical Publishing Company, Inc., New York.
64. Sridharan, A. M., A. G. Altschaeffl and S. Diamond. 1971. Pore size distribution studies. *J. Soil Mech. Found. Eng. Div., ASCE* 97(SM5): 771-787.
65. Tanada, T. 1942-1944. Hawaiian soil colloids. University of Hawaii Agr. Exp. Sta. Report. pp. 56-57.
66. Terzaghi, K. 1958. Design and performance of Sasumua Dam. *Inst. Civil Engineers Proc.* 9:369-395.
67. Topping, J. 1957. Errors of observation and their treatment. The Institute of Physics, London.
68. Tovey, N. K. and K. Y. Wong. 1973. The preparation of soils and other geological materials for the SEM. *Proc. Int. Symp. on Soil Structure, Gothenburg, Sweden*, pp. 59-67.
69. Townsend, F. C., P. G. Manke and J. V. Parcher. 1969. Effects of remolding on the properties of the lateritic soil. 48th Annual Meeting, Highway Research Board.

70. Trow, W. A. and J. D. Morton. 1969. Lateritic soils at Guardarraya, La Republica Dominicana, their development, composition, and engineering properties. Proc. Specialty Session on Engineering Properties of Lateritic Soils, 7th Int. Conf. Soil Mech. Found. Eng., Mexico City 1:75-85.
71. Tsuji, G. Y., R. T. Watanabe and W. S. Sakai. 1975. Influence of soil microstructure on water characteristics of selected Hawaiian soils. Soil Sci. Soc. Am. Proc. 39:28-33.
72. U.S. Department of Agriculture, Soil Conservation Service. 1960. Soil classification, a comprehensive system, 7th approximation. U.S. Gov. Printing Office, Washington, D.C.
73. U.S. Department of Agriculture, Soil Conservation Service. 1972. Soil survey of islands of Kauai, Oahu, Maui, Molokai, and Lanai, State of Hawaii. In cooperation with the University of Hawaii Agr. Exp. Sta., U.S. Gov. Printing Office, Washington, D.C.
74. Vallergera, B. A. and N. Rananandana. 1969. Characteristics of lateritic soils used in Thailand road construction. Highway Research Record 284:86-103.
75. Wallace, K. B. 1973. Structural behavior of residual soils of the continually wet highlands of Papua, New Guinea. Geotechnique 2: 203-218.
76. Washburn, E. W. 1921. Note on a method of determining the distribution of pore sizes in a porous material. Natl. Acad. Sci. Proc. 7:115-116.
77. Wendlandt, W. W. 1974. Thermal methods of analysis. John Wiley and Sons, Inc., New York.
78. Wentworth, C. J. and H. Winchell. 1947. Koolau basalt series, Oahu, Hawaii. Bulletin of the Geol. Soc. Am. 58:46-78.
79. Winterkorn, H. F. and E. C. Chandrashekharan. 1951. Laterite soils and their stabilization. Highway Research Board Bull. 44:10-29.
80. Wooltorton, F. L. D. 1954. The scientific basis of road design. Edward Arnold Publishers, Ltd., London.

ACKNOWLEDGMENTS

The author wishes to gratefully acknowledge the support given to this research project by the Environmental Sciences Division, Army Research Office, Durham, North Carolina, and the cooperation given by the Hawaiian Office of the Soil Conservation Service, U.S. Department of Agriculture.

Dr. R. A. Lohnes, the author's major professor, deserves a very special thank you, not only for suggesting this research problem but also for his invaluable guidance, enthusiasm, encouragement and friendship in making this dissertation possible.

A special thank you must also go to Dr. T. Demirel for his never ending encouragement, guidance, and assistance especially in the mineralogical and elemental studies performed for this dissertation; and for his support as a friend during the performance of the work.

The author is grateful to the other three able members of his graduate committee, namely, Dr. J. L. Mickle, Dr. W. H. Scholtes, and Dr. R. D. Cody.

It is difficult to single out all the other persons who have assisted with this study at one time or another. The author would like to extend his appreciation to the various faculty members and students of Soil Engineering Division, and to the other personnel of the Engineering Research Institute, for their assistance and friendship during these past two and a half years.

APPENDIX A: QUANTITATIVE X-RAY DIFFRACTION AND
FLUORESCENCE ANALYSES RESULTS

Table A1. Quantitative X-ray diffraction and fluorescence analyses results

Soil series	Determination of hematite content by quantitative X-ray diffraction			Determination of total iron content by quantitative X-ray fluorescence		
	Slope	Intercept	Hematite, %	Slope	Intercept	Total iron, %
Molokai	1.1304	0.2584	12.1	0.5797	0.2053	11.0
Lahaina	0.2971	0.1444	10.0	0.3448	0.1859	11.5
Wahiawa	1.1087	0.3110	12.8	0.6622	0.2404	12.0
Manana	0.6522	0.1077	6.1	0.2174	0.2437	15.6
Paaloa	0.4058	0.3393	19.4	0.4451	0.3166	16.7
Lihue	0.7101	0.0648	3.7	0.3830	0.2418	14.0
Puhi	0.1449	0.1846	13.9	0.9834	0.4234	16.4
(shallow)	0.3551	0.1654	10.9	2.5128	0.5481	12.8
(deep)	0.5863	0.1394	8.1	0.7246	0.4231	18.2
Kapaa	0.2681	0.0878	6.5	0.9213	0.7166	24.3
Halii	0.1594	0.1529	11.6	1.0041	0.8777	26.9
(soil matrix)	0.2826	0.2341	15.4	1.6503	0.6270	17.7
(concretion)	0.4420	0.2170	13.1	1.3561	0.5921	18.5

APPENDIX B: PORE SIZE DISTRIBUTION CURVES
OBTAINED FROM MERCURY POROSIMETRY

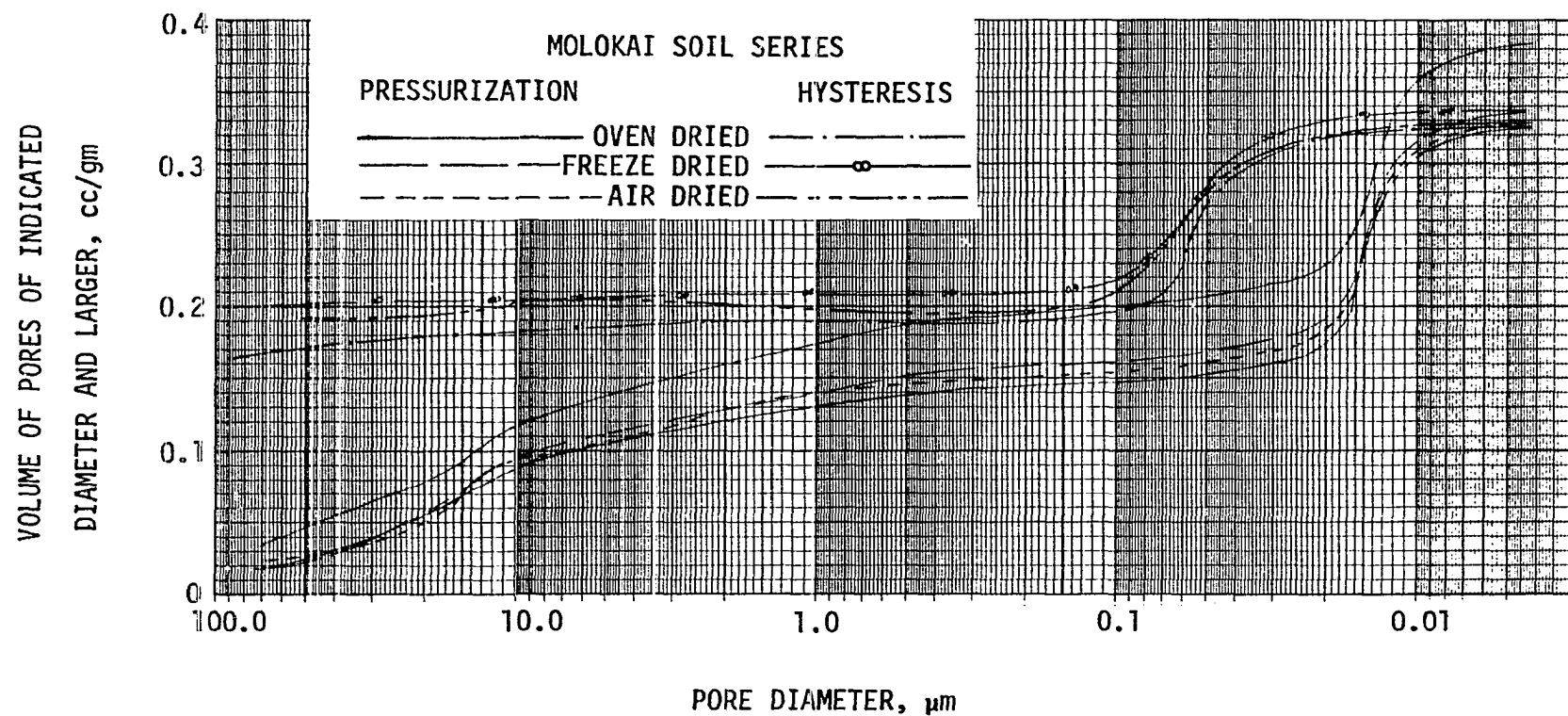


Figure B1. Pore size distribution curves for Molokai soil series

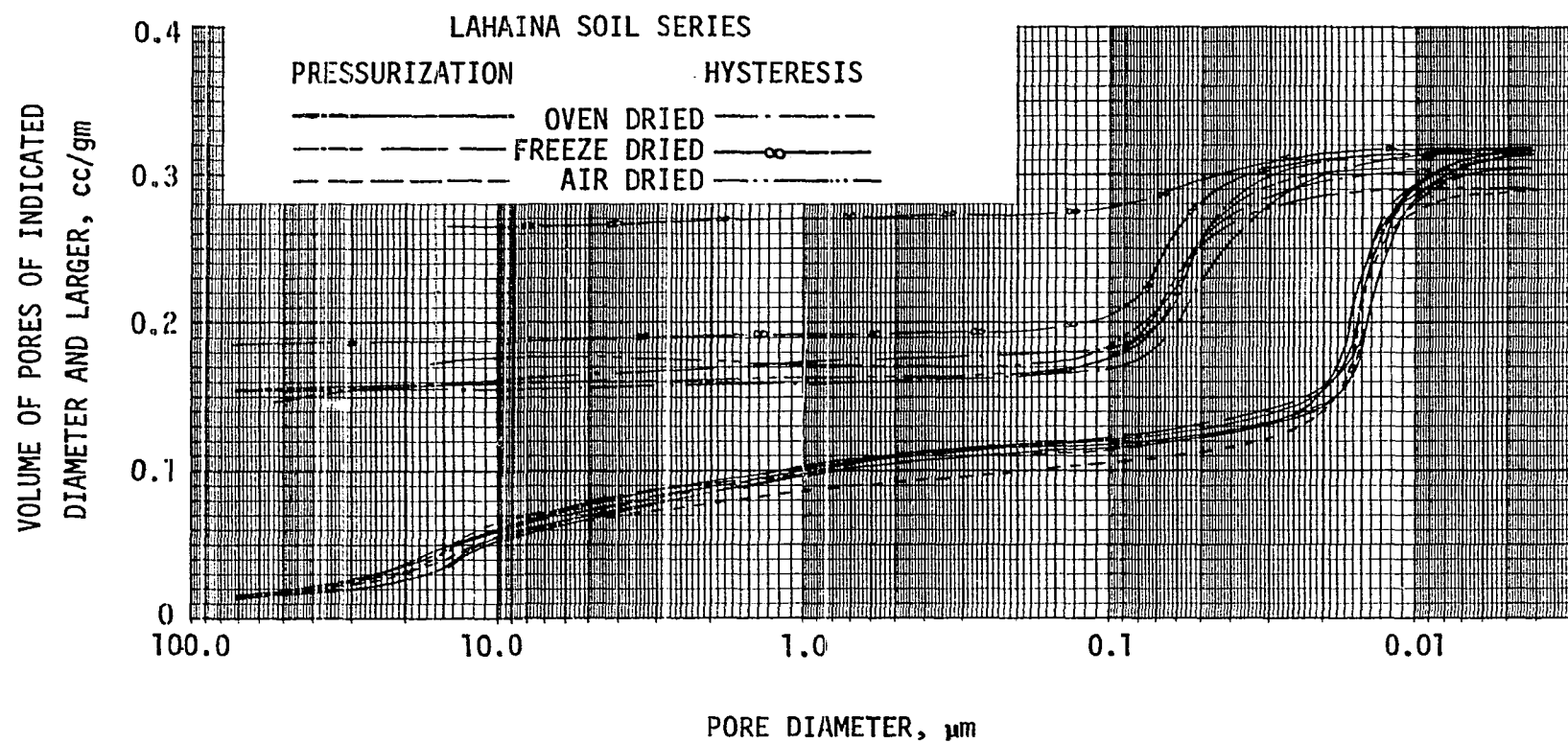


Figure B2. Pore size distribution curves for Lahaina soil series

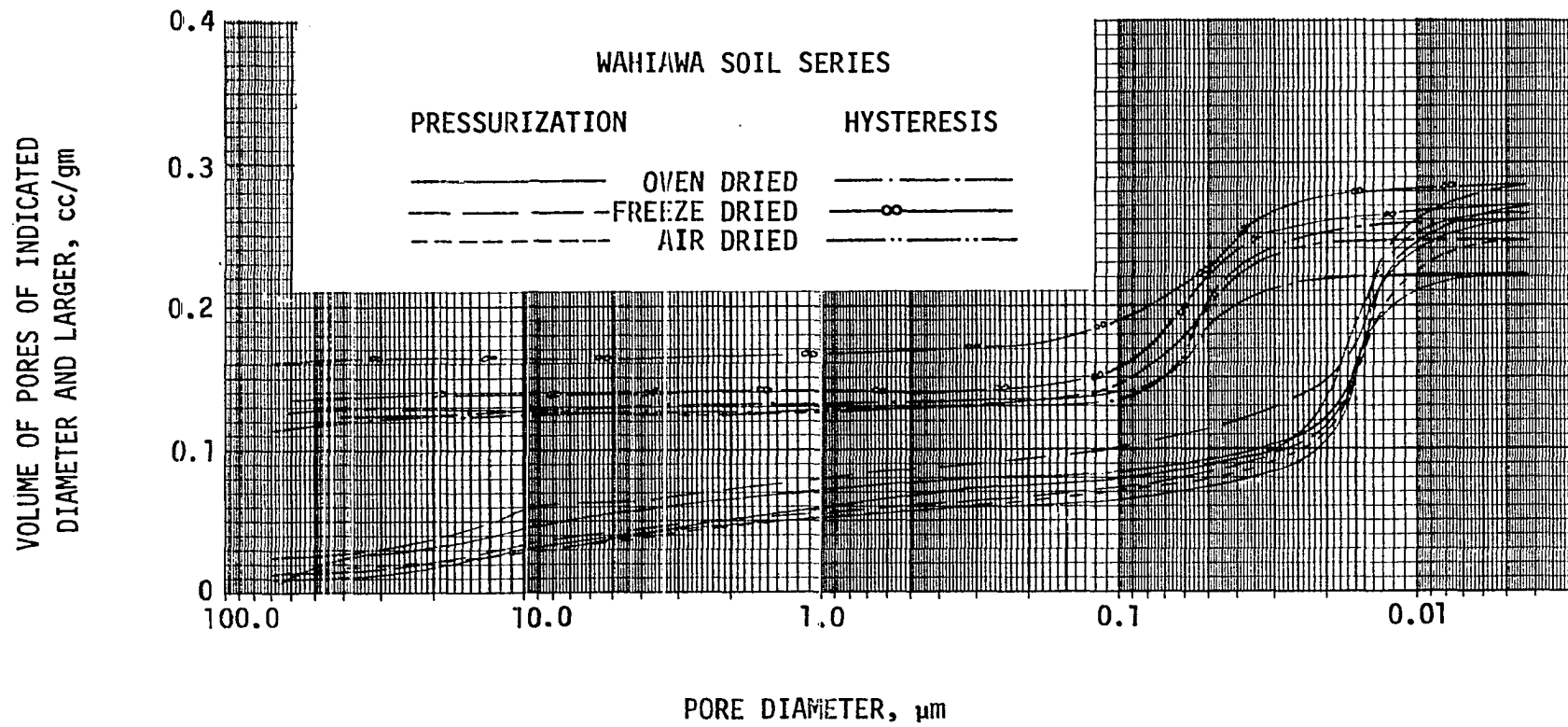


Figure B3. Pore size distribution curves for Wahaiwa soil series

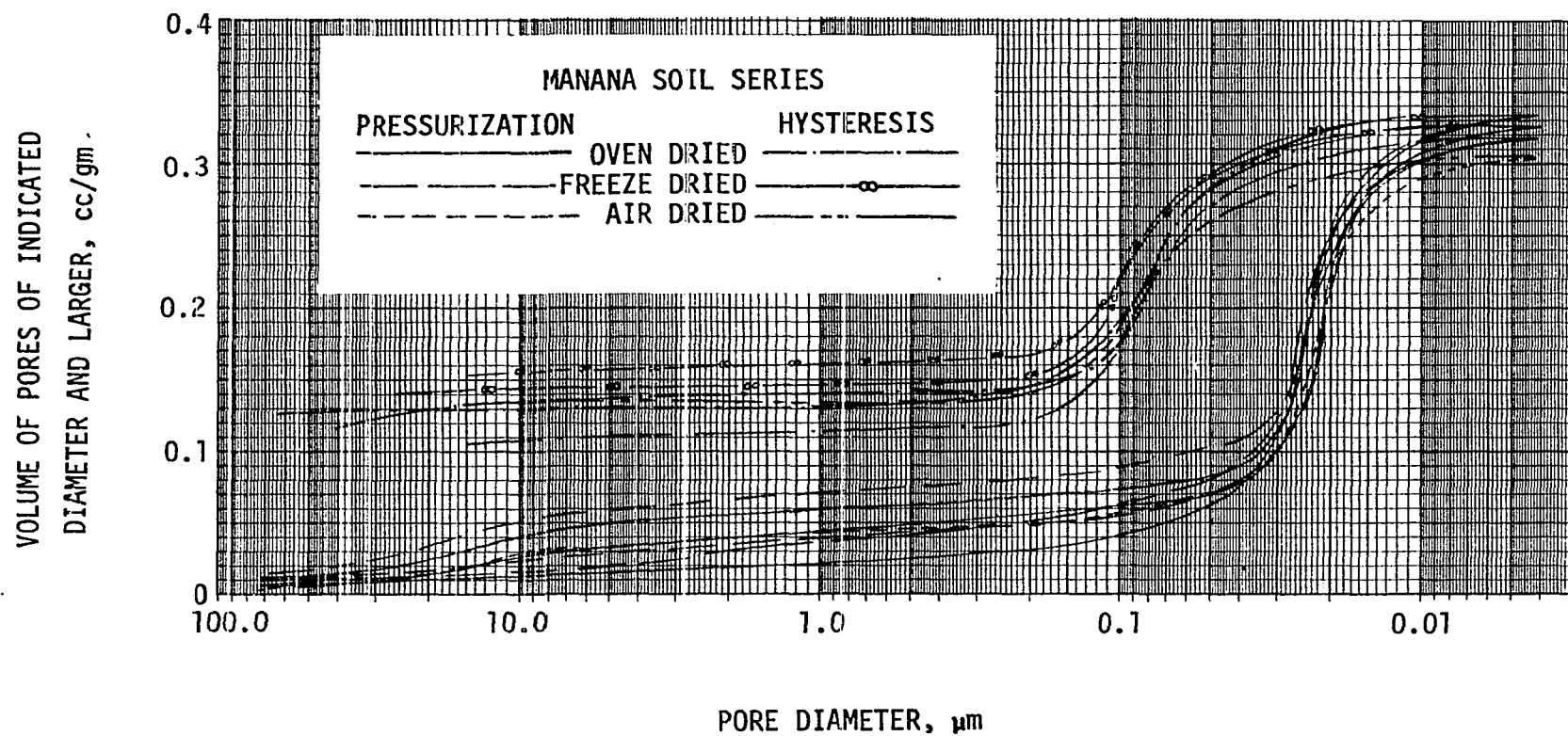


Figure B4. Pore size distribution curves for Manana soil series

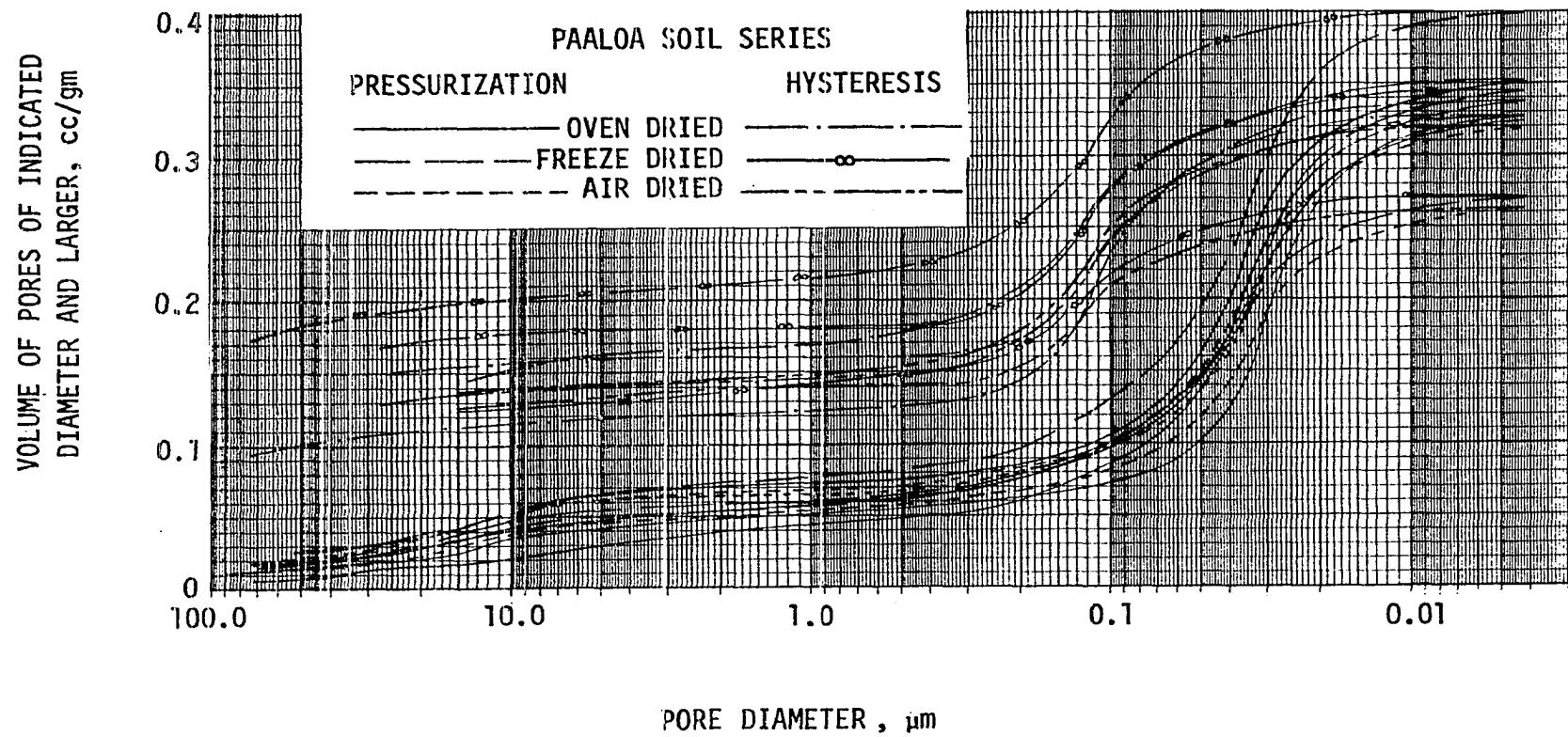


Figure B5. Pore size distribution curves for Paaloo soil series

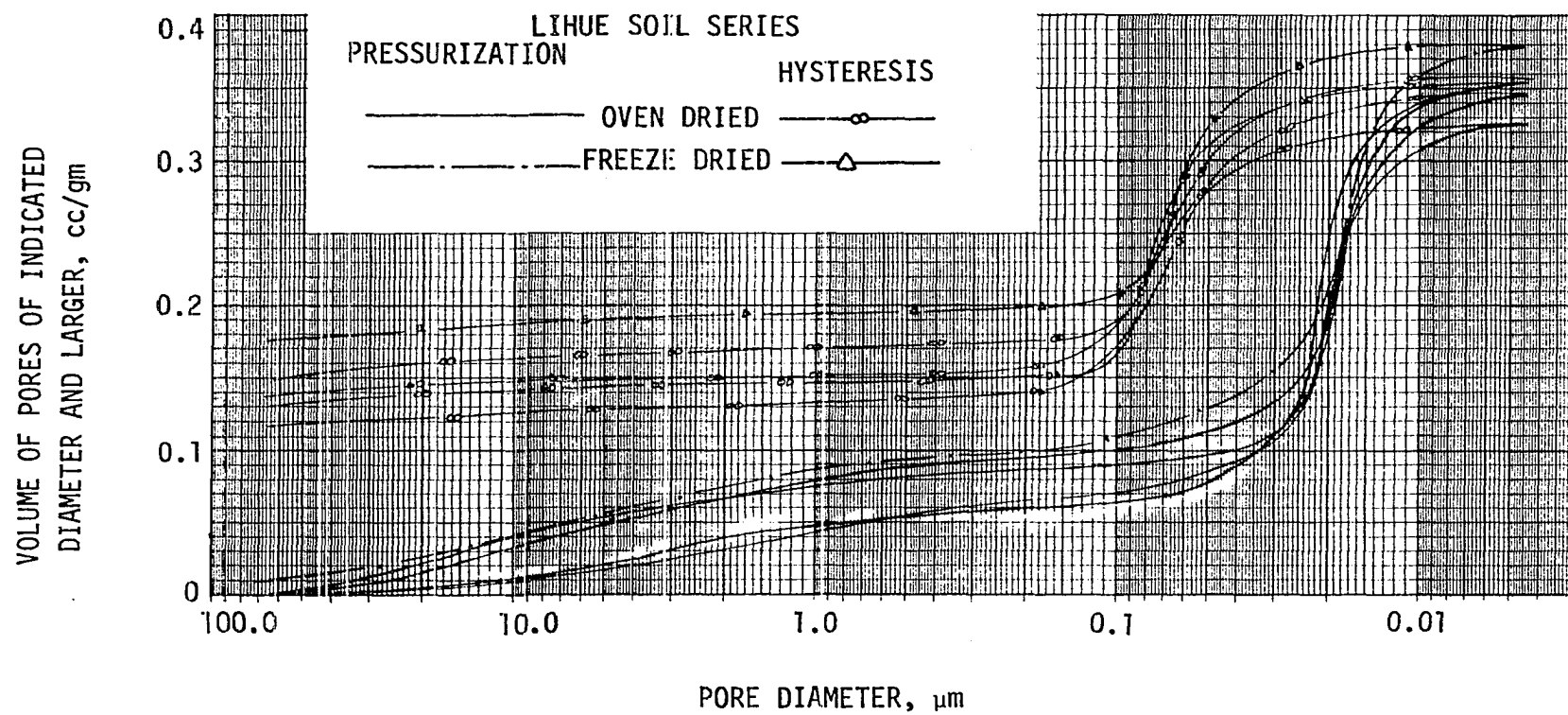


Figure B6. Pore size distribution curves for Lihue soil series

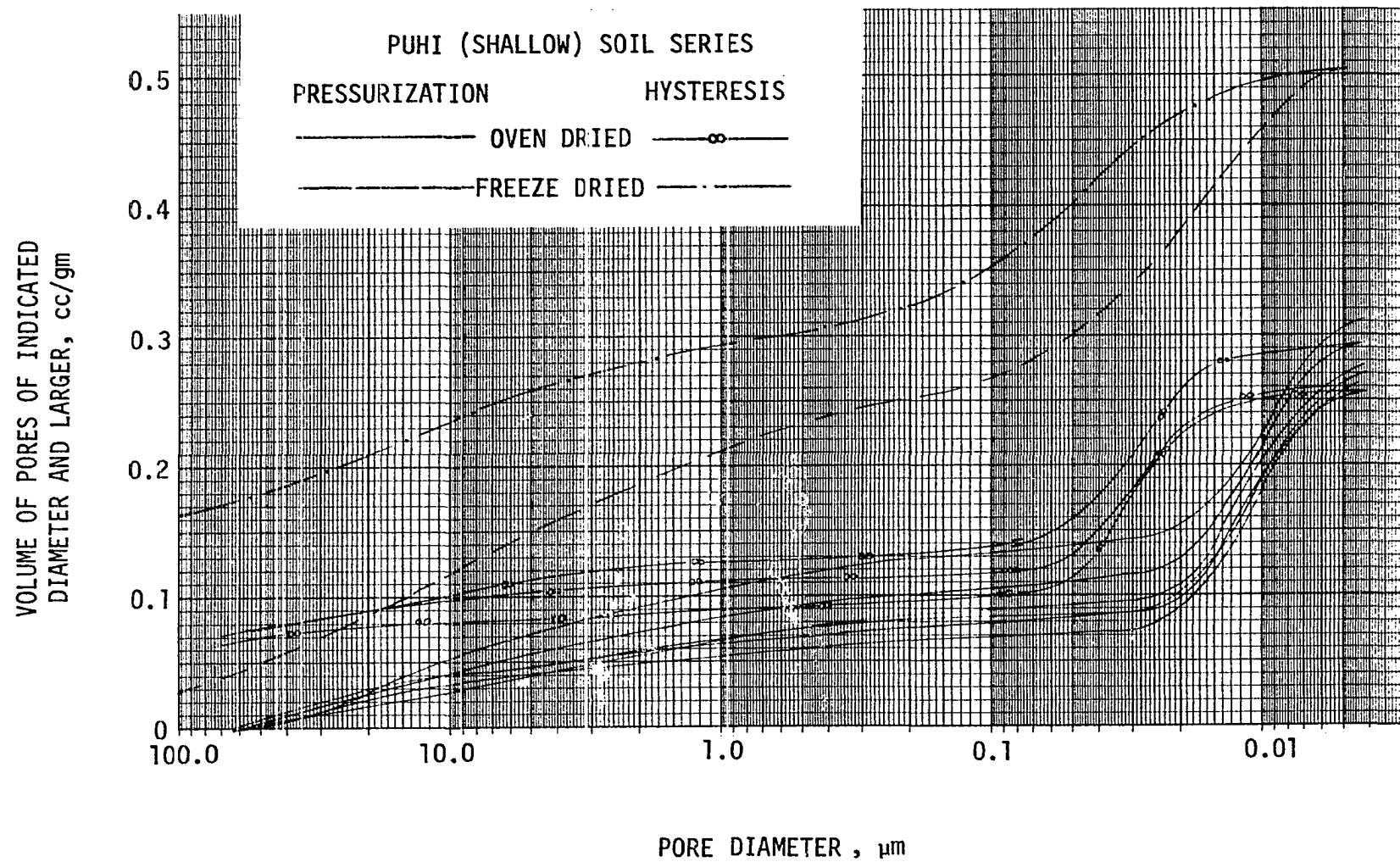


Figure B7. Pore size distribution curves for Puhi (shallow) soil series

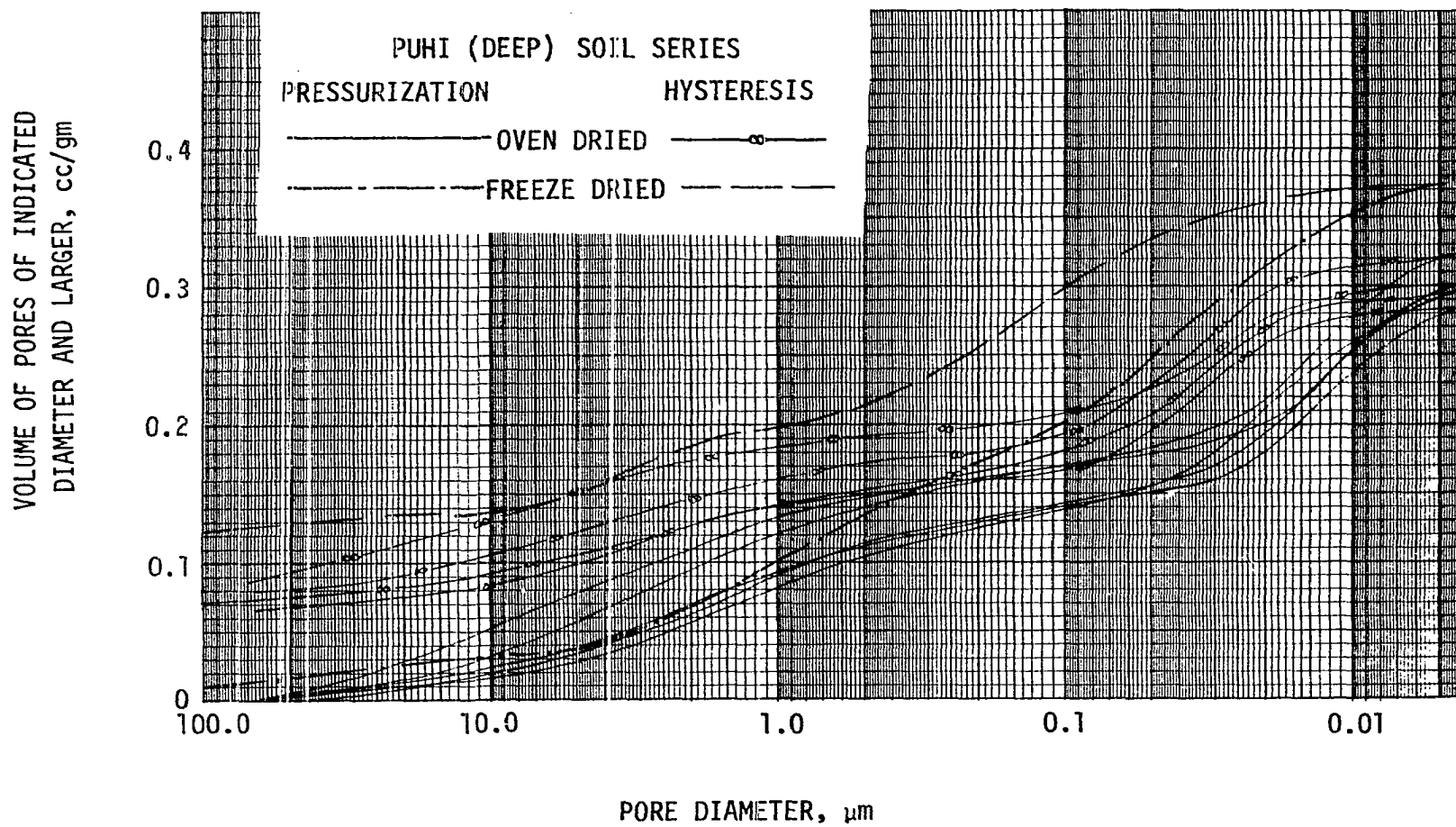


Figure B8. Pore size distribution curves for Puhi (deep) soil series

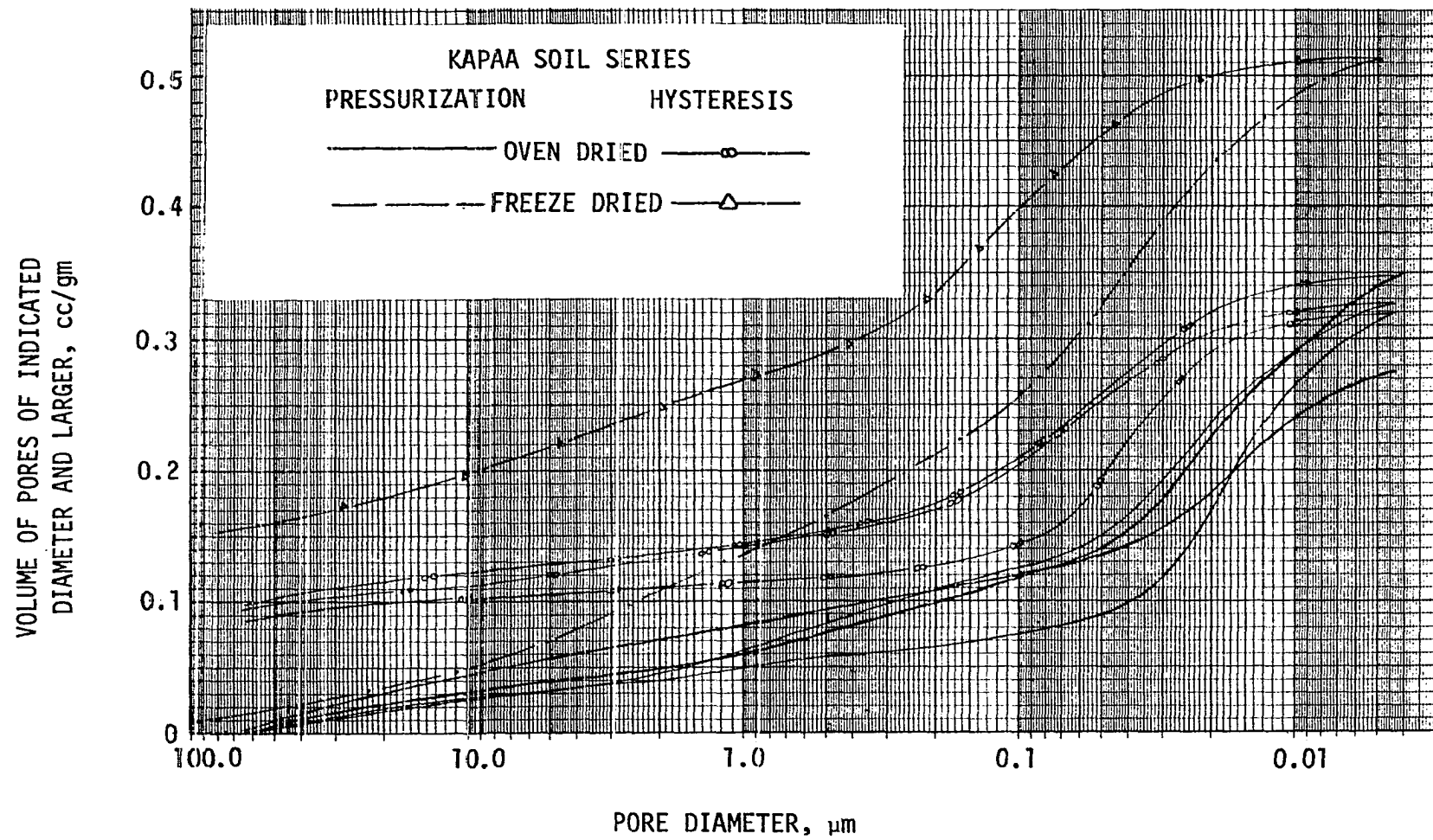


Figure B9. Pore size distribution curves for Kapaa soil series

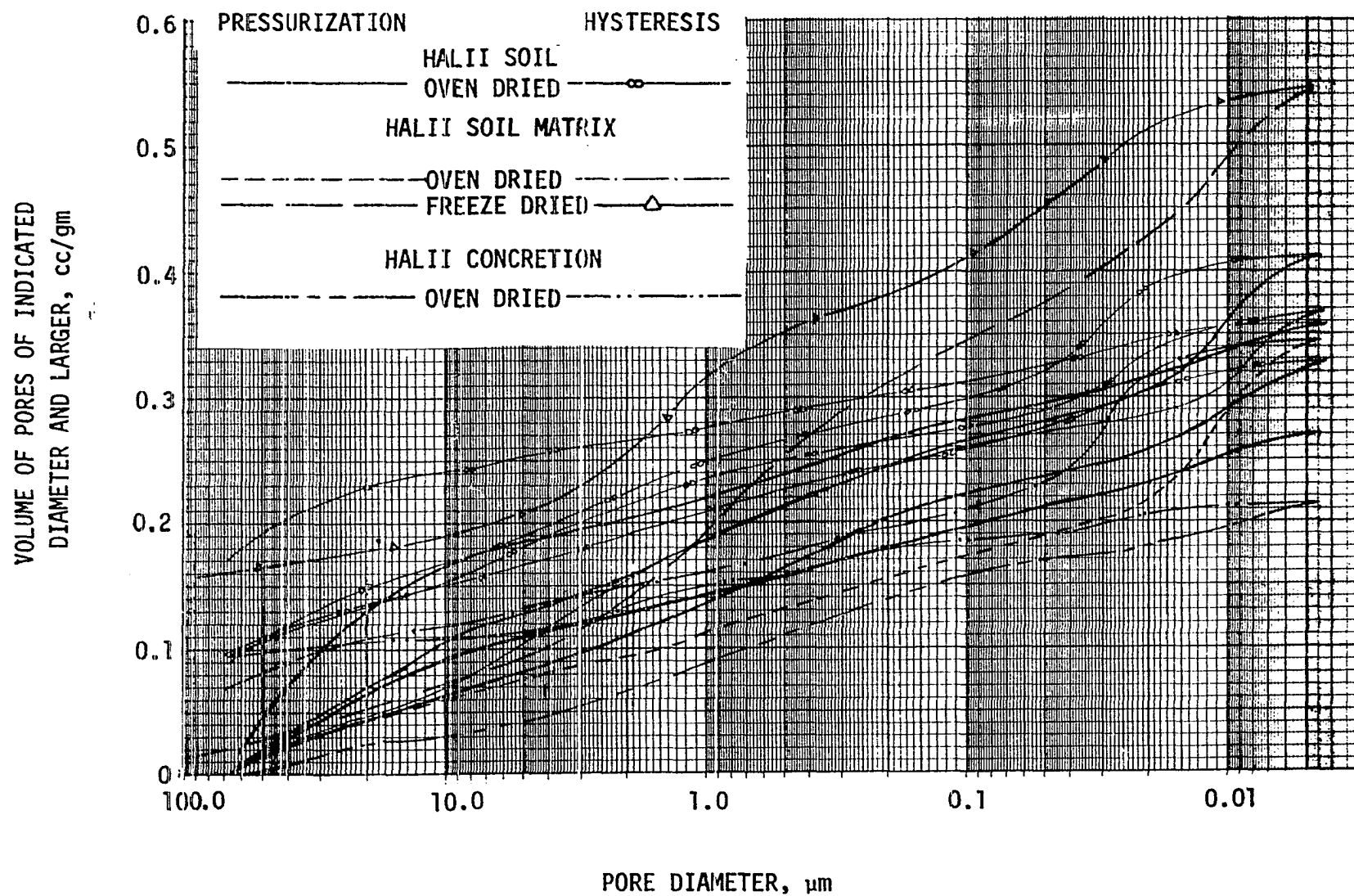


Figure B10. Pore size distribution curves for Halii soil series